Homo erectus s.l. life history and geometric morphometrics analyses of contested specimens

Tommaso Mori

Ph.D. Dissertation 2022

Eberhard Karls Universität Tübingen

Senckenberg Center for Human Evolution and Palaeoenvironment

A

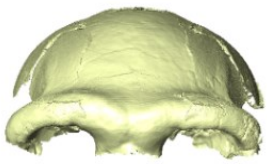

B

C

Homo erectus s.l. Life History and Geometric Morphometrics Analyses of Contested Specimens

Dissertation

der Mathematisch-Naturwissenschaftlichen Fakultät

der Eberhard Karls Universität Tübingen

zur Erlangung des Grades eines

Doktors der Naturwissenschaften

(Dr. rer. nat.)

vorgelegt von

Tommaso Mori

Aus Florenz / Italien

Tübingen

2022

Gedruckt mit Genehmigung der Mathematisch-Naturwissenschaftlichen Fakultät der Eberhard Karls Universität Tübingen.

Tag der mündlichen Qualifikation:	20/09/2022
Dekan:	Prof. Dr. Thilo Stehle
1. Berichterstatter/-in:	Prof. Dr. Katerina Harvati
2. Berichterstatter/-in:	Prof. Dr. Jacopo Moggi-Cecchi

Content

Abstract

The history and debate of *Homo erectus* are long and complex. The first fossils recovered from Trinil were assigned to *Pithecanthropus erectus*. Afterward, many different taxa were suggested, and the taxonomy of *H. erectus* has been hardly debated. Currently, scholars mainly accept two main views regarding *H. erectus* alpha taxonomy: the first considers *H. erectus* as a single "real" species. In this scenario, all specimens from Africa and Eurasia belong to the same species *H. erectus sensu lato (s.l.)*. The other view considers specimens from Asia as the only representative of the *H. erectus* species, naming it *H. erectus sensu stricto (s. str.)*. Specimens from Africa are regarded as different species, *H. ergaster*. One of the most challenging tasks in studying *H. erectus* systematics is distinguishing between intra- and interspecific variations. To understand and frame correct hypotheses regarding human evolution, studying fossil materials carefully and using state-of-the-art methods is essential.

For this reason, the main aim of this Ph.D. project is to contribute to the current knowledge and debate on the evolution of the genus *Homo* by studying three different specimens using state-of-the-art geometric morphometrics (GM) methods and virtual anthropology techniques. The specimens studied were 1) KNM-ER 42700 calvaria, 2) KNM-OG 45500 frontal bone, and 3) Kocabaş partial calotte. All the specimens are commonly attributed to *H. erectus s.l.* However, each one has some criticism that needs to be addressed.

The different works made during my Ph.D. provide new information regarding specific fossils. In particular, these works concluded that:

- Based on basicranial morphology and ontogenetic comparison, KNM-ER 42700 is most probably a young adult individual;
- After reconstructing the frontal bone and performing a GM comparative study, results indicate that KNM-OG 45500 frontal morphology is among the smallest found in *H. erectus s.l.,* and its shape retains many archaic features.
- Kocabaş calotte was fully restored, and the frontal bone was studied through GM analysis. The comparison highlighted that Kocabaş differs in the frontal and supraorbital region from the other *H. erectus s.l.* specimens. Instead, it is morphologically similar to Middle Pleistocene *Homo* specimens, particularly Bodo.

Before these detailed and comprehensive analyses, these fossils were considered *H. erectus s.l.* The picture drawn by these results seems to complicate the scenario and add new information to the open debate regarding *H. erectus s.l.*

Zusammenfassung

Die Geschichte und Debatte des *Homo erectus* ist lang und komplex. Die ersten Fossilien wurden *Pithecanthropus erectus* zugeordnet. Zu einem späteren Zeitpunkt wurden verschiedene Taxa vorgeschlagen und die Taxonomie von *H. erectus* stark diskutiert. Gegenwärtig gibt es zur Alpha-Taxonomie von *H. erectus* zwei vorherrschende Ansichten: Die erste betrachtet *H. erectus* als eine einzige „echte“ Art. In diesem Szenario gehören alle Exemplare aus Afrika und Eurasien zur selben Art *H. erectus sensu lato* (*s.l.*). Die andere Ansicht betrachtet Exemplare aus Asien als einzige Vertreter der Art *H. erectus* und bezeichnet sie *H. erectus sensu stricto* (*s. str.*). Exemplare aus Afrika gelten als andere Arten, *H. ergaster*. Eine der herausforderndsten Aufgaben beim Studium der Systematik von *H. erectus* ist die Unterscheidung zwischen intra- und interspezifischer Variabilität. Um korrekte Hypothesen über die menschliche Evolution zu verstehen und zu formulieren, ist die sorgfältige Untersuchung fossiler Materialien unter Verwendung modernster Methoden unerlässlich.

Aus diesem Grund ist das Hauptziel dieser Promotion, einen Beitrag zum aktuellen Wissen und zur Debatte über die Evolution der Gattung *Homo* zu leisten, indem drei verschiedene Fossilien mit modernsten Methoden der geometrischen Morphometrie (GM) und Techniken der virtuellen Anthropologie untersucht wurden. Die untersuchten Fossilien waren 1) das Calvarium von KNM-ER 42700, 2) das Stirnbein von KNM-OG 45500 und 3) die bruchstückhafte Kalotte von Kocabaş. Alle drei Fossilien werden allgemein *H. erectus s.l.* zugeschrieben. Jedes steht jedoch unter Kritik, die berücksichtigt werden muss.

Die verschiedenen Arbeiten, die während meiner Promotion entstanden sind, liefern neue Informationen zu bestimmten Fossilien. Die Arbeiten kamen zu den folgenden Schlüssen:

- Basierend auf der Morphologie der Schädelbasis und des ontogenetischen Vergleichs ist KNM-ER 42700 höchstwahrscheinlich ein junges erwachsenes Individuum.

- Die Rekonstruktion des Stirnbeins und Durchführung einer GM-Vergleichsstudie ergibt, dass KNM-OG 45500 zu den kleinsten Stirnbeinen von *H. erectus s.l.* gehört und morphologisch viele archaische Merkmale aufweist.

- Die Kocabaş-Kalotte wurde vollständig rekonstruiert und das Stirnbein mittels einer GM-Analyse untersucht. Der Vergleich verdeutlicht, dass sich Kocabaş in der frontalen und supraorbitalen Region von anderen *H. erectus s.l.* Exemplaren unterscheidet. Stattdessen ähnelt Kocabaş morphologisch den mittelpleistozänen *Homo*-Exemplaren, insbesondere Bodo.

Vor diesen detaillierten und umfassenden Analysen wurden die hier behandelten Fossilien als *H. erectus s.l.* angesehen. Das in dieser Arbeit generierte Bild scheint die bisherige Zuordnung zu verkomplizieren und liefert neue Informationen hinsichtlich der bestehenden Debatte über *H. erectus s.l.*

List of publications for cumulative dissertation

Publications submitted in fulfillment of the requirements of this cumulative dissertation.
Numbers in parenthesis represent the percentage of own contribution to the:
(scientific idea/data generation/analysis and interpretation/paper writing).

Accepted papers:

• Appendix I (75/100/100/90):

Mori, T., Harvati, K. Basicranial ontogeny comparison in *Pan troglodytes* and *Homo sapiens* and its use for developmental stage definition of KNM-ER 42700. *Am J Phys Anthropol*. 2019; 170: 579– 594. https://doi.org/10.1002/ajpa.23926

• Appendix II (75/100/85/75):

Mori, T., Profico, A., Reyes-Centeno, H., & Harvati, K. (2020). Frontal bone virtual reconstruction and geometric morphometric analysis of the mid-Pleistocene hominin KNM-OG 45500 (Olorgesailie, Kenya). *Journal of Anthropological Sciences*, *98*, 49-72. DOI 10.4436/JASS.98022

Manuscript ready for submission:

• Appendix III (75/100/100/100):

Mori, T., Riga, A., Aytek, A., I., Harvati, K. *(To be submitted).* A new virtual reconstruction and geometric morphometric analysis of Kocabaş hominin fossil from Turkey.

1 Introduction

History and debate regarding Homo erectus sensu lato

The history of *H. erectus* is long and complex. Initially, the rich fossil sample found in Asia were included in many different genera: *Pithecanthropus, Meganthropus,* and *Sinanthropus.* Each of them sometimes comprised multiple species. A first reduction in the number of taxa was made already by von Koenigswald and Weidenreich [1]; in their opinion, remains from Java (Trinil, Sangiran, and others) and China (Zhoukoudian) “were related to each other in the same way as two different races of present mankind”[1, page 928] and Weidenreich [2] decided to put them as subspecies within *H. erectus* taxon. Mayr [3], in his influential paper, put together *Pithecanthropus* and S*inanthropus* into *H. erectus.* Also, in the African sample, the fossil material was first described with a variety of taxa later included in *H. erectus.* For example, *Telanthropus capensis* was first moved into the genera *Pithecanthropus* [4], maintaining the specific attribution; later, it was moved into *H. erectus* [5]. Specimens from East Africa (Olduvai Gorge and the Turkana Basin) were assigned to *H. erectus* by Leakey, Walkers, and colleagues during the 1960s and 1980s [6-10].

By the 1980s, we have a highly variable species, H. erectus s.l., with a temporal and geographical distribution going from 1.9 Ma to 0.5 or 0.4 Ma in sites from South Africa to the far east as Indonesia. Recent discoveries even added new regions with specimens from Dmanisi and possibly Turkey, expanding the geographical range of *H. erectus s.l.*

The discussion regarding the alpha taxonomy of *H. erectus s.l.* is still open and lively. The debate is crucial because alpha taxonomies provide the ground basis for analyses regarding species diversity and intraspecific biological aspects, such as sexual dimorphism. One of the most challenging aspects of paleontology is the differences in how scientists define species theoretically and operationally. Regarding *H. erectus s.l.* the two extreme taxonomic and evolutionary scenarios go from the regional continuity model to the “bushy tree” model. Most scholars adhere to intermediate points of view. The two main positions correspond to a single species model or a two-species model. When considering *H. erectus* as a single “real” species, distinct from early *Homo* and later *Homo,* variation is considered the norm for a widespread polytypic species [11-21]. Geographic variants are seen as parapatric allotaxa [11] – these populations possess the same basic anatomy and can hybridize but are distinguishable from one another. Different populations from Africa or

western Asia were proposed to be ancestral to later *Homo* species [19] with a speciation event that occurred by the Early Pleistocene. Other populations, the eastern Asian ones, survived for a longer time, probably went extinct, and were replaced by the dispersal of more derived species.

In the ‘80s, the increasing cladistic approaches were also applied in paleoanthropology. The new approach focused the attention on autapomorphies to define species [22-26]. In this regard, Asian fossils tend to have a higher frequency of autapomorphic traits compared to the African fossils. These autapomorphic traits (i.e., angular torus, fissure between the mastoid process and the petrosal crest, thicker cranial bones etc.) allowed to define the species *Homo erectus sensu stricto (s. str.),* which defined all the Asian specimens, excluding the African sample [22, 23] or at least the Koobi Fora record [25-27] (at that time the African record did not include more recent discoveries such as KNM-OG 45500, KNM-ER 42700 and Daka). The African sample was interpreted as a different species, *H. ergaster,* that exhibited synapomorphies recognized in *H. sapiens* that were missing in *H. erectus* [28]. *H. ergaster* is considered as a different species comprising the African fossils from Late Pliocene and Early Pleistocene sites possibly ancestral to both lineage: one of more derived Middle Pleistocene *Homo* (possibly *H. heidelbergensis s.l.)* and the second which evolved in *H. erectus s. str.* More speciose taxonomies were proposed with the discovery of new material, especially the fossils from Dmanisi. For example, by adding *H. georgicus* a three-species model was proposed with the Georgian species having diverged from early *Homo* prior to the emergence of *H. ergaster* [29-31]. The phylogenetic relationships linking these taxa are still unclear. Researchers also propose even a bushier tree. Tattersall and Schwartz, in their works, have defined many “morphs” that, in their opinion [32], can be considered as “at the very least. . .genetically disjunct species,” such speciose scenario was also recognized within single sites, and limited time periods (e.g., Koobi Fora [33]; Dmanisi [34]). However, detailed species diagnoses and nomenclature are lacking, and a phylogenetic linkage among these different taxa has not yet been proposed.

Aim of the Ph.D. project

It is clear that the most challenging difficulty when studying *H. erectus* systematics is recognizing between intra- and interspecific variations. Are differences between fossils from Africa (i.e. Koobi Fora and West Turkana) and those from Asia related to taxonomic diversity, or the variability seen in the fossil record can be attributed to temporal and spatial variation? It is also essential to understand the pattern of variability in this sample. When studying

fossils, one of the challenges is being able to recognize the different sources of variation. For example, temporal trends can be a source of variation in *H. erectus s.l.* It is known that in this taxon, cranial shape evolution is strictly bonded to allometric variation, as cranial capacity increases over time, resulting in changes to the cranial form.

In order to understand and frame correct hypotheses regarding human evolution, we must carefully study the fossil material. Adding more specimens to the current fossil sample by finding new material will help draw correct evolutionary scenarios. However, there are also fossils that, for different reasons, were not studied using state-of-the-art methodologies; such specimens can add crucial information regarding human evolution (for example, the Apidima fossils [35]). In this context, every specimen is fundamental and can be helpful in increasing our knowledge regarding the natural history of *Homo.* For this reason, the main aim of this Ph.D. project is to contribute to the current knowledge and debate on the early phases of the evolution of the genus *Homo* by studying three different specimens (namely KNM-Er 42700, KNM-OG 45500, and Kocabaş) using state-of-the-art geometric morphometric methods and virtual anthropology techniques. Geometric morphometrics allows for a quantitative, hypothesis-driven analytical approach to studying morphological variability in the fossil sample to validate a fossil's taxonomic status or study morphological affinities. Based on shape theory and evolutionary theory, this cumulative dissertation builds upon three works:

- Paper I: Understanding the developmental stage of KNM-ER 42700
- Paper II: Reconstruct and study the morphology of KNM-OG 45500 frontal bone.
- Paper III: Reconstruct and study the morphology of Kocabaş frontal bone

The following sections introduce the methodological and theoretical approaches of this Ph.D. project. Chapter 2 (Research strategies) presents the main research goal and the specific objectives of the three papers that form this cumulative dissertation, together with the methods and material adopted. Chapter 3 (Results and discussion) summarises the key results of the three papers and reviews the contribution of this dissertation to the discussion of early Pleistocene hominin variability. Finally, the last chapter (Concluding remarks) synthesizes the conclusions and discusses future research directions.

Theoretical and methodological background.

Geometric morphometrics

Morphometrics, the measurement (metron) of shape (morphe), is a subfield of statistics with a long and well-established history. In 1888 Frances Galton was the first to introduce the correlation coefficient to study human morphology. In 1907 he was the first to propose a method to quantify facial shape. The same method has later been termed two-point shape coordinates or Bookstein-shape coordinates. The advent of multivariate statistical techniques, developed mainly in the first half of the 20th century, allowed for the development of a new branch of morphometrics analyses involving a multivariate approach. Coordinate-based methods, the statistical theory of shape, and the computational realization of deformation grids were only invented in the 1980s and they represent a significant breakthrough for morphometric analyses [36-40]. The advent of computer technology and the possibility to process large amounts of data allowed for new ways of morphological analyses. In the last thirty years, geometric morphometrics (GM) has become a well-established method for the quantification and analysis of the shape of biological forms [41-51]. GM is based on landmark coordinates. Landmarks are defined by Bookstein [37] as named *loci* (i.e. 'bridge of the nose', 'tip of the chin') and Cartesian coordinates. Names of landmarks are intended to imply correspondence (biological homology) among forms. In every other form of the sample and in the average of each form, all landmarks point have the "same" location. Landmarks' coordinates can be two or three-dimensional.

This new morphometric approach preserves the geometry of the landmark configurations throughout the analysis and thus permits the representation of statistical results as actual shapes or forms. Thanks to multivariate statistic methods, GM can enhance our possibilities in hypothesis testing and shape analyses.

Virtual reconstruction

Fossils are discovered broken or distorted; for this reason, any comparative analysis needs a reconstruction step before being conducted. Nowadays, working with fossil data in an entirely virtual environment is possible, and the reconstruction can be accomplished using a PC. In the earliest stage of this approach, the reconstruction primarily focused on the "puzzle" aspect of assembling fragments on the computer in a correct anatomical position. More recently, virtual reconstruction also adopted techniques aimed at correcting post-mortem deformation and integrating missing aspects by mirroring preserved symmetrical parts or statistically reconstructing and predicting the missing part [52-55].

My Ph.D. project aimed at using state-of-the-art GM and virtual anthropology methods to study 3 different fossils and their morphological relation to other hominin remains.

2 Objectives

The study of human evolution is a difficult task. Hypotheses of speciation and extinction events, phylogenetic relation, and taxonomic attribution in paleontology are based on the fossil evidence available. Fossils, however, are a complex source of information. The sample size for morphological analyses is the first problem for paleoanthropologists. Fossils are scarce and often do not preserve the same skeletal elements.

Moreover, it is complicated to understand specific biological aspects such as ontogeny and sexual dimorphism in extinct species. For this reason, every fossilized fragment recovered is fundamental for the advancement of this discipline in order to add new knowledge regarding the natural history of our lineage. Based on this assumption, my Ph.D. project focused on three fossils of interest that have been poorly studied and often not considered in the paleoanthropological debate of taxonomic complexity during the Early and Middle Pleistocene. Each paper of this cumulative dissertation focused on one fossil with its research question and research design. The three works aim to investigate *Homo erectus s.l.* hypodigm and its temporal and geographical variation.

Fossil of interest and specific research design

This research focused on three fossils. The specimens studied were: KNM-ER 42700, KNM-OG 45500, and Kocabaş. They are all commonly attributed to *Homo erectus s.l..* However, each has some critical aspects[56, 57], particularly KNM-OG 45500 and Kocabaş were never studied using advanced virtual anthropological methods. The following paragraphs introduce those specimens, the literature regarding previous studies, their research question, and specific research design.

Paper I - KNM-ER 42700

The first work of my Ph.D. focused on KNM-ER 42700. The fossil is a small calvaria found in the Koobi Fora Formation; its geological age has been estimated at around 1.55 million years. The first taxonomic attribution made by Spoor and colleagues [58] assigned it to *H. erectus s.l.*. However, the taxonomic status of this specimen has been debated since then. Baab [57]found in her geometric morphometrics (GM) analysis that the specimen's cranial shape was different from other *H. erectus s.l.*; instead, she found KNM-ER 42700 to be similar to later *Homo*. Spoor et al. [59] argued that the results were influenced by the

(minor) taphonomic, probable sexual dimorphism, and the ontogenetic stage of this specimen. After correcting the taphonomic damage, GM analysis results did not significantly change [60], leaving ontogeny or sexual dimorphism as the only potential factors behind the unusual cranial shape of this specimen.

Recently, Baab [61] attempted to evaluate the cranial morphology of *Homo erectus* as a whole, including subadult specimens such as KNM-WT 15000 and D 2700. KNM-ER 42700 showed no similarities with these subadult specimens [61]. In 2018, Neubauer et al. [62] presented a new virtual reconstruction and GM analysis of KNM-ER 42700's endocranial shape to understand its taxonomic affinities. The endocranial morphology of KNM-ER 42700 was found to be different from other *H. erectus s.l.* specimens, however, the authors suggested that this specimen had not reached an adult endocranial morphology [62]. This hypothesis was based on the fact that KNM-ER 42700 lies on the growth trajectory formed by Modjokerto and the other adult *H. erectus s.l.*. Based on these results, Neubauer et al. [62] proposed that probably KNM-ER 42700 had an age at death between Modjokerto and KNM-WT 15000. Following this hypothesis, KNM-ER 42700 would likely have had an age between 3 and 7 years since 95% of brain size is already attained in chimpanzees between 3-4 postnatal years and humans between 6-7 years[63].

The lack of dentition in KNM-ER 42700 does not allow us to estimate its relative age with confidence. The only useful proxy for age estimation is cranial sutures closure [20, 64]. KNM-ER 42700 shows all sutures completely fused except for the spheno-occipital synchondrosis, which is described as two-thirds fused [58, 62]. In modern humans, this condition indicates either a young adult or a late subadult age [11, 64]. However, the sutural closure pattern association/correspondence between modern humans and *H. erectus s.l.* is poorly understood [65-68]. It is challenging to study the closure pattern in *H. erectus,* given the lack of juvenile fossils and the preservation of the fossil material. Among the few young individuals ascribed to *H. erectus s.l.* D2700 has an open spheno-occipital synchondrosis [20], KNM-WT 15000 does not preserve this part, but its dentition is less developed than that of D2700; thus, it was probably younger than D2700 [68]. Variability in the suture's fusion time in modern humans, however, makes the spheno-occipital synchondrosis not a reliable proxy for the definition of the ontogenetic stage of KNM-ER 42700 [62]. Therefore, it is crucial to research the ontogenetic changes in H. erectus s.l. to clarify the age at death of KNM-ER42700 [57, 62].

Material and Methods:

In order to evaluate the ontogenetic stage of KNM-ER 42700, we decided to study modern humans and chimpanzees' ontogenetic trajectories in the basicranium, looking for a shared (presumably plesiomorphic) developmental pattern. A total of 33 landmarks were collected from an ontogenetic sample of modern humans (80), chimpanzees (51), and 12 individuals classified as *Homo erectus s.l.* Modern humans and chimpanzees were grouped according to the dental eruption and divided into four ontogenetic groups useful for analyzing ontogenetic trajectory. Usual GM workflow (Procrustes superimposition followed by principal component analysis)[37, 39, 40, 69] was used to investigate the shape space of the basicranium. Ontogenetic trajectories in modern humans and chimpanzees were analyzed by comparing the size, shape, and direction of ontogenetic changes across different age groups (more details regarding the methodological approach can be found in appendix I)[41]. Common ontogenetic aspects between the two trajectories were found and tested to determine whether they could help discriminate age groups in modern humans and chimpanzees. A regression of size on the extracted shape variables was used to investigate common ontogenetic allometry. Shape variables useful for age class estimation were used to evaluate the *Homo erectus s.l.* sample and KNM-ER 42700.

Paper II - KNM-OG 45500

The specimen focus of the second work was KNM-OG 45500 (also referred to as KNM-OL 45500 in the literature). This fossil was recovered *in situ* in 2003 in a stratigraphic layer rich in Acheulean handaxes [70]. Datation of underlying and overlying volcano layers using the single-crystal $^{40}Ar/^{39}Ar$ method gave an age between ca. 974 and 747 ka. KNM-OG 45500 was found close to the lower layer; hence, the age proposed for this specimen ranged between 970 and 900 ka [70]. KNM-OG 45500 was attributed to *H. erectus s.l.* on the basis of morphological evidence of the frontal bone, such as midline keeling, shelf-like morphology of the post-toral sulcus, lack of torsion in the toral anterior surface, and double-arched supraorbital shape. It has been described as one of the smallest African *Homo erectus s.l.* [70]. KNM-OG 45500 frontal bone size is smaller than fossils from Kenya (e.g. KNM-ER3733 and KNM-WT15000, dated to between 1.8-1.5 Ma), but it seems to be closer to the later OH12 fragmented specimen from Olduvai (dated to ca. 1.2-1.1 Ma) [71, 72]. Its

morphology is considered similar to Early Pleistocene African specimens such as Daka BOU-VP-2/66 (Ethiopia) and KNM-ER3733 (Kenya) [70].

Despite its interesting morphological feature, since 2004 it was never accomplished a virtual reconstruction of the frontal bone and comprehensive analysis of this district. For this reason, this work aimed to reconstruct the specimen and compare its morphology to other fossil specimens using GM methods.

Material and methods

KNM-OG 45500 frontal bone was virtually reconstructed by mirror-imaging the left preserver structures on the right side and *vice versa.* Afterward, the posterior margin of the coronal suture was estimated by reconstructing the bregma position; estimation was performed multiple times. Once reconstructed, the frontal squama and supraorbital region morphology was studied using GM methods. A total of 80 landmarks and semilandmarks were collected. The comparative sample comprised geographically diverse fossils (n=20) and modern human samples (n=30). The aligned Procrustes coordinates, centroid size distribution, and pairwise Procrustes distances between specimens were analyzed using different methods, such as principal component analysis, cluster analysis, and correlation tests to investigate morphological affinities of KNM-OG 45500 to the fossil sample.

Paper III - Kocabaş

Workers discovered the Kocabaş remains during the processing of the travertine blocks brought from the travertine area to the factory (Dalmersan), as reported by Prof. Dr. Mehmet Cihak Alçiçek [73]. There, the blocks were sliced at *ca* 35 cm of thickness. The partial calotte was embedded in one of the blocks and unfortunately cut by the factory's sawing procedure. The process only left three fragments of the calotte: a partial right parietal bone, the right part of the frontal preserving the lateral aspect of the supraorbital torus, and a partial left parietal in articulation with a fragment of the left posterior portion of the frontal bone (not preserving the supraorbital torus). Although this fossil's exact provenance is unknown, it is considered to derive from the Upper Travertine level, which was the only one exploited at the time of discovery in 2002 [74, 75].

Kappelman et al. [73] described the specimen for the first time and assigned it to *H. erectus s.l..* The classification was based on non-metric features such as prominent supraorbital torus, a distinct post-toral sulcus, and few linear measurements [73]. This first conclusion was supported by several subsequent studies [75-78]. Linear measurement analysis and cladistic approach supported the conclusion that Kocabaş belonged to *H.*

erectus s.l. hypodigm [75, 78]. However, works based on GM approach did not convincingly support such a taxonomic affiliation. Only two GM comparative shape analyses have been published to date [56, 77], both showing that the Kocabaş frontal morphology is similar both to *H. erectus s.l.* and to middle Pleistocene African (Broken Hill 1 and Bodo [77]) or Eurasian fossils (Ceprano and Arago [56]). Both works did not completely restore the frontal bone but focused on different portions of the frontal squama. Moreover, the taxonomic groupings used by Vialet et al. [77], do not conform to commonly accepted taxonomic attributions of the Pleistocene fossil record, potentially influencing their interpretation of the results. In 2018 a new work was published where Vialet and colleagues [78] performed a metric and cladistic analysis, concluding again that Kocabaş belonged to *H. erectus s.l.* However, this most recent analysis also shows some shortcomings. The metric analysis only comprised four linear measurements; after the data collection, no size correction was performed, and the four measurements were analyzed through principal component analysis (PCA). However, such an analysis reflects only size differences, an expected result given the nature of PCA, an exploratory method looking for the greater source of variation, which, in this case, is size differences. No other clear pattern or separation between the different samples used was found. In the cladistic analysis, Kocabaş showed closer relation to the late early Pleistocene fossil (ca. 1 Ma BP, Buia, Daka, KNM-OG 45500). However, the authors did not include any middle Pleistocene fossils in this latter analysis. Therefore, it was impossible to test any relationship between Kocabaş and later hominin taxa. The taxonomic status of this important specimen, therefore, remains controversial.

The aim of this work was to perform a complete restoration of the frontal squama using state-of-the-art virtual anthropology methods and to perform a GM analysis to evaluate the morphological affinities of this specimen to early Pleistocene and middle Pleistocene fossils.

Material and Methods

The calotte of Kocabaş was restored by aligning and mirroring the three preserved fragments. The remaining missing portion of the medial aspect of the frontal squama and supraorbital torus was reconstructed by applying the Thin Plate Spline (TPS) interpolation algorithm of target fossils onto the reconstructed Kocabaş specimen (more details regarding the reconstruction steps can be found in appendix III). For the GM analyses, we collected a total of 80 landmarks on the frontal bone (11 osteometric points, 14 bilateral curve semilandmarks, and 41 surface semilandmarks). The comparative sample includes 21

fossils from different chronological periods and geographical areas and 30 adult modern humans from different populations. Shape analyses were performed through the use of principal component analysis on the Procrustes aligned landmarks' coordinates. Principal component analysis was used to explore the shape space of frontal morphologies. We performed different analyses with different datasets and samples to compare Kocabaş anatomy to different fossils and evaluate the reconstruction steps' influence on the results. The Procrustes distance among the fossil specimens was used to make a cluster analysis and build a phenetic tree. The first four PC scores were used to calculate a discriminant function between *H. erectus s.l.* and Middle Pleistocene Homo groups. Cross-validation of the function was estimated, and a classification procedure was applied to the different Kocabaş reconstructions.

3 Results and discussions

Paper I - KNM-ER 42700

The first paper concludes that the ontogenetic trajectories in Chimpanzee and modern Humans are different. Test statistics using the trajectory approach [41, 79-81] revealed that there is a significant difference in the direction (p-value= 0.0001) and size (p-value= 0.02) of the two trajectories. The pattern of shape change between consecutive age groups, however, is similar between the two (p-value= 0.49).

The difference in the size of the trajectories means that one species undergoes more shape changes than the other; in this case, Chimpanzees tend to change more in the shape of the basicranium than modern Humans in the analyzed ontogenetic period. The difference in direction means that the trajectories are not parallel. The trajectories' shapes are similar, indicating that main events in the ontogeny (dental eruption period) follow similar developmental steps.

However, despite the differences between the two trajectories, some common aspects exist. The overall trajectories are n-dimensional vectors where n is the number of PCs, and the vector's value is the mean PC score of each age group in the two taxa. A projection of the two-dimensional trajectories is presented in the PCA plot in figure 1. Decomposing the trajectory and analyzing each vector along each PCs highlight the presence of an ontogenetic vector along PC2 show the same direction (from negative values to positive ones) in both taxa. PC2 scores distribution in the different age groups follows the same trend in modern humans and chimpanzees. Kendall's tau results showed a strong correlation between age group and PC2 scores when not considering species affiliation, indicating that the values of PC2 in the different age groups have a similar distribution across the two taxa. These common aspects can be related to a shared plesiomorphic shape change of the basicranium in the hominin ontogeny. Such feature suggests that *Homo erectus s.l.* basicranial ontogeny could have had similar developmental changes. PC2, in this context, can be used as a proxy for age class estimation.

In the PCA plot, all adult fossils tend to have high PC2 scores. In particular, KNM-ER 42700 shows higher PC2 scores than KNM-WT 15000, a juvenile individual that might be older than KNM-ER 42700. These results suggest that KNM-ER 42700 probably already attained an adult basicranial morphology.

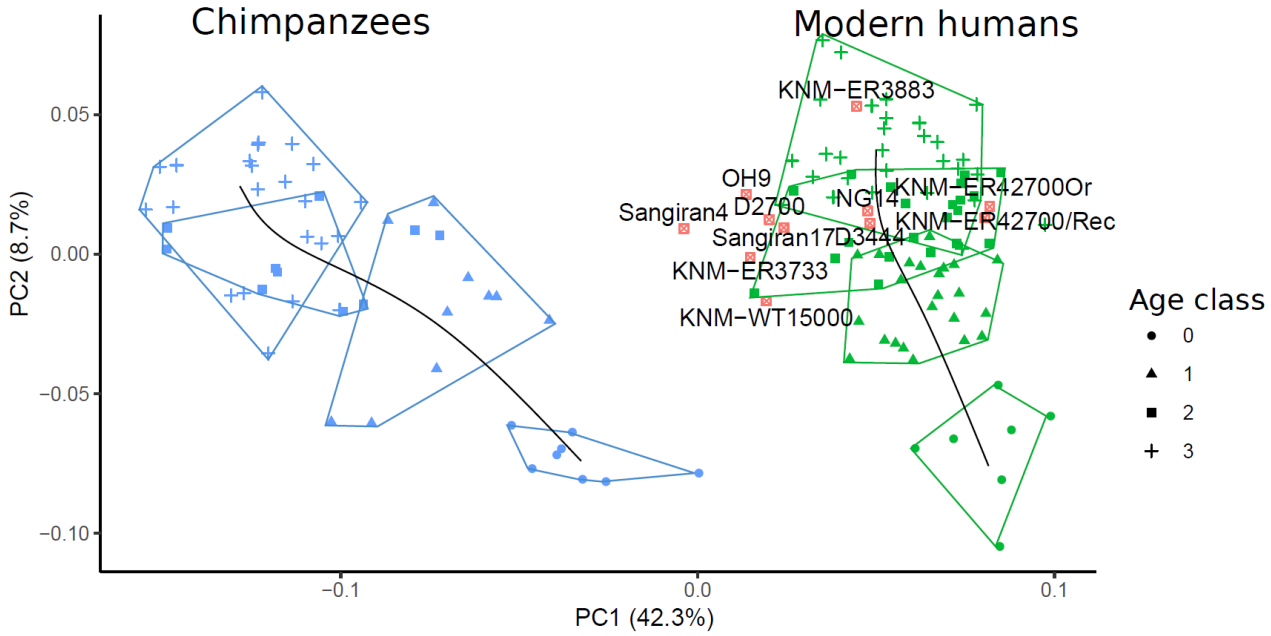

FIGURE 1. Trajectories comparison in PC1 and PC2. Colors: Blue = Chimpanzees, Green= Modern Humans, Red = Projected *H. erectus* . Symbols: ● = Age category 0, ■ = Age category 1, ▲ = Age category 2, + =Age category 3. Trajectories in bold line.

This work found that *Pan* and *Homo* do not share the same developmental trajectory. However, common developmental components are present when considering specific PC vectors. In this analysis, KNM-ER 42700 does not show a basicranial morphology of a very young individual. Thus the results do not support previous work suggesting a very young age at death [62]. Based on its basicranial morphology, it is more plausible that this specimen was an adult or young adult, confirming the initial hypothesis suggested by Spoor et al. [58].

Also, the second analysis of the reduced dataset (see original article in appendix I) shows that Modjokerto has a very low PC2 score consistent with its presumed age at death [82, 83]. This result confirms that the common ontogenetic vector along PC2 also discerns developmental stages in *H. erectus s.l.* However, such conclusions must be cautiously approached, given the limited number of young subadults in the fossil sample and the incomplete preservation of Modjokerto's cranial base.

Paper II - KNM-OG 45500

The first result obtained from this work was the KNM-OG 45500 reconstruction (Figure 2). The reconstructed parts are the right supraciliary arch and the left margin of the supraorbital torus at the height of the zygomatic process of the frontal bone.

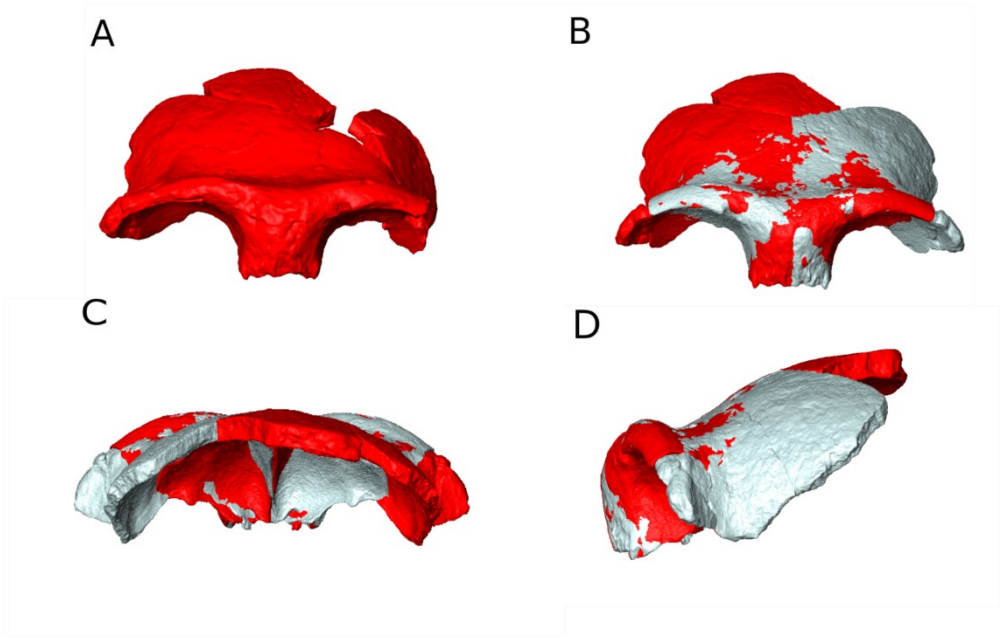

Figure 2 - KNM-OG 45500 Reconstruction: (A) Original specimen (dark red); (B) frontal view of superimposition of the mirrored specimen (light grey) on the original one in order to reconstruct the missing areas; (C) posterior view; (D) lateral view. [Image scan courtesy of the National Museums of Kenya]

The PCA plot of the first two components is shown in Figure 3. PC1 separates the recent modern humans and the fossil specimens. PC2 separates the other groups from the Middle Pleistocene Homo specimens (Bodo, Dali, Petralona, and Kabwe). Fossils are placed in this plot following temporal clustering along PC1 and PC2. Early Pleistocene *H. erectus s.l.* usually tend to have low PC1 scores, and later fossils tend to have higher PC1 scores. All the five reconstructions of KNM-OG 45500 fall within or closest to the *H. erectus s.l.* convex hull. Specifically, they tend to show a position in the PCA plot close to Early Pleistocene *H. erectus s.l.* fossils. In the plot, the label KNM-OG 45500 represents the specimen with bregma taken on the posterior margin of the frontal squama, while KNM-OG 45500 rec represents the different bregma reconstruction. In the first case, KNM-OG 45500 plots well within the *H. erectus s.l.* convex hull; in the second, the reconstructions plot on the margin of the *H. erectus s.l*. convex hull.

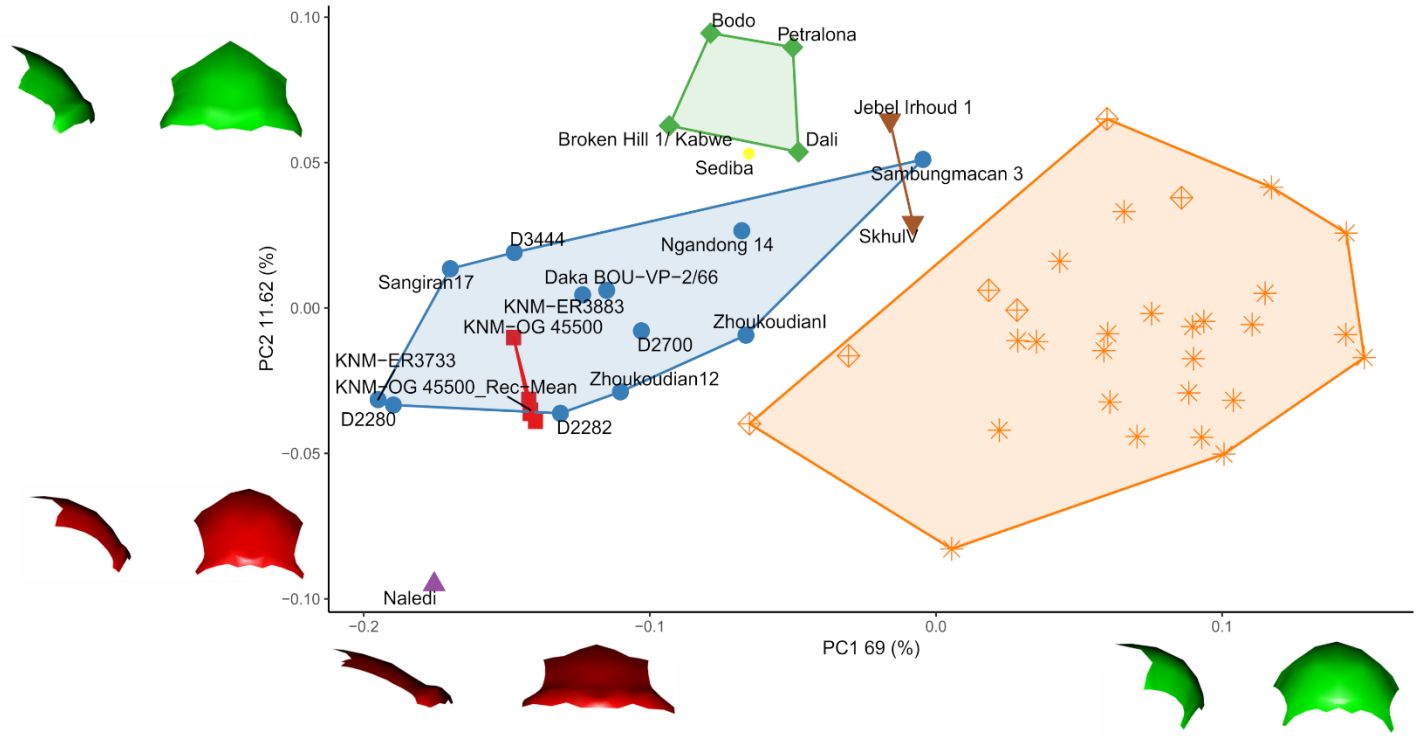

Figure 3 - PCA plot of fossil specimens and recent modern humans. Convex hulls based on group attribution from Table 2. Colors and shape: orange symbols = recent modern humans (Australian in crossed diamond); blue circle= H. erectus s.l.; green diamond= Middle-Pleistocene Homo; brown downward triangle= early H. sapiens; yellow small circle= Au. sediba; purple triangle= H. naledi; red square = KNM-OG 45500. Surfaces (frontal bone in lateral view) are shape transformations along +/-2 std. dev. from mean along PC axes.

UPGMA cluster results are shown in Figure 4. This phenetic tree shows a first basal split that generates two main clusters. The two clusters separate the fossil sample based on their chronology except for *Au. sediba* and *H. naledi* specimens. KNM-OG 45500 mean landmark configuration closest specimens are the African KNM-ER 3733 and *H. naledi* composite reconstruction DNH1 and DNH3.

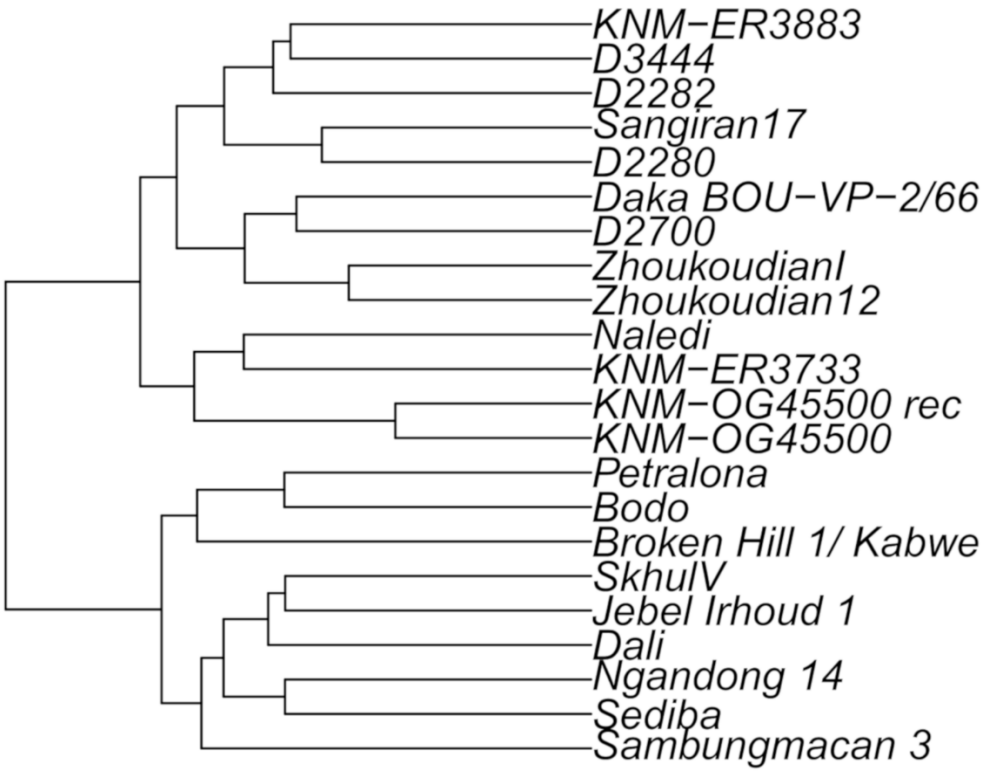

Figure 4 - UPGMA cluster analysis based on pairwise Procrustes distances matrix.

The size of KNM-OG 45500 is extremely small given its chronological age. LogCS values are closest to the Georgian fossils from Dmanisi. In comparison, Daka fossil has a much higher logCS despite being relatively close in time and space to KNM-OG 45500.

The results indicate that KNM-OG 45500 retains many archaic traits such as small overall size, an elongated frontal squama, and a relatively thin supraorbital torus. These morphologies place the reconstructions near the margin of the *H. erectus s.l.* convex hull and closer to the early specimens from Dmanisi and Kenya. The GM results agreed with previous taxonomic attribution [70], and the reconstruction confirmed that the original frontal bone was probably about 8mm longer.

Endocranial volume (ECV) has been estimated for KNM-OG 45500 to be between 622 cm^3 and <800 cm^3 [61, 70]. The logCS of KNM-OG 45500 is similar to the Dmanisi specimens, where the ECV spans from 601 cm^3 (D2700) to 730 cm^3 (D2280) [21] for this reason probably the lower limit of the estimation is more precise. Specimens that are closer in chronology and geographic position: Daka BOU-VP-2/66 (Ethiopia) and Buia UA 31 (Eritrea), by comparison, have ECV values of 986 cm^3 [84] and 995 cm^3 [85], respectively. This indicates that they probably were more than 1/3 larger than the ECV of KNM-OG 45500.

A comparison of the frontal bone size in terms of logCS between Daka BOU-VP-2/66 and KNM-OG 45500 shows that difference in size between these two fossils is larger than the size range observed among the modern humans sampled (see figure 6 in appendix II).

If KNM-OG 45500 is accepted as a member of *H. erectus s.l,* it means that in this taxon, there was greater size variability during this time period (ca. 900 Ka) than previously thought. Its small size and relatively young chronology do not follow the general trend of an increase in cranial/brain size over time, often described as a norm in the evolution of *Homo erectus* [63, 86-91].

The shape analysis of the frontal bone also highlights significant trends and clusters. The analyzed sample, as previously described, plots along PC1 following what seems to be a temporal trend. The shape analysis appears to cluster *H. erectus s.l.* fossils in different paleodemes [92]. Low PC1 scores are associated with the African early Pleistocene Nariokotome paleodeme [92]. Such paleodeme seems relatively homogeneous until ca. 1 Ma, comprising KNM-OG 45500 and Daka BOU-VP-2/66. The Dmanisi paleodeme is similar in frontal morphology to the African Nariokotome paleodeme. Asian paleodemes from Sangiran, Zhoukoutien, and Ngandong seem to express a morphological trajectory with more archaic frontal morphologies initially similar to the Early Pleistocene African and Eurasian morphology (Sangiran 17, associated with a low PC1 score in Fig. 3) and subsequently more derived morphologies (Zhoukoutien and Ngandong, associated with higher PC1 values in Fig. 3) in later periods. However, given the small sample size and the specific cranial district analyzed, which does not consider the full cranial morphology, such conclusions must be taken cautiously. Moreover, it is unclear what are the relationships among these paleodemes [21, 23, 93-100]. Nevertheless, also these results highlight that the high variability expressed by *H. erectus s.l.* could be linked to the taxon's great geochronological and associated paleoenvironmental spread, spanning from the Early to Late Pleistocene from Africa to Southeast Asia [101].

In summary, the results of this work confirm that this specimen is morphologically similar to Early Pleistocene fossils from Africa and Eurasia. In both its shape and size, it is most similar to Early Pleistocene specimens taxonomically assigned to *H. erectus/ergaster.* Overall, the results concur with the originally proposed taxonomy of KNM-OG 45500 and similarly highlight how KNM-OG 45500 extends the taxon’s range of size variation at this chronology.

Paper III - Kocabaş

In Paper III, the Kocabaş specimen was reconstructed. Different reconstructions were made using different reference target fossils to estimate the missing medial portion of the frontal bone. An example of a complete reconstruction of this fossil is presented in figure 5.

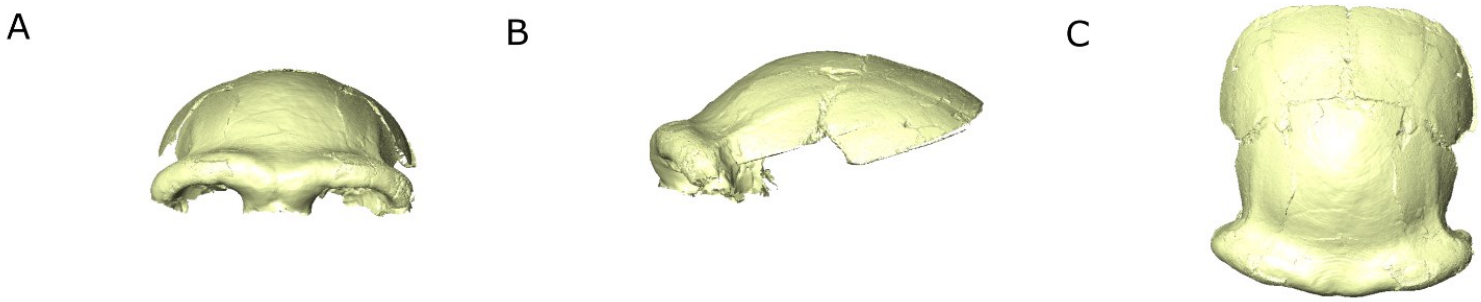

Figure 5 Full reconstruction of the medial portion of the frontal bone. Reconstruction based on Petralona specimen. A - Frontal view; B - Lateral view; C - Superior view.

Analyses performed on this fossil were similar to the analyses done in Paper-II. The shape analysis results are presented in figure 6. The PC1 and PC2 investigate the same shape space already analyzed for KNM-OG 45500. The position of the different reconstructions forms a cluster that plots outside the *H. erectus s.l.* and Middle Pleistocene Homo (MPH) convex hulls. Compared to *H. erectus s.l.* reconstructions have higher PC2 scores, while in comparison to MPH, the reconstructions have lower PC1 scores. This position in the PCA plot indicates a supraorbital morphology closer to MPH specimens but a frontal squama relatively less rounded and more “shelf-like” than MPH, similar to early Pleistocene *H. erectus s.l.* We performed multiple shape analyses to evaluate the reconstruction influence (reducing the dataset to the only preserved landmarks and semilandmarks taken on the original fragments) and compare Kocabaş to the OH9 specimen. Different plots of the first two components resulting from these analyses can be found in the extended Paper (Appendix III). Results overall: i) confirm the relative similarities of Kocabaş to other MPH; ii) comparison to OH9 show similar supraorbital morphology (high PC2 score) but quite different temporal line morphology (flatter for OH9 and with a more evident postorbital constriction).

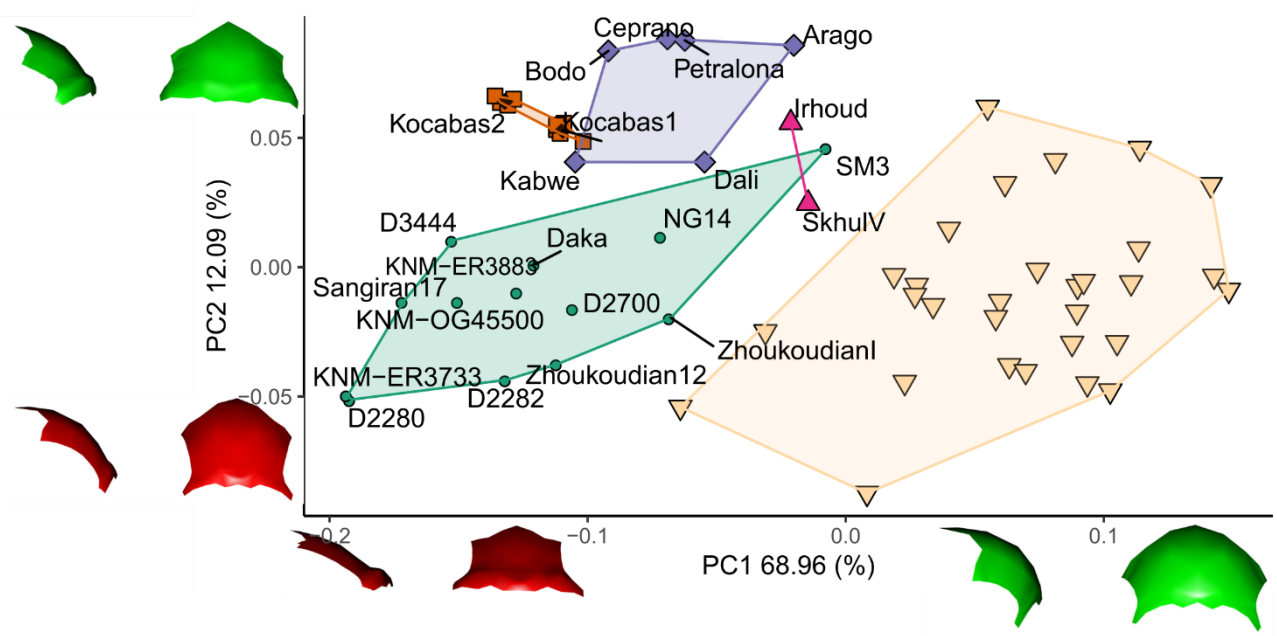

Figure 6. PCA plot of fossil specimens and recent modern humans. Convex hulls based on group attribution from Table 2. Symbols: yellow triangle = modern humans, green circle = *H. erectus s.l.*, purple diamond = Middle-Pleistocene *Homo,* pink triangle = early *H. sapiens*, brown square = Kocabaş reconstructions (black diamond = mean configuration of each reconstruction). Surface shape transformations along +/-2 std. dev. from mean along PC axes are shown below (PC1) and on the plot's left side (PC2).

A phenogram using the UPGMA cluster analysis based on the pairwise Procrustes distance matrix between the fossil specimens was generated (Figure 7). This analysis evaluates overall morphological similarities between specimens. Instead of the multiple reconstructions, Kocabaş mean landmarks configuration was used to calculate the pairwise Procrustes distance to the other fossils. Kocabaş's mean configuration closest specimen is Bodo and clusters together with the other MPH European specimens. Also, the linear discriminant analysis based on the first four PCs classified all the reconstructions made as MPH, not *H. erectus s.l.*

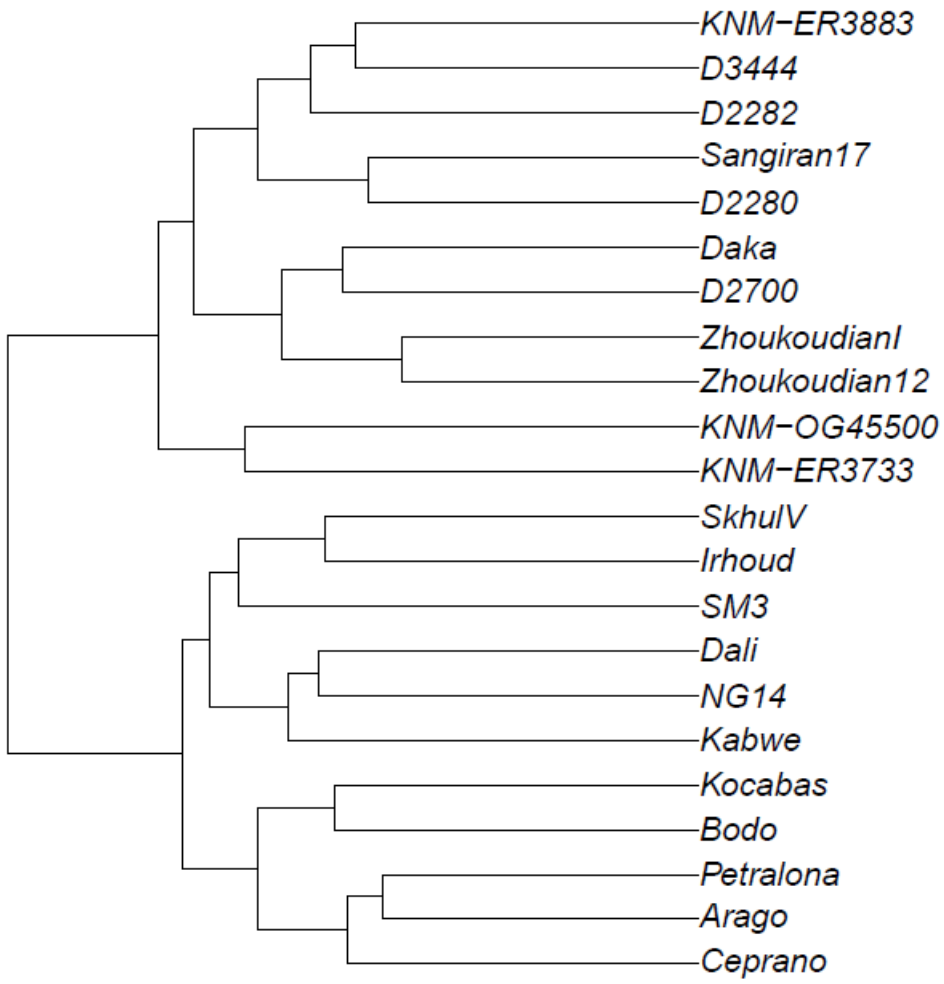

Figure 7. UPGMA cluster analysis based on pairwise Procrustes distances between individuals.

These results indicate that Kocabaş is more similar to the MPH specimens than *H. erectus s.l.*. Such results disagree with previous works [73, 75-78], which concluded that Kocabaş was a representative of *H. erectus s.l.* with closer affinities to the Daka, Buia, and KNM-OG 45500 specimens [78]. In this context, the taxonomic attribution of Kocabaş remains an open question, given the debate regarding the taxonomic definition of MPH [49, 102-105]. In any case, Kocabaş exhibits a frontal morphology similar to Bodo, so it is more reasonable considering Kocabaş as a member of the same taxonomic unit as Bodo. Discussion regarding the phylogenetic relation between Kocabaş and Bodo taxonomic unit is tight to the chronology of Kocabaş. Unfortunately, Kocabaş datation has been a difficult task. The first dating placed it around 400Ka BP (U-Th analysis) and 500 Ka BP (thermoluminescence method) [73, 106]; a date of 1.1 Ma was proposed based on ESR technique [107]. The last dating based on paleomagnetic and cosmogenic nucleotide

studies gave an age around 1 to 1.5 Ma BP [74]. All these different results, together with the history of the discovery of this specimen, led Muttoni and colleagues to not consider the hominin partial calotte as a well-dated specimen [108]. For these reasons, depending on the exact age of Kocabaş, there are different hypotheses regarding its phylogenetic relation:

1) If the oldest age is confirmed, then Kocabaş could represent the earliest representative of the same taxon of Bodo, as it presents morphology consistent with but less derived than later specimens already assigned to this group.

2) If the age is younger than 1 Ma and closer to precedent chronology (ca 500Ka BP), Kocabaş could belong to the same taxonomic unit of Bodo, representing a Eurasian paleodeme.

4 Concluding remarks

Geometric morphometric and virtual anthropology were confirmed as suitable tools for analyzing and comparing paleoanthropological remains. Geometric morphometric approaches allowed for quantifying and visualizing complex patterns (i.e., ontogenetic trajectories) and complex morphology (i.e., frontal squama and supraorbital torus). The fossil reconstruction provided a deeper understanding of KNM-OG 45500 and Kocabaş, allowing for a more thorough comparative study of these specimens with other fossil remains. The new reconstruction, moreover, can be made available to other scientists to perform future analyses and comparisons.

The different works made during my Ph.D. provide new information regarding specific fossils. Specifically, we concluded that:

- KNM-ER 42700 is most probably a young adult individual;
- KNM-OG 45500 is among the smallest *H. erectus s.l.* at this chronology, with a quite archaic frontal morphology;
- Kocabaş does not fit into the variation of *H. erectus s.l.* but shows morphological similarities with Bodo and other MPH.

Before these detailed and comprehensive analyses, these fossils were considered *H. erectus s.l.* The picture drawn by these results seems to complicate the scenario. First, the ontogenetic analysis confirmed KNM-ER 42700 enigmatic taxonomic status. Based on these results, it is more probable that KNM-ER 42700 is a young adult than a juvenile specimen. Recently Baab et al. [109] tested ontogenetic trajectories of the neurocranium to address the ontogenetic status of KNM-ER 42700. They concluded that KNM-ER 42700 might be a juvenile *H. erectus s.l.* however, in their opinion, it could also represent a young adult individual leaving the question still open to debate.

KNM-OG 45500 shows a frontal morphology close to African *H. erectus/ergaster*; these results also show this fossil's many archaic features, from its morphology to its overall small size. We confirm previous works regarding its taxonomic attribution, but the frontal analysis showed temporal differences in the *H. erectus s.l.* group. Such differences can be related to the high geographic and temporal variability of the sample, but it could be possible that these differences are linked to taxonomic diversity.

Kocabaş's results are difficult to contextualize, given the uncertainty of its chronological age. However, the shape analysis indicates morphological affinities with MPH,

specifically Bodo. For this reason, it is important in future analyses and discussions to consider its morphology as not part of *Homo erectus s.l.* variability.

Overall, my Ph.D. project added to current knowledge regarding *H. erectus s.l.* in different ways. Frontal morphology changes over time in the *H. erectus* sample, as seen in this cumulative dissertation's second and third work. Such shape change in time seems to be related to anagenetic evolution in *H. erectus s.l.* [91]. Our results support this hypothesis, but KNM-OG 45500 does not follow the expected trend in shape and size given its geological age. Another small-sized specimen is KNM-ER 42700, but in this case, its chronology does not make it an outlier in terms of expected size vs. actual size. KNM-ER 42700 interpretation of a young adult, in my opinion, exclude such specimens from the *H. erectus s.l.* hypodigm. At the moment, it is difficult to place KNM-ER 42700 as a member of other species; therefore, I agree with the original proposal made by Baab to place it in *H. sp.* [61]. Kocabaş needs further clarification of its chronology. As recently happened for the dating of member four at Sterkfontein [110], changing chronology affects the evolutionary and phylogenetic inference that scientists can make. However, as written above, Kocabaş morphology should not be considered part of *H. erectus s.l.* variability. *H. erectus s.l.* is confirmed to be a highly variable and widespread taxon, but this thesis confirms that it is essential to study incomplete specimens to avoid exaggerating the taxon's variability. Framing the correct evolutionary hypothesis relies upon a correct taxonomic attribution of different specimens. New fossils or new studies using new technologies on old findings can help draw more precise evolutionary inferences that can help us understand the natural history of our lineage.

Future directions

The presented cumulative dissertation, as with every scientific research, opens up new questions that underline the future direction of study. Regarding KNM-ER 42700, further effort must be made to study ontogenetic trajectories of extinct taxa to have a clearer picture of the impact of different ontogenetic stages on specific shapes.

KNM-OG 45500's associated temporal bone is another source of information that need to be considered and analyzed to confirm results obtained from the frontal bone analysis. In this regard, an alignment of the temporal bone to the frontal bone could lead to a more accurate estimate of the endocranial volume to better evaluate the size difference between this specimen and other pene-contemporaneous fossils.

The analysis made on Kocabaş required a more solid chronological framework. The uncertainty regarding its original stratigraphic location made it difficult to place it in a solid chronological setting. It could probably be helpful to try directly dating this specimen in the future.

The final remark regards the frontal bone analysis itself. The comparison between fossils and modern humans highlighted trends and similarities that need further attention. Among the exciting aspects highlighted, future research should focus on Late Pleistocene Asian specimens (such as SM3) to better investigate its derived frontal morphology.

References

1. von Koenigswald, G. and F. Weidenreich, *The relationship between Pithecanthropus and Sinanthropus.* Nature, 1939. **144**.
2. Weidenreich, F., *Some problems dealing with ancient man.* American Anthropologist, 1940. **42**(3): p. 375-383.
3. Mayr, E. *Taxonomic categories in fossil hominids*. in *Cold Spring Harbor Symposia on Quantitative Biology*. 1950. Cold Spring Harbor Laboratory Press.
4. Simonetta, A., *Catalogo e sinonimia annotata degli ominoidi fossili ed attuali (1758–1955).* Atti Soc. Toscana Sci. Nat., Pisa, Ser. B, 1957. **64**: p. 53-113.
5. Robinson, J.T., *The australopithecines and their bearing on the origin of man and of stone tool-making.* South African Journal of Science, 1961. **57**: p. 3-16.
6. Brown, F., et al., *Early Homo erectus skeleton from west lake Turkana, Kenya.* Nature, 1985. **316**(6031): p. 788-792.
7. Leakey, L.S., *New finds at Olduvai gorge.* Nature, 1961. **189**(4765): p. 649-650.
8. Leakey, R. and A.C. Walker, *Further hominids from the Plio-Pleistocene of Koobi Fora, Kenya.* American Journal of Physical Anthropology, 1985. **67**(2): p. 135-163.
9. Leakey, R.E., *New hominid fossils from the Koobi Fora formation in northern Kenya.* Nature, 1976. **261**(5561): p. 574-576.
10. Walker, A. and R.E. Leakey, *The hominids of east Turkana.* Scientific American, 1978. **239**(2): p. 54-67.
11. Antón, S.C., *Natural history of Homo erectus.* American Journal of Physical Anthropology, 2003. **122**(37): p. 126-170.
12. Baab, K.L., *The taxonomic implications of cranial shape variation in Homo erectus.* Journal of Human Evolution, 2008. **54**(6): p. 827-847.
13. Harrison, T., *Cladistic concepts and the species problem in hominoid evolution*, in *Species, species concepts and primate evolution*. 1993, Springer. p. 345-371.
14. Howell, F., *Evolution of African mammals.* Maglio VJ and Cooke HBS (eds), 1978: p. 154-248.
15. Howells, W.W., *Homo erectus—who, when and where: a survey.* American Journal of Physical Anthropology, 1980. **23**(S1): p. 1-23.
16. Rightmire, G.P., *Comparisons of Homo erectus from Africa and southeast Asia.* Courier Forschungsinstitut Senckenberg, 1984. **69**: p. 83-98.
17. Rightmire, G.P., *Species recognition and Homo erectus.* Journal of human evolution, 1986. **15**(8): p. 823-826.
18. Rightmire, G.P., *The Evolution of Homo Erectus: Comparative Anatomical Studies of an Extinct Human Species*. 1990, Cambridge: Cambridge University Press.
19. Rightmire, G.P., *Evidence from facial morphology for similarity of Asian and African representatives of Hhomo erectus.* American Journal of Physical Anthropology: The Official Publication of the American Association of Physical Anthropologists, 1998. **106**(1): p. 61-85.
20. Rightmire, G.P., D. Lordkipanidze, and A. Vekua, *Anatomical descriptions, comparative studies and evolutionary significance of the hominin skulls from Dmanisi, Republic of Georgia.* Journal of Human Evolution, 2006. **50**(2): p. 115-141.
21. Rightmire, G.P., A. Margvelashvili, and D. Lordkipanidze, *Variation among the Dmanisi hominins: Multiple taxa or one species?* American journal of physical anthropology, 2019. **168**(3): p. 481-495.

22. Andrews, P., *An alternative interpretation of the charac ters used to define Homo erectus. The Early Evolution of Man with Special Emphasis on Southeast Asia and Africa.* Cour. Forsch. Inst. Senckenberg, Frankfurt am Main, 1984. **69**: p. 167-175.
23. Stringer, C.B., *The definition of Homo erectus and the existence of the species in Africa and Europe.* Cour. Forsch. Inst. Senckenberg, Frankfurt am Main, 1984. **69**: p. 131-143.
24. Tattersall, I., *Species recognition in human paleontology.* Journal of Human Evolution, 1986. **15**(3): p. 165-175.
25. Wood, B., *Koobi Fora research project: Hominid cranial remains*. Vol. 4. 1991: Oxford University Press, USA.
26. Wood, B.A., *The origin of Homo erectus.* Cour. Forsch. Inst. Senckenberg, 1984. **69**: p. 99-111.
27. Wood, B., *Taxonomy and evolutionary relationships of Homo erectus.* Courier Forschungsinstitut Senckenberg, 1994. **171**: p. 159-165.
28. Wood, B., *Origin and evolution of the genus Homo.* Nature, 1992. **355**(6363): p. 783.
29. de Lumley, M.-A., et al., *Les restes humains du Pliocène final et du début du Pléistocène inférieur de Dmanissi, Géorgie (1991–2000). I–Les crânes, D 2280, D 2282, D 2700.* L'anthropologie, 2006. **110**(1): p. 1-110.
30. Gabounia, L., et al., *Découverte d'un nouvel hominidé à Dmanissi (Transcaucasie, Géorgie).* Comptes Rendus Palevol, 2002. **1**(4): p. 243-253.
31. Martinón-Torres, M., et al., *Dental remains from Dmanisi (Republic of Georgia): morphological analysis and comparative study.* Journal of Human Evolution, 2008. **55**(2): p. 249-273.
32. Tattersall, I., *Species concepts and species identification in human evolution.* Journal of Human Evolution, 1992. **22**(4-5): p. 341-349.
33. Schwartz, J. and I. Tattersall, *The human fossil record. Volume two. Craniodental morphology of genus Homo (Africa, Asia).* 2003, New York: Wiley.
34. Schwartz, J.H. and I. Tattersall, *The Human Fossil Record. Vol. 4: Craniodental Morphology of Early Hominids (Genera, Australopithecus, Paranthropus, Orrorin), and Overview*. 2005: NJ: John Wiley & Sons.
35. Harvati, K., et al., *Apidima Cave fossils provide earliest evidence of Homo sapiens in Eurasia.* Nature, 2019. **571**(7766): p. 500-504.
36. Bookstein, F.L., *Principal warps: Thin-plate splines and the decomposition of deformations.* IEEE Transactions on pattern analysis and machine intelligence, 1989. **11**(6): p. 567-585.
37. Bookstein, F.L., *Morphometric tools for landmark data: geometry and biology.* 1991, Cambridge: Cambridge University Press. 435.
38. Bookstein, F.L., *Morphometric tools for landmark data: geometry and biology*. 1997: Cambridge University Press.
39. Mitteroecker, P. and P. Gunz, *Advances in Geometric Morphometrics.* Evolutionary Biology, 2009. **36**(2): p. 235-247.
40. Rohlf, F.J. and D. Slice, *Extensions of the Procrustes Method for the Optimal Superimposition of Landmarks.* Systematic Biology, 1990. **39**(1): p. 40-59.
41. Adams, D.C. and M.L. Collyer, *A general framework for the analysis of phenotypic trajectories in evolutionary studies.* Evolution, 2009. **63**(5): p. 1143-1154.
42. Athreya, S., *The frontal bone in the genus Homo: a survey of functional and phylogenetic sources of variation.* J. Anthropol. Sci., 2012. **90**: p. 1-22.
43. Baab, K.L., *Defining Homo erectus*, in *Handbook of paleoanthropology*, W. Henke and I. Tattersall, Editors. 2015, Springer: Berlin, Heidelberg. p. 2189-2219.

44. Bastir, M., A. Rosas, and P. O'Higgins, *Craniofacial levels and the morphological maturation of the human skull.* Journal of Anatomy, 2006. **209**(5): p. 637-654.
45. Gunz, P., P. Mitteroecker, and F.L. Bookstein, *Semilandmarks in three dimensions*, in *Modern morphometrics in physical anthropology*, D.E. Slice, Editor. 2005, Springer: Boston, MA. p. 73-98.
46. Gunz, P., et al., *Neandertal introgression sheds light on modern human endocranial globularity.* Current Biology, 2019. **29**(1): p. 120-127. e5.
47. Neubauer, S., P. Gunz, and J.-J. Hublin, *Endocranial shape changes during growth in chimpanzees and humans: A morphometric analysis of unique and shared aspects.* Journal of Human Evolution, 2010. **59**(5): p. 555-566.
48. O'HIGGINS, P., *The study of morphological variation in the hominid fossil record: biology, landmarks and geometry.* The Journal of Anatomy, 2000. **197**(1): p. 103-120.
49. Profico, A., et al., *Filling the gap. Human cranial remains from Gombore II (Melka Kunture, Ethiopia; ca. 850 ka) and the origin of Homo heidelbergensis.* J. Anthropol. Sci., 2016. **94**: p. 1-24.
50. Reyes-Centeno, H., et al., *Genomic and cranial phenotype data support multiple modern human dispersals from Africa and a southern route into Asia.* Proceedings of the National Academy of Sciences of the United States of America, 2014. **111**(20): p. 7248-7253.
51. Smith, H.F., et al., *A 3-D geometric morphometric study of intraspecific variation in the ontogeny of the temporal bone in modern Homo sapiens.* Journal of Human Evolution, 2013. **65**(5): p. 479-489.
52. Bräuer, G., *The origin of modern anatomy: By speciation or intraspecific evolution?* Evolutionary Anthropology: Issues, News, and Reviews, 2008. **17**(1): p. 22-37.
53. Gunz, P., et al., *Principles for the virtual reconstruction of hominin crania.* Journal of Human Evolution, 2009. **57**(1): p. 48-62.
54. Weber, G.W., *Virtual anthropology.* American Journal of Physical Anthropology, 2015. **156**: p. 22-42.
55. Weber, G.W. and F.L. Bookstein, *Virtual anthropology: a guide to a new interdisciplinary field*. 2011, Wien, Austria: SpringerWienNewYork.
56. Aytek, A.İ. and K. Harvati, *The human fossil record from Turkey*, in *Paleoanthropology of the Balkans and Anatolia*, K. Harvati and M. Roksandic, Editors. 2016, Springer: Dordrecht. p. 79-91.
57. Baab, K.L., *A re-evaluation of the taxonomic affinities of the early Homo cranium KNM-ER 42700.* Journal of human evolution, 2008. **55**(4): p. 741-6.
58. Spoor, F., et al., *Implications of new early Homo fossils from Ileret, east of Lake Turkana, Kenya.* Nature, 2007. **448**: p. 688.
59. Spoor, F., et al., *The taxonomic status of KNM-ER 42700: A reply to Baab (2008a).* Journal of human evolution, 2008. **55**(4): p. 747-750.
60. Bauer, C.C. and K. Harvati, *A virtual reconstruction and comparative analysis of the KNM-ER 42700 cranium.* Anthropologischer Anzeiger, 2015. **72**(2): p. 129-140.
61. Baab, K.L., *The role of neurocranial shape in defining the boundaries of an expanded Homo erectus hypodigm.* Journal of Human Evolution, 2016. **92**: p. 1-21.
62. Neubauer, S., et al., *Reconstruction, endocranial form and taxonomic affinity of the early Homo calvaria KNM-ER 42700.* Journal of Human Evolution, 2018.
63. Lieberman, D.E., *The evolution of the human head*. 2011: The belknap press of Harvard university press.
64. Antón, S.C., *Cranial growth in Homo erectus: how credible are the Ngandong juveniles?* American Journal of Physical Anthropology, 1999. **108**(2): p. 223-236.

65. Dean, C. and H.M. Liversidge, *Age estimation in fossil hominins: comparing dental development in early Homo with modern humans.* Annals of Human Biology, 2015. **42**(4): p. 415-429.
66. Robson, S.L. and B. Wood, *Hominin life history: reconstruction and evolution.* Journal of Anatomy, 2008. **212**(4): p. 394-425.
67. Smith, B.H., *Dental development as measure of life history in primates.* Evolution, 1989. **43**(3): p. 683-688.
68. Smith, S.L., *Skeletal age, dental age, and the maturation of KNM-WT 15000.* American Journal of Physical Anthropology, 2004. **125**(2): p. 105-120.
69. Gower, J.C., *Generalized procrustes analysis.* Psychometrika, 1975. **40**(1): p. 33-51.
70. Potts, R., et al., *Small Mid-Pleistocene Hominin Associated with East African Acheulean Technology.* Science, 2004. **305**(5680): p. 75-78.
71. Rightmire, G.P., *Cranial remains of Homo erectus from Beds II and IV, Olduvai Gorge, Tanzania.* American Journal of Physical Anthropology, 1979. **51**(1): p. 99-115.
72. Tamrat, E., et al., *Revised magnetostratigraphy of the Plio-Pleistocene sedimentary sequence of the Olduvai Formation (Tanzania).* Palaeogeography, Palaeoclimatology, Palaeoecology, 1995. **114**(2-4): p. 273-283.
73. Kappelman, J., et al., *First Homo erectus from Turkey and implications for migrations into temperate Eurasia.* American Journal of Physical Anthropology, 2008. **135**(1): p. 110-116.
74. Lebatard, A.-E., et al., *Dating the Homo erectus bearing travertine from Kocabaş (Denizli, Turkey) at at least 1.1 Ma.* Earth and Planetary Science Letters, 2014. **390**: p. 8-18.
75. Vialet, A., G. Guipert, and M. Cihat Alçiçek, *Homo erectus found still further west: Reconstruction of the Kocabaş cranium (Denizli, Turkey).* Comptes Rendus Palevol, 2012. **11**(2): p. 89-95.
76. Guipert, G., A. Vialet, and M.C. Alcicek. *The Homo erectus from Kocabaş in Turkey and the first settlements in Eurasia*. in *American Journal of Physical Anthropology*. 2011. WILEY-BLACKWELL 111 RIVER ST, HOBOKEN 07030-5774, NJ USA.
77. Vialet, A., et al., *La calotte crânienne de l'Homo erectus de Kocabaş (Bassin de Denizli, Turquie).* L'Anthropologie, 2014. **118**(1): p. 74-107.
78. Vialet, A., et al., *The Kocabaş hominin (Denizli Basin, Turkey) at the crossroads of Eurasia: New insights from morphometric and cladistic analyses.* Comptes Rendus Palevol, 2018. **17**(1): p. 17-32.
79. Adams, D.C., E. Otárola-Castillo, and E. Paradis, *geomorph: an r package for the collection and analysis of geometric morphometric shape data.* Methods in Ecology and Evolution, 2013. **4**(4): p. 393-399.
80. Collyer, M.L. and D.C. Adams, *Analysis of two-state multivariate phenotypic change in ecological studies.* Ecology, 2007. **88**(3): p. 683-692.
81. Collyer, M.L. and D.C. Adams, *Phenotypic trajectory analysis: comparison of shape change patterns in evolution and ecology.* Hystrix, the Italian Journal of Mammalogy, 2013. **24**(1): p. 75-83.
82. Antón, S.C., *Developmental age and taxonomic affinity of the Mojokerto child, Java, Indonesia.* American Journal of Physical Anthropology, 1997. **102**(4): p. 497-514.
83. Balzeau, A., D. Grimaud-Hervé, and T. Jacob, *Internal cranial features of the Mojokerto child fossil (East Java, Indonesia).* Journal of Human Evolution, 2005. **48**(6): p. 535-553.
84. Gilbert, W.H. and B. Asfaw, *Homo erectus: Pleistocene Evidence from the Middle Awash, Ethiopia*. Vol. 1. 2008, Berkeley and Los Angeles, California: University of California Press.
85. Bruner, E., et al., *The endocast of the one-million-year-old human cranium from Buia (UA 31), Danakil Eritrea.* American journal of physical anthropology, 2016. **160**(3): p. 458-468.

86. Antón, S.C., *Defining Homo erectus: size considered.* Handbook of paleoanthropology, 2007. **3**: p. Chapter 11.
87. Lordkipanidze, D., et al., *A Complete Skull from Dmanisi, Georgia, and the Evolutionary Biology of Early Homo.* Science, 2013. **342**(6156): p. 326-331.
88. Plavcan, J.M., *Body size, size variation, and sexual size dimorphism in early Homo.* Current Anthropology, 2012. **53**(S6): p. S409-S423.
89. Rightmire, G.P., *Brain size and encephalization in early to mid-Pleistocene Homo.* American Journal of Physical Anthropology: The Official Publication of the American Association of Physical Anthropologists, 2004. **124**(2): p. 109-123.
90. Rightmire, G.P., *Homo erectus and Middle Pleistocene hominins: brain size, skull form, and species recognition.* Journal of human evolution, 2013. **65**(3): p. 223-252.
91. Baab, K.L., et al., *Reconstruction and analysis of the DAN5/P1 and BSN12/P1 Gona Early Pleistocene Homo fossils.* Journal of Human Evolution, 2022. **162**: p. 103102.
92. Howell, F.C., *Paleo-Demes, Species Clades, and Extinctions in the Pleistocene Hominin Record.* Journal of Anthropological Research, 1999. **55**(2): p. 191-243.
93. Delson, E., et al., *The Sambungmacan 3 Homo erectus calvaria: a comparative morphometric and morphological analysis.* The Anatomical Record: An Official Publication of the American Association of Anatomists, 2001. **262**(4): p. 380-397.
94. Openoorth, W., *Homo (Javanthropus) soloensis, een pleistoceene mensch van Java.* Wetesch Mededee. Dienst Mijnbauw Nederl Indie, 1932. **20**: p. 49-74.
95. Schwartz, J.H. and I. Tattersall, *Defining the genus Homo.* Science, 2015. **349**(6251): p. 931-932.
96. Tattersall, I., *Homo ergaster and Its Contemporaries*, in *Handbook of Paleoanthropology*, W. Henke and I. Tattersall, Editors. 2015, Springer Berlin Heidelberg: Berlin, Heidelberg. p. 2167-2187.
97. Weidenreich, F., *Morphology of Solo man.* Anthropological Paper of the American Museum of Natural History, 1951. **43**(3): p. 205-290.
98. Widianto, H. and V. Zeitoun, *Morphological description, biometry and phylogenetic position of the skull of Ngawi 1 (east Java, Indonesia).* International Journal of Osteoarchaeology, 2003. **13**(6): p. 339-351.
99. Wolpoff, M.H., et al., *The case for sinking Homo erectus: 100 years of Pithecanthropus is enough.* Courier Forschungsinstitut Senckenberg, 1994. **171**: p. 341-361.
100. Zeitoun, V., et al., *Solo man in question: Convergent views to split Indonesian Homo erectus in two categories.* Quaternary International, 2010. **223-224**: p. 281-292.
101. Antón, S.C., R. Potts, and L.C. Aiello, *Evolution of early Homo: An integrated biological perspective.* Science, 2014. **345**(6192): p. 1236828.
102. Delson, E. and C. Stringer, *The naming of Homo bodoensis by Roksandic and colleagues does not resolve issues surrounding Middle Pleistocene human evolution.* Evolutionary Anthropology: Issues, News, and Reviews, 2022. **n/a**(n/a).
103. Rightmire, G.P., *Homo in the Middle Pleistocene: Hypodigms, variation, and species recognition.* Evolutionary Anthropology: Issues, News, and Reviews: Issues, News, and Reviews, 2008. **17**(1): p. 8-21.
104. Roksandic, M., P. Radović, and J. Lindal, *Revising the hypodigm of Homo heidelbergensis: A view from the Eastern Mediterranean.* Quaternary International, 2018. **466**: p. 66-81.
105. Roksandic, M., et al., *Resolving the "muddle in the middle": The case for Homo bodoensis sp. nov.* Evolutionary Anthropology: Issues, News, and Reviews, 2022. **31**(1): p. 20-29.
106. Altunel, E., *Pamukkale travertenlerinin morfolojik özellikleri, yaşları ve neotektonik önemleri.* MTA dergisi, 1996. **118**: p. 47-64.

107. Engin, B., O. Güven, and F. Köksal, *Electron spin resonance age determination of a travertine sample from the southwestern part of Turkey.* Applied Radiation and Isotopes, 1999. **51**(6): p. 689-699.
108. Muttoni, G., G. Scardia, and D.V. Kent, *Early hominins in Europe: The Galerian migration hypothesis.* Quaternary Science Reviews, 2018. **180**: p. 1-29.
109. Baab, K.L., et al., *Assessing the status of the KNM-ER 42700 fossil using Homo erectus neurocranial development.* Journal of Human Evolution, 2021. **154**: p. 102980.
110. Granger, D.E., et al., *Cosmogenic nuclide dating of Australopithecus at Sterkfontein, South Africa.* Proceedings of the National Academy of Sciences, 2022. **119**(27): p. e2123516119.

Appendix I

This is the proof version of the original article:

Mori T, Harvati K. Basicranial ontogeny comparison in *Pan troglodytes* and *Homo sapiens* and its use for developmental stage definition of KNM-ER 42700. *Am J Phys Anthropol*. 2019;170:579-594. https://doi.org/10. 1002/ajpa.23926

Basicranial ontogeny comparison in *Pan troglodytes* and *Homo sapiens* and its use for developmental stage definition of KNM-ER 42700

Tommaso Mori[1], Katerina Harvati[1,2]

[1] Palaeoanthropology, Senckenberg Centre for Human Evolution and Palaeoenvironment, Eberhard Karls Universität Tübingen, Rümelinstrasse 23, 72070, Tübingen, Germany.

[2] DFG Centre for Advanced Studies "Words, Bones, Genes, Tools: Tracking linguistic, cultural and biological trajectories of the human past", Eberhard Karls Universität Tübingen, Rümelinstrasse 23, 72070, Tübingen, Germany.

Keywords: ontogeny, *Homo erectus*, geometric morphometric, growth and development, human evolution.

Corresponding author: Tommaso Mori, Palaeoanthropology, Senckenberg Centre for Human Evolution and Palaeoenvironment, Eberhard Karls Universität Tübingen, Rümelinstrasse 23, 72070, Tübingen, Germany.

E-mail: tommaso.mori@ifu.uni-tuebingen.de

ABSTRACT:

Objective: This study aims to develop a comparative basis for assessing the developmental stage of KNM-ER 42700 based on the ontogenetic pattern of the ectocranial surface of the basicranium in modern humans and chimpanzees.

Materials and methods: A total of 33 landmarks were collected from an ontogenetic sample of modern humans (80), chimpanzees (51), and twelve individuals classified as *Homo erectus s.l.* Ontogenetic trajectories were analyzed, and common aspects were extracted for the purpose of discriminating age groups. A regression of size on the extracted shape variables was used to investigate common ontogenetic allometry.

Results: The basicranial development of chimpanzees and humans follows different trajectories; however, similarities are also present. The common shape component of development extracted can be used to define age groups in both chimpanzees and modern humans. The extracted shape component presents a similar ontogenetic and static-allometric pattern in these two species. The developmental stages of *Homo erectus s.l.* specimens were attributed following these common

traits. Our analysis correctly assigned developmental stages to those specimens of Homo erectus for which developmental ages are known.

Discussion: The component used for assessing the developmental stage has an ontogenetic allometric component. However, this shape component can discriminate age group irrespective of size and is no longer related to size when static allometry is considered. Adult *H. erectus s.l.* specimens were attributed to the adult category. KNM-WT 15000 fell with the late juvenile age group, whereas D2700 plotted in the region of overlap between the juvenile and adult age groups and Mojokerto with the younger age groups, as predicted by their known developmental ages. KNM-ER 42700 fell within the adult variability despite its incompletely fused spheno-occipital synchondrosis.

INTRODUCTION:

Homo erectus sensu lato (s.l). is the earliest fossil human species that shows modern human body proportions, an increase of brain size, as well as various other derived features (Baab, 2008, 2016; Rightmire, 1990; Schwartz, 2004). Its vast time range and geographic distribution have been linked with its observed high morphological variability (Antón, 2003; Baab, 2015; Lordkipanidze et al., 2013; Rightmire, 1990; Rightmire, Lordkipanidze, & Vekua, 2006; F. Spoor et al., 2007). This variability, however, has also been interpreted in terms of taxonomic diversity, with some authors proposing the presence of more species (Andrews, 1984; Schwartz, 2004; Stringer, 1984). Understanding the factors that affect this variation, including geography, time, sexual dimorphism and developmental changes, is therefore imperative for the interpretation of the *Homo erectus s.l.* hypodigm.

A case in point is the specimen KNM-ER 42700, described by Spoor et al. (2007) as an exceptionally small *H. erectus s.l.* individual. KNM-ER 42700 is a small neurocranium recovered from the Koobi Fora Formation, with an estimated geological age of 1.55 million years. Spoor and colleagues (Spoor et al. 2007) assigned it to *H. erectus s.l.* due to the presence of features considered typical for this taxon (i.e., frontal and parietal keeling, mediolaterally narrow temporomandibular joint, distinct coronal and sagittal orientation of the tympanic and petrous elements, and a posterior midsagittal profile with a low occipital upper scale and opisthocranion positioned close to lambda). A multivariate analysis of calvaria dimensions showed that the specimen fell within *H. erectus s.l.* variability. This conclusion, however, was disputed on the basis of a 3D geometric morphometrics (GM) analysis of its overall cranial shape by Baab (2008). Baab (2008) found that the specimen's cranial shape fell outside the range of variation of *H. erectus s.l.*, suggesting shape similarities with later *Homo*. She proposed that the cranium might represent a yet unrecognized *Homo* taxon. In response, Spoor et al. (2008) suggested that the specimen's unusual shape was due to the (minor)

taphonomic distortion of its frontal bone and/or to its not fully adult status. Virtual reconstruction of the specimen correcting the taphonomic damage did not significantly alter its shape or the results of the comparative shape analysis (Bauer and Harvati 2015), leaving ontogeny as the only potential factor behind the unusual cranial shape of this specimen.

Recently, Baab (2016) attempted to evaluate the cranial morphology of *H erectus s.l.* as a whole. In her shape analysis, she could identify a shared morphology between specimens from Asia, Georgia and East Africa. KNM-ER 42700, however, showed a distinct morphology that was unique and not presents even in subadult specimens such as KNM-WT 15000 and D2700 (Baab, 2016). Furthermore, Neubauer et al. (2018) presented a new reconstruction and GM analysis of KNM-ER 42700 endocranial shape to understand its taxonomic affinities. Their study showed that this specimen differs in its endocranial morphology from other *H. erectus s.l.* specimens and the authors hypothesized that it is a young individual who had not yet reached adult endocranial morphology (Neubauer et al. 2018). Neubauer et al. (2018) proposed a probable age for the KNM-ER 42700 individual between Mojokerto and KNM-WT 15000. Several different ages at death have been proposed for Mojokerto, ranging from 0 to 8 years (Antón, 1997; Balzeau, Grimaud-Hervé, & Jacob, 2005; Coqueugniot, Hublin, Veillon, Houët, & Jacob, 2004; O'Connell & DeSilva, 2013). A computed tomography-based analysis of this specimen showed that the anterior fontanelle had not yet closed, suggesting an age at death at between 0.5 and 1.5 years (Coqueugniot et al., 2004). KNM-WT 15000 is an early adolescent, with an age estimation spanning from 10 to 14 years (Dean & Smith, 2009; S. L. Smith, 2004). Therefore, following the hypothesis by Neubauer et al. (2018) of incomplete brain growth in KNM-ER 42700, this specimen should also be quite young. *H. erectus s.l.* seems to follow a different pattern of brain growth from that of modern humans, being intermediate between modern humans and chimpanzees (O'Connell & DeSilva, 2013). A not fully-grown brain in KNM-ER 42700 would therefore indicate a possible age between 3 and 7 years, since 95% of brain size is already attained in chimpanzees between 3-4 postnatal years and in humans between 6-7 years (Lieberman, 2011).

Since KNM-ER 42700 lacks dentition, its dental age cannot be determined. Suture closure provides the only direct evidence of its developmental stage (Antón, 1999; Rightmire et al., 2006). The spheno-occipital synchondrosis of KNM-ER 42700 is described as two-thirds fused (Neubauer et al., 2018; F. Spoor et al., 2007) whereas the other cranial sutures are completely fused. Such a condition usually indicates either a young adult or a late subadult age in modern humans (Antón, 1999, 2003; Lieberman, 2011). However, the ontogeny of *H. erectus s.l.* and its association/correspondence with modern human sutural closure patterns remains poorly understood (Antón, 2003; Dean & Liversidge, 2015; Robson & Wood, 2008; B. H. Smith, 1989; S. L. Smith,

2004). Moreover, a comparison of sutural closure of KNM-ER 42700 with those of other juvenile *H. erectus s.l.* fossils it is limited by the small number of young specimens known and their preservation status. D2700 is an almost complete cranium exhibiting an open spheno-occipital synchondrosis (Rightmire et al., 2006), whereas KNM-WT 15000 does not preserve this part of the cranium but its dentition is less developed than that of D2700, suggesting a younger age than D2700 (S. L. Smith, 2004). Neubauer and coauthors did not rely on the spheno-occipital synchondrosis as a proxy for the attribution of the ontogenetic stage for KNM-ER 42700 because this suture's fusion time varies greatly among modern humans (Neubauer et al., 2018). In their opinion a premature closure of spheno-occipital synchondrosis due to a pathological condition of KNM-ER 42700 is unlikely but, if present, could interfere with the interpretation of species affinity for this specimen. Therefore, additional research on the ontogenetic changes in *H. erectus s.l.* is needed to clarify the developmental age of the KNM-ER 42700 specimen (Baab, 2008, 2016; Neubauer et al., 2018).

This study aims to perform an ontogenetic assessment of KNM-ER 42700 based on the ectocranial morphology of the basicranium. Basicranial ontogeny has been studied in modern human and chimpanzee individuals using ontogenetic samples (Bastir & Rosas, 2004; Bastir, Rosas, & O'Higgins, 2006; Mitteroecker, Gunz, Bernhard, Schaefer, & Bookstein, 2004; Terhune, Kimbel, & Lockwood, 2013). Due to the absence of an ontogenetic comparative sample in the fossil record of *H. erectus s.l.*, we compare ontogenetic trajectories of extant species and find common traits that can reasonably be considered to be plesiomorphic ontogenetic features, in order to use them as a comparative basis for assessing the developmental stage of KNM-ER 42700. The ectocranial surface shows superstructures which continue to change over development for a longer time compared to the endocranial surface until early adulthood (Balolia, Soligo, & Lockwood, 2013; Neubauer et al., 2018). This gives the possibility to track morphological changes until a later ontogenetic stage than is possible with the endocranium. Furthermore, the basicranium is considered to retain both a phylogenetic and an ontogenetic signal (Bastir & Rosas, 2004; Harvati, 2003; Harvati & Weaver, 2006a, 2006b; Lieberman, McBratney, & Krovitz, 2002; Lieberman, Ross, & Ravosa, 2000; Reyes-Centeno, Ghirotto, & Harvati, 2017; Terhune et al., 2013). Basicranial morphology has previously been used to infer the ontogenetic stage of specific fossil specimens (Antón, 1997; Terhune et al., 2013), while geometric morphometric (GM) analyses have shown that modern humans, great apes and Neanderthals follow a common ontogenetic trajectory in endocranial shape changes after the eruption of the deciduous dentition (Mitteroecker et al., 2004; Neubauer, Gunz, & Hublin, 2009; Scott, Neubauer, Hublin, & Gunz, 2014). These findings suggest the existence of a shared, and presumably ancestral, hominin developmental pathway. Given this previous work, we hypothesize that basicranial ontogeny also retains some plesiomorphic aspects useful for our aim.

Previous works (Adams & Collyer, 2009; Adams, Otárola-Castillo, & Paradis, 2013; Collyer & Adams, 2007; Collyer, Sekora, & Adams, 2014) have shown how to analyze and compare phenotypic trajectories across multiple evolutionary levels. In order to analyze ontogeny, we use the same phenotypic trajectories approach. In our case, as different phenotypic levels, we use dental eruption stages, a reliable proxy for ontogenetic comparison (Simons & Frost, 2016). This approach allows us to investigate non-linear trajectories that most often are difficult to quantify with conventional methods (Adams & Collyer, 2009; Collyer & Adams, 2007, 2013; Gunz, Neubauer, Maureille, & Hublin, 2010; Mitteroecker et al., 2004; Mitteroecker, Gunz, & Bookstein, 2005; Scott et al., 2014).

In this framework, we, therefore, aim to test the following hypotheses. First, that the two extant species (modern humans and chimpanzees) exhibit a common developmental trajectory, which can be used to study the developmental stage of our *H. erectus s.l.* sample. This can be evaluated by analyzing the ontogenetic trajectories in the two extant taxa and comparing shape change during the examined ontogenetic period. Second, KNM-ER 42700 is expected to show a young basicranial shape according to the suggestion made by Neubauer et al. (2018) of a not fully grown brain. This hypothesis will be tested by comparing KNM-ER 42700 with other juvenile *H. erectus s.l.* such as D2700, KNM-WT 15000 and Mojokerto through its position in the common hominin trajectory.

MATERIALS AND METHODS

Our sample of chimpanzees and modern humans consisted of a cross-sectional representation of crania, ranging in age from the eruption of the deciduous teeth to adulthood. The sample used included 80 *Homo sapiens* and 51 *Pan troglodytes.* Both sexes were used for each species, and sex was determined based on the archived museum record. Juvenile individuals with unknown sex attribution were not sexed and are instead labeled as sex unknown (Table 1). The geographic origins and subspecific information of the sample are indicated in Table 2. The human sample comprised part of the anthropological collection of the Florence Natural History Museum and the Tübingen human osteology collection. The chimpanzee sample originated from the Senckenberg (Frankfurt) collection, the Digital Morphology Museum of the Kyoto University Primate Research Institute and the Smithsonian Museum collection. We used both physical crania as well as virtual models to compile our dataset. Virtual 3D models (PLY format) were extracted from medical computed tomography (CT) scans of dried skulls. Definitions of the developmental age groups, following previous ontogenetic studies (Mitteroecker et al., 2004; Neubauer et al., 2009; Terhune et al., 2013), and sample distributions are provided in Table 1. Dental age groups were used for basicranial development proxy instead of size. This facilitated the comparison of individuals at different

ontogenetic stages irrespective of absolute size, which is known to differ between humans and chimpanzees in both the adult values and growth curves (Scott et al., 2014; Simons & Frost, 2016). A detailed description of the chimpanzee and modern human sample with information regarding every individual used here is provided in the excel sheet file as supporting information. The *H. erectus s.l.* sample comprised specimens with relatively complete basicrania. It included medical CT scans (slice thickness=1 mm, slice interval=0.5 and pixel size= 0.25mm) and 3D surface models developed using high resolution casts housed in the Department of Anthropology, American Museum of Natural History, New York, or from original fossils. The fossil sample used in the analysis was composed of 9 fossils for the full landmark configuration and a total of 12, less complete, specimens that were used in a second, reduced, landmark dataset analysis. The list of fossil and developmental stage attribution is reported in Table 3. KNM-ER 42700 is represented twice: once using a high-resolution cast from the University of Tübingen collection (KNM-ER 42700/Or) and a second time using the virtual reconstruction published by Bauer and Harvati (Bauer & Harvati, 2015), which corrected the minor effects of taphonomy on the specimen (KNM-ER 42700/Rec).

Landmark digitization

A total of thirty-three landmarks (Harvati & Weaver, 2006a; von Cramon-Taubadel & Smith, 2012) were registered on the ectocranial surface of the cranial base (see Table 4 and Figure 1 for each landmark's definition and exact position). A microscribe (MicroScribe G2x Digitizing System, Immersion Corp., San José) was used for placing landmarks on the physical crania. Landmarks on the 3D sample were digitized using the software Avizo. All measurements were taken by the same author (T.M.). The landmarks on the fossil sample were registered using both a microscribe (on casts) as well as digitally with the Avizo software (on 3D ply files of original fossils; see Table 2).

Due to the fossils' preservation status (missing or distorted basicranial areas) bilaterally missing points or distorted areas were mirrored and symmetrized from the better-preserved side of the specimens using the reflected relabeling method (Mardia, Bookstein, & Moreton, 2000). Missing landmarks on the sagittal plane were computed using mean substitution based on Procrustes aligned *H. erectus s.l.* specimens with the *Morpheus* et al. (2014) software (which allows for landmark computation based on generalized Procrustes analysis (GPA) mean substitution), followed by rescaling to the original size of the specimens. A list of reconstructed landmarks for each fossil using GPA mean substitution and reflecting relabeling technique is presented in the supporting information Table S1.

We used a subset of the original landmark set in order to be able to include the young but incomplete Mojokerto specimen in the analysis. Given the poor preservation of this specimen, we were able to collect a total of 14 landmarks. We collected landmarks on the right side of this specimen and mirrored them so as to obtain the full dataset. The list of landmarks used is defined in Table 4.

Statistical analysis

The analyses performed were conducted in R (Team, 2013) using the Geomorph package (Adams et al., 2013), as well as the software IBM SPSS (Field, 2013; Norusis, 1993). Both landmark sets were superimposed with generalized Procrustes analysis (GPA) (Gower, 1975; Rohlf & Slice, 1990), in which the sum of squared distances between homologous landmarks is minimized by rotating, translating to the same reference system, and scaling them to the same size. Centroid size was calculated for each individual. The Procrustes coordinates together with centroid size were used for all following statistical analyses (Adams et al., 2013; Bookstein, 1991; Mitteroecker & Gunz, 2009; Rohlf & Slice, 1990; Slice, 2007).

In order to test the repeatability of landmark acquisition, two specimens were digitized 10 times on 10 different days: one chimpanzee (catalog n° SMF-PA 355, Senckenberg collection) and one very young modern human medical CT scan (Florence collection, catalog n° 740). Subsequently, an intra-observer error was evaluated for each landmark based on a relative standard deviation threshold of 5%. Given that the standard deviation of each landmark (among all twenty repetitions) was lower than the threshold, the precision of landmark acquisition was considered acceptable. To test inter-method error (Robinson & Terhune, 2017; Shearer et al., 2017), given the use of microscribe and virtually acquired landmarks in our analysis, we collected landmarks 6 times from the same specimen (Tuebingen collection, catalog n° 1018) virtually and with the microscribe. Pairwise Procrustes distances between repetitions were determined after generalized Procrustes analysis (GPA). Distance distributions were visualized using a boxplot. We generated a boxplot for each method and a boxplot from the two methods merged together. Statistical differences between the distribution of distances were determined via one-way ANOVA between methods and the mixed method as a grouping variable, testing the null hypothesis that mean differences between groups is equal to zero. Different methods did not increase the amount of error in our analysis (results in the support information Figure S1 and Table S2).

Before further analysis, we evaluated whether the basicranial shape was sexually dimorphic in modern humans and chimpanzees. We performed a Procrustes shape ANOVA (Adams et al., 2013) only on the adult group of the two species. Each adult group was Procrustes superimposed separately in order to explore only the specific adult shape space. Shape variables of the two species were used

in the Procrustes ANOVA and sex attribution was used as the grouping factor. No significant differences in basicranial shape were found among sexes (results of Proc. ANOVA in the supporting information Table S3- S4).

The developmental trajectories for *Pan troglodytes* and *Homo sapiens* were computed in R, following the method described by Adams and Collyer (2009; 2007, 2013). This method (Adams & Collyer, 2009; Adams et al., 2013; Collyer & Adams, 2007, 2013; Collyer et al., 2014) allows for a quantitative comparison between two or more trajectories. The first step of the analysis performed a GPA of modern humans and chimpanzees' raw coordinates, then the Procrustes coordinates were used to build specific trajectories. Trajectories were compared in terms of differences in size (MD), direction (angle Θ) and shape ($D_{Shape)}$. Trajectory size expresses the amount of shape change (Procrustes distance) exhibited by a species along its ontogeny; in this case, total trajectory size was measured as the summed lengths of vectors between sequential ontogenetic stages building the trajectory. Differences in size between trajectories describe a difference in the amount of morphological change (i.e. species one change more in shape than species two). Trajectory direction (angle of the trajectory) is described as "the orientation of first principal component (PC1) of the covariance matrix estimated from the trajectory points, standardized by the starting (ancestral) point" (Adams & Collyer 2009, pages 1145-1146). This trait measures the overall difference in angle between the two trajectories. Differences in the angle between trajectories indicate differences in their direction. If the trajectories show no difference in angle (Θ= 0) they are considered to be parallel; otherwise, they are considered to be divergent. When two trajectories are parallel it means that the shape difference between the two species does not change during ontogeny, but it remains the same along the analyzed period. The third component quantified by the analysis is the shape of the trajectory. This attribute is considered only when we want to explore a trajectory that undergoes three or more levels of shape changes. In our case, four levels were used, as we had four ontogenetic stages. The shape of the trajectory can be considered as the pattern of shape variation along the trajectory. Differences between the trajectory's shapes can be quantified as the Euclidean distances (D_{Shape}) between corresponding ontogenetic levels across the two scaled and aligned phenotypic trajectories. In order to quantify differences between trajectory shape, we used a least-square superimposition alignment that is a similar approach to the superimposition step used for landmark analysis in geometric morphometric. The difference in shape between the trajectories indicates whether the two trajectories have a similar "morphology". In our case, this indicated whether the ontogenetic classes appeared along the two trajectories with a similar pattern. In our analysis trajectories were built using the Procrustes mean configuration of each age category of the two species (Adams & Collyer, 2009; Collyer & Adams, 2013). Shape change from the youngest category (category 0) to the oldest

(category 3) passed through intermediate levels (categories 1 and 2). Test statistics on differences between two trajectories in terms of size (overall path length), angle (direction), and shape (pattern of shape variation) were calculated based on 9999 residual randomization permutations.

A principal component analysis (PCA) on the Procrustes coordinates were used to visualize and explore shape changes in our modern humans and chimpanzees' samples. Trajectories were built using the mean shape of each age group in each species. These mean shapes corresponded in the principal component analysis to mean PC scores of each age group, and connecting consecutive age groups allowed us to visualize a projection of the trajectory in the PCA plot. Trajectories were visualized as smoothed curves (B-splines with least-square mean scores of each age group as control points) in Figure 2. This also means that a trajectory can be defined as a multidimensional vector where each PC is one dimension of it. PCA in this way provided the possibility to investigate the two trajectories, to isolate different PCs that built the overall vector, and to visualize shape changes related to this vector (Adams & Collyer, 2009; Collyer & Adams, 2013).

In order to fully investigate each aspect of the ontogenetic shape space, we performed a Kendall tau test (Kendall, 1948) of each PC score's distribution using age groups as ordinal variable and disregarding the taxonomic affiliation. This non-parametric test allows us to find which PCs are correlated to the ordinal variable age group in both species. In order to ascertain that such PCs have a similar ontogenetic pattern, the specific PC vectors that build each ontogenetic trajectory were evaluated for similarity across both species by using a permutation test between different age classes. Such PCs can be used to analyze common developmental traits present in both species because they likely represent plesiomorphic developmental features and were selected for further analysis. It is important to notice, however, that such extracted PC vectors do not represent the full ontogenetic trajectories of modern humans or chimpanzees. Even though these vectors represent only one aspect of the full ontogenetic trajectories of these taxa, they are important for our aim because of their correlation to the ontogenetic progression in both species. Furthermore, to evaluate how species and age categories differ in their basicranial morphology, we explored shape space in which wireframes of our dataset were morphed along the major PC axes to visualize how shape varied along PCs.

Our aim is to find common traits that can be used to infer the developmental stage. For this reason, the PC scores distribution highlighted by the Kendall tau correlation test were used in a permutation test (1000 random permutations) to assess statistical differences between age groups. This allowed us to make pairwise comparisons for every age group for each taxon at both an intra- and an inter-specific level. Differences between groups were considered significant at a 0.05 alpha level. A sequential Bonferroni (Rice, 1989) correction was applied given the multiple tests performed.

A significant p rejects the null hypothesis that the difference between the two groups means is equal to 0.

In order to explore whether these PCs were influenced by centroid size, and therefore allometry, we also performed a linear regression and calculated a Pearson´s correlation coefficient between the logarithm of centroid size (LogCS) and the PC scores (Viðarsdóttir, O'Higgins, & Stringer, 2002) that were correlated to age group in the extant species. We analyzed ontogenetic allometry using the entire sample and static allometry using adults in both species.

We added the fossil sample to the PCA calculated on the covariance matrix of our extant samples by projecting each individual on the original PC axes. We chose to project our fossil sample in order to not influence the ontogenetic nature of the original PCA, as our aim was to infer the developmental stage based on this comparative framework. The previously selected common developmental PCs were therefore used to estimate the developmental stage of the fossils.

For the second analysis including the Mojokerto specimen, after the GPA of the raw coordinates, we performed a PCA and projected each fossil on the original PC axes. We did not perform further ontogenetic analysis in this reduced dataset since the lower number of variables reduced the overall ontogenetic signal. However, in this analysis using Mojokerto as a control specimen, we could investigate the relationship between KNM-ER 42700 and this very young individual (Antón, 1997; Balzeau et al., 2005; Coqueugniot et al., 2004).

RESULTS

Ontogenetic trajectories and PCA of extant taxa

Regarding the full dataset, our trajectory analysis based on Procrustes coordinates across the four ontogenetic stages shows that the two extant taxa undergo a different pattern of development. Test statistics using the trajectory approach (Adams & Collyer, 2009; Adams et al., 2013; Collyer & Adams, 2007, 2013) (with 9999 residual randomization permutations) revealed that there is a significant difference in the direction ($p= 0.0001$) and size ($p= 0.02$) of the two trajectories (see Table 5). Overall, chimpanzees displayed greater shape change during development. The trajectories do not seem to differ in the pattern (shape of the trajectory) of shape change that a species undergoes during development ($p = 0.49$).

Figure 2 shows a projection of the two trajectories in the PCA plot. Visual inspection of PC1 and PC2 reveals that the trajectories of *Homo* and *Pan* are not parallel, with each of them showing a distinct morphology since the earliest age stage. In general, a difference in the size of the trajectories ($MD_{P,H} =0.043$) is defined as the difference between the Procrustes distances covered by one

trajectory compared to the other (Adams and Collyer 2009; Adams et al. 2013; Collyer and Adams 2007; Collyer and Adams 2013). In this case, chimpanzees cover bigger Procrustes distances during ontogeny than modern humans. PC1 tends to discriminate between *Homo* and *Pan.* Younger chimpanzees appear to be closer to the human group on PC1 than their adult counterparts. The first component also separates age classes in the chimpanzees but not in modern humans. Along PC2, instead, there is not a clear separation between the two species. However, both species show a similar ontogenetic progression. In this specific PCA, adults tend to have higher PC2 scores while the infant age groups have lower PC2 values.

The PCA of the Mojokerto dataset can be visualized in Figure 3. In this case, there is slightly more overlap between the two taxa as well as among different age classes. However, a similar, monotonic, ontogenetic pattern is retained along PC2.

Shape Changes

PC1 discriminates, as mentioned above, between humans and chimpanzees. Humans show relatively longer occipital condyles (Figure 4), a less sagittally flexed nuchal plane, and a proportionally more prominent mastoid process. The area anterior to the foramen magnum in modern humans is much more compact, presenting a petrotympanic crest in combination with a relatively less laterally extended glenoid fossa. Inion is more superiorly located in chimpanzees (low PC1 scores) than humans, the nuchal plane faces more posteriorly in chimpanzees.

PC2 separates age categories in both taxa. It exhibits an increase in the mastoid process projection from lower values to higher ones indicating an increase in the pneumatization of this area (Figure 5). The articular fossa expands laterally in older specimens (higher PC2 scores). Overall, the nuchal plane has a more rounded and flexed morphology as PC2 values increase (the nuchal line from inion to opisthion). The occipital condyles undergo a twist that makes them more parallel to the sagittal plane. The anterior basicranium becomes medio-laterally wider with higher PC2 scores.

In the reduced dataset which includes the Mojokerto specimen, PC2 retains a similar common developmental pattern. The shape change associated with PC2 is mainly driven by an increase in the pneumatization of the mastoid area (Figure 6).

Common developmental shape change

A Kendall's tau correlation test between age group and PC values shows that PC2 is strongly correlated with this ordinal variable ($R=0.69$, $p < 0.0001$). This is the only PC associated with development both in modern humans and chimpanzees.

The ontogenetic trajectory is computed starting from the mean configuration of each age group. PC2 comprises a common ontogenetic vector between modern humans and chimpanzees that is part of the multivariate vector constituting the entire trajectory. Both vectors appear to have similar scores in age classes in both groups. This is evident graphically in the PCA plot (Figure 2), which shows that humans tend to reach higher PC2 scores than chimpanzees. PC2 discriminates age groups in the modern humans' sample clearly, but there is more overlap between the chimpanzee age groups along this axis. The permutation pairwise comparison allowed us to detect the differences between mean PC2 values in each group (species and age category). After a sequential Bonferroni correction results are presented in Table 6. When considering the intraspecific differences between age groups, PC2 values significantly differ among different age groups in modern humans. In contrast, chimpanzees show no significant differences in the last consecutive age groups (i.e. between age class 1:2 and 2:3). However, the entire PC2 vector is correlated to age class with significant differences between adults (age class 3) and the earliest stages (age class 0 and 1). Our interspecific comparison shows that PC2 values are not different for the same age groups in the two species until age class 2. At the end of development (transition from age class 2 to 3), however, chimpanzees appear to have changed shape less than modern humans along with this component. In fact, the adult group of chimpanzees is more similar to the second age group of modern humans (see Table 6). However, there is a trend in both species to change basicranial shape in a similar manner during ontogeny, giving us a common and shared, likely ancestral, young to adult pattern that can be used to address the developmental stage of unknown fossil specimens. In order to evaluate sexual dimorphism in this specific shape component, we conducted a student t-test using PC2 scores of the adults with sex as grouping variable per species. No significant difference was found between PC2 scores between males and females in either species (result in supporting information Table S5- S6).

The linear regression between the PC2 values and log centroid size shows how this shape component is related to size (Figure 7). Results show that a significant association exists between size and PC2 values for both extant species (chimps $R=0.63$ $p=0.023$, humans $R=0.8$ $p=0.01$) when the entire sample is considered. Chimpanzees have higher PC2 scores compared to humans for smaller size values. However, the adult PC2 scores exhibit no significant correlation with LogCS in either species; in fact, they both have a weak correlation $R<0.3$ and p above 0.05, showing that this component is not allometric in the adult sample. Regression lines in the plot (Figure 7) show the ontogenetic allometry in the sample. This plot demonstrates that, for the same size values, PC2 can span from human infants (age group 0) to the adult chimpanzees (age group 3). This suggests that despite an allometric correlation of this component to size its power to discriminate age groups at an interspecific level is not related to size.

H. erectus s.l. have high size values, exceeding sometimes the variability of adult modern humans. KNM-ER 42700 is the only specimen of small size that falls outside the range of adult modern human variation but within the adult chimpanzees' distribution (Figure 7).

PCA with projection of *H. erectus* specimens

Figure 2 shows the projection of *Homo erectus s.l.* specimens on PCs 1 and 2. They overlap with the human sample on PC1. KNM-ER 42700 (both the original cast and the virtual reconstruction) shows the highest positive scores on PC1 among the *H. erectus s.l.* individuals, though still falling within the ranges of the modern human samples. Given the results about the developmental trajectory, in this specific shape space, PC2 is used as a young-to-adult shape vector. Overall, fossils tend to have positive PC2 values, all plotting in the range of variation between young adult and adult modern human categories, as expected. KNM-WT 15000, the youngest specimen included, has the lowest PC2 score. However, it still plots relatively close to the other fossils and within the area of overlap between adults and late juveniles (i.e. our age categories 3 and 2), as does D2700 and all other specimens except KNM-ER 3883. KNM-ER 3883 shows the highest PC2 score among our fossil sample. Both the original as well as the reconstruction of KNM-ER 42700 plot very close to each other, in the area of overlap between age categories 3 (adults) and 2 (late juveniles), indicating that taphonomic deformation does not have a major effect on the shape of the basicranium in this specimen.

The projection of fossils in the PCA of the reduced dataset is similar to that of the full dataset with respect to the shape changes on these PC axes. Mojokerto shows the lowest PC2 score and it plots close to the age category 0, as expected given its younger age attribution (Balzeau et al., 2005; Coqueugniot et al., 2004). The other additional specimens all plot within the adult variability. As in the first analysis, KNM-ER 42700 plots in the area of overlap between age categories 3 (adult) and 2 (late juveniles)

DISCUSSION

The hypotheses that formed the basis of our study were found to be only partially supported. We found that *Pan* and *Homo* do not share the same developmental trajectory; however, they share a common developmental component. We further could not support a young developmental stage for KNM-ER 42700, as proposed by (Neubauer et al., 2018). Based on its basicranial morphology this specimen seems more likely to be an adult or young-adult, as originally suggested by Spoor et al. (2007). Moreover, the second analysis of the reduced dataset shows that the very young fossil specimen Mojokerto has a PC2 score consistent with its age attribution (Antón, 1997; Balzeau et al.,

2005). This result confirms our assumption that the *Pan-Homo* common developmental shape variable (PC2) can be used to discriminate between very young and adult stages in *H. erectus s.l.* However, it must be approached with caution, given the limited nature of our fossil sample, especially in terms of young subadults, and the incomplete preservation of the cranial base of Mojokerto. Although we tried to reduce the effect of any taphonomic distortion on this specimen by mirroring, symmetrizing and projecting the specimen on PCA such bias may still have some influence on our results, also considering the possible introduction of artificial shape variation linked to every reconstruction/symmetrization method applied in virtual anthropology (Weber, 2015).

Neubauer et al. (2018) concluded that most probably KNM-ER 42700 represents a much younger *H. erectus s.l.* individual than previously thought. Their hypothesis is based on an allometric analysis using the Mojokerto child as a young individual to build an ontogenetic trajectory. As previously emphasized, studying the ontogeny of fossil species can be a difficult task because of the lack of a complete ontogenetic sample. Therefore, it is perhaps not sufficient to build an ontogenetic allometry regression with only one young specimen, as was done by Neubauer et al. (2018). In fact, their regression is strongly influenced by the Mojokerto specimen, which acts as an influential point that affects the regression line (Chatterjee 1986). In contrast, here we investigated development based on common ontogenetic traits of chimpanzees and modern humans, in order to form a comparative basis for assessing the developmental stage of KNM-ER 42700. We aimed to find a shape component that could give us a result independent of the overall size of the specimen, unlike the approach taken by Neubauer et al. (2018). In fact *H. erectus s.l.* cranial size is known to be highly variable (Antón, 2003; Baab, 2015); therefore using size as a proxy to infer the ontogenetic stage could be challenging. Moreover, it is problematic to compare full ontogeny (association of growth and development during time) between modern humans and chimpanzees because of differences in overall size and in the growth rate in these two taxa (Robson & Wood, 2008; B. H. Smith, Crummett, & Brandt, 1994). We, therefore, prefer to analyze shape space, since a common developmental component in two related taxa (modern humans and chimpanzees) not related to size (when considering static allometry in adult samples) can be used to infer the developmental stage of specimens with an unknown ontogenetic trajectory. In our analysis, PC2, extracted from the ontogenetic trajectories of the two species, provides a useful proxy to infer the ontogenetic status of an individual (Figure 2).

Ontogenetic trajectory comparison and common ontogenetic component.

The ontogenetic trajectories of the basicranium in humans and chimpanzees are different. GM studies have shown different results regarding a shared cranial ontogenetic trajectory in the Homininae clade (Ackermann & Krovitz, 2002; Bastir & Rosas, 2004; Berge & Penin, 2004; Cobb

& O'Higgins, 2004; Dean & Wood, 1984; Gunz et al., 2010; Mitteroecker et al., 2004; Mitteroecker et al., 2005; Neubauer, Gunz, & Hublin, 2010; Neubauer et al., 2009; Penin, Berge, & Baylac, 2002). However, even if the two trajectories are different, they share some common aspects. Developmental steps during ontogeny have a similar pattern of shape changes between these two species, suggesting that key events during ontogeny (dental eruption) are followed by a similar developmental direction. In our analysis *Pan troglodytes* and *Homo sapiens* show distinct shapes starting with the earliest developmental stage studied, and their divergence continues during later ontogenetic stages, as indicated by their non-parallel trajectories. However, PC2 is a component of the trajectory that, during ontogeny, has a similar direction in both taxa, as shown in Figure 2, possibly representing a shared plesiomorphic aspect of hominin ontogeny, a trait likely present also in the common ancestor of chimpanzees and modern humans. This, in turn, suggests that *Homo erectus s.l.* could be reasonably assumed to have had similar developmental changes in their basicranium. These common developmental changes include an increase in the size of the mastoid process, probably due to the progressive pneumatization of the temporal region (Turgut & Tos, 2007); a lateral expansion of the articular fossa; and a rounding of the nuchal area in adults relative to the flatter nuchal planes of young individuals. The Kendall's tau results highlighted the strong correlation between age group and PC2 scores when species affiliation is not considered, indicating that this is the only component that has a similar distribution along with age groups across taxa. The resulting ontogenetic vector along PC2 from the ontogenetic trajectory can be defined as a common developmental vector in this case. It is important to note that PC2 is a part of the overall trajectory and it captures only the shape changes related to ontogeny in both species; it does not represent the entirety of ontogenetic shape changes in modern humans or chimpanzees. The pairwise comparisons between age group demonstrate that PC2 changes in a similar manner between age class 0 and 1 in both taxa, but then is slowed in chimpanzees compared to humans. This may be related to the morphological changes linked to PC2, which involve a projection of the mastoid process that does not reach the same dimensions in chimpanzees as in humans. Nevertheless, when the full trajectory is considered (Table 5), chimpanzees cover more Procrustes distances than modern humans. This indicates that, at the end of their growth, human adults appear to be relatively more similar to their younger counterparts than chimpanzee adults compared to their offspring, even though the latter complete their development earlier in terms of absolute time (B. H. Smith, 1989; B. H. Smith et al., 1994). This observation has been frequently made in the past (Dean & Wood, 1984; Godfrey & Sutherland, 1996; Gould, 1979; Mitteroecker et al., 2004; Mitteroecker et al., 2005; Shea, 1983, 1988, 1989). It also means that there are specific ontogenetic changes on other PCs such as PC1 for chimpanzees. However, these specific ontogenetic changes are not considered by us for the developmental stage attribution of fossil

specimens. In fact, such shape changes can be autapomorphic traits and can not be safely used without knowing the real ontogenetic trajectory of the fossil taxon.

A point that should be given further consideration is variation in ontogenetic trajectories across populations of the same species. Some studies have found intraspecific differences in the ontogenetic trajectories of the hominoid cranium (Massey, 2018; Terhune, Robinson, & Ritzman, 2014; Viðarsdóttir & Cobb, 2004). However, among modern humans, temporal bone differences between populations are evident already before the eruption of the first molar (H. F. Smith, Ritzman, Otárola-Castillo, & Terhune, 2013). After that stage, the growth trajectories of different human populations do not differ. Among chimpanzees, ontogenetic trajectories differ at the population level for the nuchal area but not for the rest of the basicranium (Massey, 2018). In our analysis, we tried to reduce genetic variability and therefore limited our human sample to European individuals. Given the relative scarcity of chimpanzees in collections accessible to us, however, we were obliged to use a wider range of geographical origin for our chimpanzee sample (see Table 3). However, while our adult chimpanzee samples derive from different geographic regions, the earlier ontogenetic groups (from age group 0 to 2) mainly comprise individuals originating from Liberia, strongly suggesting that differences in shape among this group are mainly driven by ontogeny. Furthermore, if we consider only the adults (superimposing them separately and then running a PCA), there is no clear separation in shape space between geographic clusters (Figure S2). Adult chimpanzees seem to display higher variability in the shape space compared to younger age groups. This probably is related to the presence of different subspecies in our sample. Despite the possibility of somewhat different ontogenetic trajectories in different chimpanzee populations (Massey, 2018), we consider that the extracted common ontogenetic vector (PC2) is significantly associated with age regardless of subspecies. Indeed, all the adult specimens show higher PC2 scores compared to the youngest age group.

Another caveat of our analysis concerns the earliest part of the ontogeny, which is not well-represented in our study. To fully analyze the postnatal ontogenetic trajectory, we would require an ontogenetic group composed solely of specimens with no deciduous dentition and another of specimens only with deciduous. Unfortunately, this is extremely difficult to achieve given the rarity of very young individuals in collections. However, our study's main goal is to determine the age of KNM-ER 42700, which has been proposed to represent either a young adult or a child between the ages of 3 and 7 years. We, therefore, consider that our analysis is sufficient for this purpose.

In summary, our results suggest that the basicranium retains a developmental signal throughout ontogeny. Common shape changes found in two closely related taxa such as *Pan*

troglodytes and *Homo sapiens* have been reported previously (Gunz et al., 2010; Neubauer et al., 2010; Neubauer et al., 2009; Scott et al., 2014) and have been considered plesiomorphic developmental characteristics. Our results suggest that also in this case there is a plesiomorphic attribute in this shape component. The placement of juvenile fossil specimens in our analysis suggests that these plesiomorphic ontogenetic shape changes are also present in *H. erectus s.l.* and were therefore used here to evaluate the developmental age of KNM-ER 42700. Future analyses should further confirm the plesiomorphic nature of the ontogenetic shape changes described here by investigating other fossil taxa and additional extant hominoids.

The common component PC2 comprises a common ontogenetic allometric aspect (Klingenberg, 2016) since the two species exhibit a similar correlation with size. This is expected given the ontogenetic nature of our cross-sectional sample (Klingenberg 2016). However, when considering only the adult groups in both species, static allometry is not strongly correlated with basicranial shape ($R<0.3$ and $p>0.05$). This means that, once full maturity is reached, size does not affect PC2 values. Considering that human infants show low PC2 scores, but their size is comparable to that of adult chimpanzees, PC2 discriminates different developmental stages irrespective of size. In this framework, the extracted component is considered plesiomorphic and useful for our aim but also it could give results about the developmental stage despite the overall size of an unknown specimen – something that is difficult to achieve when considering overall cranial or endocranial shape.

Developmental stage definition in *H. erectus s.l.*

We explored the similarities found in the shape changes along ontogeny to address the ontogenetic status of *H. erectus s.l.* individuals. These fossils plot very close to the human samples on PC1. For the two young fossil individuals included here, KNM-WT 15000 and D2700 (Dean et al., 2001; S. L. Smith, 2004; Vekua et al., 2002), their developmental stage, determined on the basis of their dental and cranial development, generally agrees with their PC2 scores. This is most evident for KNM-WT 15000, whose PC2 score falls in the area of overlap between the ranges of age categories 1, 2 and 3. D2700 is thought to be almost adult; its PC2 score plots in the area of overlap of age categories 2 and 3. Both specimens are usually considered as already showing an adult overall morphology (Baab, 2016; Rightmire et al., 2006). All other fossil specimens show PC2 scores falling in the range of overlap of young adult and adult individuals, except for KNM-ER 3883, which plots exclusively with the adults. Shape changes along PC2 show that the pneumatization of the mastoid region is strongly associated with positive PC2 scores, and thus variation in this feature within *H. erectus s.l.* could affect an individual's PC2 score. The mastoid area has some dimorphic features in modern humans

(Rosas & Bastir, 2002), but, no sexual dimorphism was found both in modern humans and chimpanzees regarding PC2 scores distribution, thus supporting that difference along PC2 are mainly driven by ontogenetic status. In our second analysis, we were able to expand our fossil sample to include the young *H. erectus s.l.* specimen from Mojokerto. Results clearly showed the separation between Mojokerto and the other specimens along PC2, as this specimen's PC2 score overlapped those of the youngest age groups (0 and 1) of our analysis. Overall, therefore, *H. erectus s.l.* has a distribution that follows the trend seen in modern humans and chimpanzees. Furthermore, in this second dataset, only KNM-ER 3883 and Mojokerto were reconstructed by mirroring the preserved side. All the other specimens used in the analysis were not reconstructed, thus reducing the possible influence of taphonomy and reconstruction on the results. The similarity of the results of our two analyses (full vs reduced datasets) increases our confidence that taphonomy and landmark reconstruction do not strongly influence our results. Moreover, by projecting our fossil specimens in the PCA plot we reduced the effect of taphonomy to the PC axes investigated.

Neubauer et al. (2018) recently argued that KNM-ER 42700 is younger than originally thought because the fusion of the spheno-occipital synchondrosis is not a reliable proxy for age estimation in extinct species. They suggested that this individual never completed its endocranial growth, associating its small overall size with a young age. Since 95% of brain size is already attained in chimpanzees between ages 3 and 4 and in humans between ages 6 and 7 (Lieberman, 2011), an immature brain for KNM-ER 42700 would indicate a developmental stage corresponding to the age categories 0 and 1 in our analysis. If this hypothesis is correct, we would expect KNM-ER 42700 to show a PC2 score between our age categories 0 and 1. Instead, KNM-ER 42700 falls within the area of overlap of the modern human adult/late subadult categories, with a PC2 score similar to most other *H. erectus s.l.* adult specimens in our analysis and to D2700, a late subadult. This result is inconsistent with the hypothesis of Neubauer et al. (2018). Instead, it agrees with previous work arguing that this specimen reached an overall adult or young adult stage despite its not fully-fused spheno-occipital syncondhrosis and small cranial size (Baab, 2008, 2016; F. Spoor et al., 2007). We also note that it would be difficult for this individual to further increase its cranial capacity, as its already fused cranial sutures (with the exception of the spheno-occipital synchondrosis) could not have allowed for a substantial expansion of the brain. Our results are therefore consistent with previous work suggesting that KNM-ER 42700 attained its adult morphology despite its incompletely fused spheno-occipital synchondrosis (Baab, 2016; F. Spoor et al., 2007).

CONCLUSION

We used ontogenetic trajectory analysis on a cross-sectional sample of chimpanzee and modern human basicrania, in order to assess the developmental age of the enigmatic fossil human specimen KNM-ER 42700. Common ontogenetic traits between modern humans and chimpanzees are helpful to define the plesiomorphic developmental features retained during hominin evolution. Our results show that these features provide an avenue for determining the developmental stage in *H. erectus s.l.* specimens lacking dentition or other proxies traditionally used for age determination. This is because both analyzed species show a common ontogenetic vector involving a distinct morphology for each age group. Future analysis using different extant and extinct hominins should further investigate this aspect in order to extend such method to other fossil species. In agreement with previous work, our results show that KNM-ER 42700 had reached an adult stage at death even if it shows an overall very small cranial size and an incompletely fused spheno-occipital synchondrosis. It is reasonable to assume that this specimen would likely not have shown extensive morphological changes had it survived to a later point in life. We propose that its morphology is not greatly affected by incomplete growth and that the hypothesis that it represents a much younger individual (Neubauer et al., 2018), cannot be supported. Under this light and given the results from other studies showing that KNM-ER 42700 lies outside the range of shape variation of *H. erectus s.l.* (Baab, 2016; Bauer & Harvati, 2015; Neubauer et al., 2018; Stringer, 1984), our results suggest that either this specimen represents an as yet unidentified hominin species; or, that the intraspecific, possibly sex-related, shape variation of *H. erectus s.l.* was much higher than previously appreciated. This work encourages the use of our approach for age determination in fossil specimens lacking dental remains.

ACKNOWLEDGMENT

We thank Dr. M. Zavattaro for access to specimens from the Museum of Natural History, University of Florence collection. We are grateful to the Kyoto University Primate Research Institute (KUPRI) digital morphology museum for access to the CT Scans used in this work. We want to thank the Senckenberg museum (Dr. F. Schrenk, Dr. C. Hemm) in Frankfurt for the scans of SMF-PA specimens and the access to the Sangiran material. We thank the Smithsonian's Division of Mammals (Dr. K. Helgen) and Human Origins Program (Dr. M. Tocheri) for the scans of USNM specimens used in this research (http://humanorigins.si.edu/evidence/3d-collection/primate 30.07.2018). These scans were acquired through the generous support of the Smithsonian 2.0 Fund and the Smithsonian's Collections Care and Preservation Fund. We are grateful to Dr. E. Delson for access to scanned specimens from the American Museum of Natural History, New York. We thank Dr. J. Moggi-Cecchi for his support during data acquisition. T.M. thanks, Dr. H. Reyes-Centeno, Dr. F. A. Karakostis and Dr. A. Strauss for their help and precious advice. T. M. wants to thank Francesca for her faithful support. This study was supported by the University of Tübingen and the German Research Foundation (DFG-FOR 2237).

DATA AVAILABILITY STATEMENT

Raw coordinates data used in the analysis are available from the corresponding author upon reasonable request.

REFERENCES

Ackermann, R. R., & Krovitz, G. E. (2002). Common patterns of facial ontogeny in the hominid lineage. *The Anatomical Record, 269*(3), 142-147.

Adams, D. C., & Collyer, M. L. (2009). A general framework for the analysis of phenotypic trajectories in evolutionary studies. *Evolution, 63*(5), 1143-1154. doi:https://doi.org/10.1111/j.1558-5646.2009.00649.x

Adams, D. C., Otárola-Castillo, E., & Paradis, E. (2013). geomorph: an r package for the collection and analysis of geometric morphometric shape data. *Methods in Ecology and Evolution, 4*(4), 393-399. doi:https://doi.org/10.1111/2041-210X.12035

Andrews, P. (1984). An alternative interpretation of the charac ters used to define Homo erectus. The Early Evolution of Man with Special Emphasis on Southeast Asia and Africa. *Cour. Forsch. Inst. Senckenberg, Frankfurt am Main, 69*, 167-175.

Antón, S. C. (1997). Developmental age and taxonomic affinity of the Mojokerto child, Java, Indonesia. *American Journal of Physical Anthropology, 102*(4), 497-514. doi:https://doi.org/10.1002/(SICI)1096-8644(199704)102:4<497::AID-AJPA6>3.0.CO;2-P

Antón, S. C. (1999). Cranial growth in Homo erectus: how credible are the Ngandong juveniles? *American Journal of Physical Anthropology, 108*(2), 223-236. doi:https://doi.org/10.1002/(SICI)1096-8644(199902)108:2<223::AID-AJPA7>3.0.CO;2-8

Antón, S. C. (2003). Natural history of Homo erectus. *American Journal of Physical Anthropology, 122*(37), 126-170. doi:https://doi.org/10.1002/ajpa.10399

Baab, K. L. (2008). A re-evaluation of the taxonomic affinities of the early Homo cranium KNM-ER 42700. *Journal of Human Evolution, 55*(4), 741-746; discussion 747-750. doi:https://doi.org/10.1016/j.jhevol.2008.02.013

Baab, K. L. (2015). *Defining Homo erectus* (Vol. 3): Springer.

Baab, K. L. (2016). The role of neurocranial shape in defining the boundaries of an expanded Homo erectus hypodigm. *Journal of Human Evolution, 92*, 1-21. doi:https://doi.org/10.1016/j.jhevol.2015.11.004

Balolia, K. L., Soligo, C., & Lockwood, C. A. (2013). Sexual Dimorphism and Facial Growth Beyond Dental Maturity in Great Apes and Gibbons. *International Journal of Primatology, 34*(2), 361-387. doi:https://doi.org/10.1007/s10764-013-9666-z

Balzeau, A., Grimaud-Hervé, D., & Jacob, T. (2005). Internal cranial features of the Mojokerto child fossil (East Java, Indonesia). *Journal of Human Evolution, 48*(6), 535-553. doi:https://doi.org/10.1016/j.jhevol.2005.01.002

Bastir, M., & Rosas, A. (2004). Comparative ontogeny in humans and chimpanzees: Similarities, differences and paradoxes in postnatal growth and development of the skull. *Annals of Anatomy - Anatomischer Anzeiger, 186*(5), 503-509. doi:https://doi.org/10.1016/S0940-9602(04)80096-7

Bastir, M., Rosas, A., & O'Higgins, P. (2006). Craniofacial levels and the morphological maturation of the human skull. *Journal of Anatomy, 209*(5), 637-654. doi:https://doi.org/10.1111/j.1469-7580.2006.00644.x

Bauer, C. C., & Harvati, K. (2015). A virtual reconstruction and comparative analysis of the KNM-ER 42700 cranium. *Anthropologischer Anzeiger, 72*(2), 129-140. doi:https://doi.org/10.1127/anthranz/2015/0387

Berge, C., & Penin, X. (2004). Ontogenetic allometry, heterochrony, and interspecific differences in the skull of African apes, using tridimensional Procrustes analysis. *American Journal of*

Physical Anthropology: The Official Publication of the American Association of Physical Anthropologists, 124(2), 124-138.
Bookstein, F. L. (1991). *Morphometric tools for landmark data: geometry and biology.*: Cambridge Univ. Press.
Cobb, S. N., & O'Higgins, P. (2004). Hominins do not share a common postnatal facial ontogenetic shape trajectory. *Journal of Experimental Zoology Part B: Molecular and Developmental Evolution, 302*(3), 302-321.
Collyer, M. L., & Adams, D. C. (2007). Analysis of two-state multivariate phenotypic change in ecological studies. *Ecology, 88*(3), 683-692. doi:doi:10.1890/06-0727
Collyer, M. L., & Adams, D. C. (2013). Phenotypic trajectory analysis: comparison of shape change patterns in evolution and ecology. *Hystrix, the Italian Journal of Mammalogy, 24*(1), 75-83. doi:https://doi.org/10.4404/hystrix-24.1-6298
Collyer, M. L., Sekora, D. J., & Adams, D. C. (2014). A method for analysis of phenotypic change for phenotypes described by high-dimensional data. *Heredity, 115*, 357. doi:https://doi.org/10.1038/hdy.2014.75

Coqueugniot, H., Hublin, J. J., Veillon, F., Houët, F., & Jacob, T. (2004). Early brain growth in Homo erectus and implications for cognitive ability. *Nature, 431*, 299. doi:https://doi.org/10.1038/nature02852
Dean, C., Leakey, M. G., Reid, D., Schrenk, F., Schwartz, G. T., Stringer, C., & Walker, A. (2001). Growth processes in teeth distinguish modern humans from Homo erectus and earlier hominins. *Nature, 414*, 628. doi:https://doi.org/10.1038/414628a
Dean, C., & Liversidge, H. M. (2015). Age estimation in fossil hominins: comparing dental development in early Homo with modern humans. *Annals of Human Biology, 42*(4), 415-429. doi:https://doi.org/10.3109/03014460.2015.1046488
Dean, C., & Smith, B. H. (2009). Growth and Development of the Nariokotome Youth, KNM-WT 15000. In F. E. Grine, J. G. Fleagle, & R. E. Leakey (Eds.), *The First Humans – Origin and Early Evolution of the Genus Homo: Contributions from the Third Stony Brook Human Evolution Symposium and Workshop October 3 – October 7, 2006* (pp. 101-120). Dordrecht: Springer Netherlands.
Dean, C., & Wood, B. A. (1984). Phylogeny, Neoteny and Growth of the Cranial Base in Hominoids. *Folia Primatologica, 43*(2-3), 157-180.
Field, A. (2013). *Discovering statistics using IBM SPSS Statistics (4th edition)*. London: Sage.
Godfrey, L. R., & Sutherland, M. R. (1996). Paradox of peramorphic paedomorphosis: heterochrony and human evolution. *American Journal of Physical Anthropology: The Official Publication of the American Association of Physical Anthropologists, 99*(1), 17-42.
Gould, S. J. (1979). Ontogeny and Phylogeny. *Science and Society, 43*(1), 104-106.
Gower, J. C. (1975). Generalized procrustes analysis. *Psychometrika, 40*(1), 33-51. doi:https://doi.org/10.1007/bf02291478
Gunz, P., Neubauer, S., Maureille, B., & Hublin, J.-J. (2010). Brain development after birth differs between Neanderthals and modern humans. *Current Biology, 20*(21), R921-R922. doi:https://doi.org/10.1016/j.cub.2010.10.018
Harvati, K. (2003). Quantitative analysis of Neanderthal temporal bone morphology using three-dimensional geometric morphometrics. *American Journal of Physical Anthropology: The Official Publication of the American Association of Physical Anthropologists, 120*(4), 323-338.
Harvati, K., & Weaver, T. D. (2006a). Human cranial anatomy and the differential preservation of population history and climate signatures. *The Anatomical Record Part A: Discoveries in Molecular, Cellular, and Evolutionary Biology, 288A*(12), 1225-1233. doi:https://doi.org/10.1002/ar.a.20395

Harvati, K., & Weaver, T. D. (2006b). Reliability of cranial morphology in reconstructing Neanderthal phylogeny *Neanderthals revisited: new approaches and perspectives* (pp. 239-254): Springer.
Kendall, M. G. (1948). *Rank correlation methods*: Charles Griffin & Co. Ltd., London.
Klingenberg, C. P. (2016). Size, shape, and form: concepts of allometry in geometric morphometrics. *Development Genes and Evolution, 226*(3), 113-137. doi:https://doi.org/10.1007/s00427-016-0539-2
Lieberman, D. E. (2011). *The evolution of the human head*: The belknap press of Harvard university press.
Lieberman, D. E., McBratney, B. M., & Krovitz, G. (2002). The evolution and development of cranial form in *Homo sapiens*. *Proceedings of the National Academy of Sciences, 99*(3), 1134-1139. doi:https://doi.org/10.1073/pnas.022440799
Lieberman, D. E., Ross, C. F., & Ravosa, M. J. (2000). The primate cranial base: ontogeny, function, and integration. *American Journal of Physical Anthropology, Suppl 31*, 117-169. doi:10.1002/1096-8644(2000)43:31+<117::aid-ajpa5>3.3.co;2-9
Lordkipanidze, D., Ponce de León, M. S., Margvelashvili, A., Rak, Y., Rightmire, G. P., Vekua, A., & Zollikofer, C. P. E. (2013). A Complete Skull from Dmanisi, Georgia, and the Evolutionary Biology of Early *Homo*. *Science, 342*(6156), 326-331. doi:https://doi.org/10.1126/science.1238484
Mardia, K. V., Bookstein, F. L., & Moreton, I. J. (2000). Statistical assessment of bilateral symmetry of shapes. *Biometrika, 87*(2), 285-300. doi:https://doi.org/10.1093/biomet/87.2.285
Massey, J. (2018). Pattern Of Cranial Ontogeny In Populations Of Gorilla And Pan. *Retrieved from the University of Minnesota Digital Conservancy, http://hdl.handle.net/11299/200300.*
Mitteroecker, P., & Gunz, P. (2009). Advances in Geometric Morphometrics. *Evolutionary Biology, 36*(2), 235-247. doi:https://doi.org/10.1007/s11692-009-9055-x
Mitteroecker, P., Gunz, P., Bernhard, M., Schaefer, K., & Bookstein, F. L. (2004). Comparison of cranial ontogenetic trajectories among great apes and humans. *Journal of Human Evolution, 46*(6), 679-698. doi:https://doi.org/10.1016/j.jhevol.2004.03.006
Mitteroecker, P., Gunz, P., & Bookstein, F. L. (2005). Heterochrony and geometric morphometrics: a comparison of cranial growth in Pan paniscus versus Pan troglodytes. *Evolution & Development, 7*(3), 244-258. doi:https://doi.org/10.1111/j.1525-142X.2005.05027.x
Neubauer, S., Gunz, P., & Hublin, J.-J. (2010). Endocranial shape changes during growth in chimpanzees and humans: A morphometric analysis of unique and shared aspects. *Journal of Human Evolution, 59*(5), 555-566. doi:https://doi.org/10.1016/j.jhevol.2010.06.011
Neubauer, S., Gunz, P., & Hublin, J. J. (2009). The pattern of endocranial ontogenetic shape changes in humans. *Journal of Anatomy, 215*(3), 240-255. doi:https://doi.org/10.1111/j.1469-7580.2009.01106.x
Neubauer, S., Gunz, P., Leakey, L., Leakey, M., Hublin, J.-J., & Spoor, F. (2018). Reconstruction, endocranial form and taxonomic affinity of the early Homo calvaria KNM-ER 42700. *Journal of Human Evolution*. doi:https://doi.org/10.1016/j.jhevol.2018.04.005
Norusis, M. J. (1993). *SPSS for windows: advanced statistics, release 6.0*: SPSS Incorporated Chicago.
O'Connell, C. A., & DeSilva, J. M. (2013). Mojokerto revisited: Evidence for an intermediate pattern of brain growth in Homo erectus. *Journal of Human Evolution, 65*(2), 156-161. doi:https://doi.org/10.1016/j.jhevol.2013.04.007
Penin, X., Berge, C., & Baylac, M. (2002). Ontogenetic study of the skull in modern humans and the common chimpanzees: neotenic hypothesis reconsidered with a tridimensional Procrustes analysis. *American Journal of Physical Anthropology: The Official Publication of the American Association of Physical Anthropologists, 118*(1), 50-62.

Reyes-Centeno, H., Ghirotto, S., & Harvati, K. (2017). Genomic validation of the differential preservation of population history in modern human cranial anatomy. *American Journal of Physical Anthropology, 162*(1), 170-179.
Rice, W. R. (1989). Analyzing tables of statistical tests. *Evolution, 43*(1), 223-225.
Rightmire, G. P. (1990). *The Evolution of Homo Erectus: Comparative Anatomical Studies of an Extinct Human Species*. Cambridge: Cambridge University Press.
Rightmire, G. P., Lordkipanidze, D., & Vekua, A. (2006). Anatomical descriptions, comparative studies and evolutionary significance of the hominin skulls from Dmanisi, Republic of Georgia. *Journal of Human Evolution, 50*(2), 115-141. doi:https://doi.org/10.1016/j.jhevol.2005.07.009
Robinson, C., & Terhune, C. E. (2017). Error in geometric morphometric data collection: Combining data from multiple sources. *American Journal of Physical Anthropology, 164*(1), 62-75.
Robson, S. L., & Wood, B. (2008). Hominin life history: reconstruction and evolution. *Journal of Anatomy, 212*(4), 394-425. doi:https://doi.org/10.1111/j.1469-7580.2008.00867.x
Rohlf, F. J., & Slice, D. (1990). Extensions of the Procrustes Method for the Optimal Superimposition of Landmarks. *Systematic Biology, 39*(1), 40-59. doi:https://doi.org/10.2307/2992207
Rosas, A., & Bastir, M. (2002). Thin-plate spline analysis of allometry and sexual dimorphism in the human craniofacial complex. *American Journal of Physical Anthropology: The Official Publication of the American Association of Physical Anthropologists, 117*(3), 236-245.
Schwartz, J. H. (2004). Getting to Know Homo erectus. *Science, 305*(5680), 53.
Scott, N., Neubauer, S., Hublin, J.-J., & Gunz, P. (2014). A Shared Pattern of Postnatal Endocranial Development in Extant Hominoids. *Evolutionary Biology, 41*(4), 572-594. doi:https://doi.org/10.1007/s11692-014-9290-7
Shea, B. T. (1983). Paedomorphosis and neoteny in the pygmy chimpanzee. *Science, 222*(4623), 521-522. doi:https://doi.org/10.1126/science.6623093
Shea, B. T. (1988). Heterochrony in Primates. In M. L. McKinney (Ed.), *Heterochrony in Evolution: A Multidisciplinary Approach* (pp. 237-266). Boston, MA: Springer US.
Shea, B. T. (1989). Heterochrony in human evolution: The case for neoteny reconsidered. *American Journal of Physical Anthropology, 32*(S10), 69-101.
Shearer, B. M., Cooke, S. B., Halenar, L. B., Reber, S. L., Plummer, J. E., Delson, E., & Tallman, M. (2017). Evaluating causes of error in landmark-based data collection using scanners. *PloS one, 12*(11), e0187452.
Simons, E. A., & Frost, S. R. (2016). Constructing cranial ontogenetic trajectories: A comparison of growth, development, and chronological age proxies using a known-age sample of Macaca mulatta. *American Journal of Physical Anthropology, 161*(2), 296-308. doi:https://doi.org/10.1002/ajpa.23031
Slice, D. E. (2007). Geometric Morphometrics. *Annual Review of Anthropology, 36*(1), 261-281. doi:https://doi.org/10.1146/annurev.anthro.34.081804.120613
Smith, B. H. (1989). Dental development as measure of life history in primates. *Evolution, 43*(3), 683-688. doi:https://doi.org/10.1111/j.1558-5646.1989.tb04266.x
Smith, B. H., Crummett, T. L., & Brandt, K. L. (1994). Ages of eruption of primate teeth: A compendium for aging individuals and comparing life histories. *American Journal of Physical Anthropology, 37*(S19), 177-231. doi:https://doi.org/10.1002/ajpa.1330370608
Smith, H. F., Ritzman, T., Otárola-Castillo, E., & Terhune, C. E. (2013). A 3-D geometric morphometric study of intraspecific variation in the ontogeny of the temporal bone in modern Homo sapiens. *Journal of Human Evolution, 65*(5), 479-489. doi:https://doi.org/10.1016/j.jhevol.2013.01.017
Smith, S. L. (2004). Skeletal age, dental age, and the maturation of KNM-WT 15000. *American Journal of Physical Anthropology, 125*(2), 105-120. doi:https://doi.org/10.1002/ajpa.10376

Spoor, F., Leakey, M. G., Anton, S. C., & Leakey, L. N. (2008). The taxonomic status of KNM-ER 42700: A reply to Baab (2008a). *Journal of Human Evolution, 55*(4), 747-750.
Spoor, F., Leakey, M. G., Gathogo, P. N., Brown, F. H., Antón, S. C., McDougall, I., . . . Leakey, L. N. (2007). Implications of new early Homo fossils from Ileret, east of Lake Turkana, Kenya. *Nature, 448*, 688. doi:https://doi.org/10.1038/nature05986
Stringer, C. B. (1984). The definition of Homo erectus and the existence of the species in Africa and Europe. *Cour. Forsch. Inst. Senckenberg, Frankfurt am Main, 69*, 131-143.
Team, R. C. (2013). R: A language and environment for statistical computing.
Terhune, C. E., Kimbel, W. H., & Lockwood, C. A. (2013). Postnatal temporal bone ontogeny in Pan, Gorilla, and Homo, and the implications for temporal bone ontogeny in Australopithecus afarensis. *American Journal of Physical Anthropology, 151*(4), 630-642. doi:https://doi.org/10.1002/ajpa.22318
Terhune, C. E., Robinson, C. A., & Ritzman, T. B. (2014). Ontogenetic variation in the mandibular ramus of great apes and humans. *Journal of morphology, 275*(6), 661-677.
Turgut, S., & Tos, M. (2007). Correlation between temporal bone pneumatization, location of lateral sinus and length of the mastoid process. *The Journal of Laryngology & Otology, 106*(6), 485-489. doi:https://doi.org/10.1017/S0022215100119942
Vekua, A., Lordkipanidze, D., Rightmire, G. P., Agusti, J., Ferring, R., Maisuradze, G., . . . Zollikofer, C. (2002). A New Skull of Early Homo from Dmanisi, Georgia. *Science, 297*(5578), 85-89. doi:https://doi.org/10.1126/science.1072953
Viðarsdóttir, U. S., O'Higgins, P., & Stringer, C. (2002). A geometric morphometric study of regional differences in the ontogeny of the modern human facial skeleton†. *Journal of Anatomy, 201*(3), 211-229. doi:https://doi.org/10.1046/j.1469-7580.2002.00092.x
Viðarsdóttir, U. S., & Cobb, S. (2004). Inter-and intra-specific variation in the ontogeny of the hominoid facial skeleton: testing assumptions of ontogenetic variability. *Annals of Anatomy-Anatomischer Anzeiger, 186*(5-6), 423-428.
von Cramon-Taubadel, N., & Smith, H. F. (2012). The relative congruence of cranial and genetic estimates of hominoid taxon relationships: Implications for the reconstruction of hominin phylogeny. *Journal of Human Evolution, 62*(5), 640-653. doi:https://doi.org/10.1016/j.jhevol.2012.02.007
Weber, G. W. (2015). Virtual anthropology. *American Journal of Physical Anthropology, 156*, 22-42.

Figure captions:

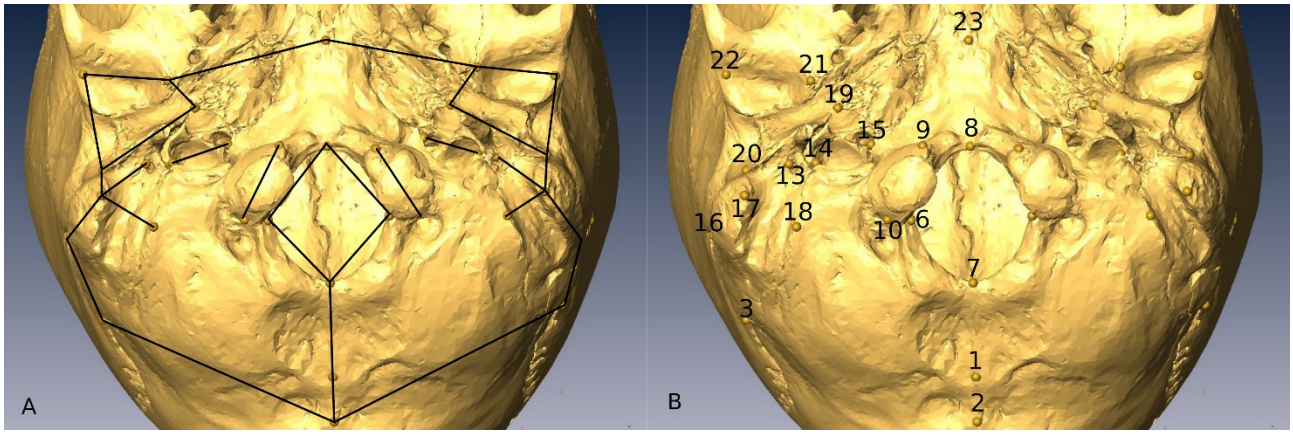

FIGURE 1. (a) Wireframe configuration and (b) Landmarks position.

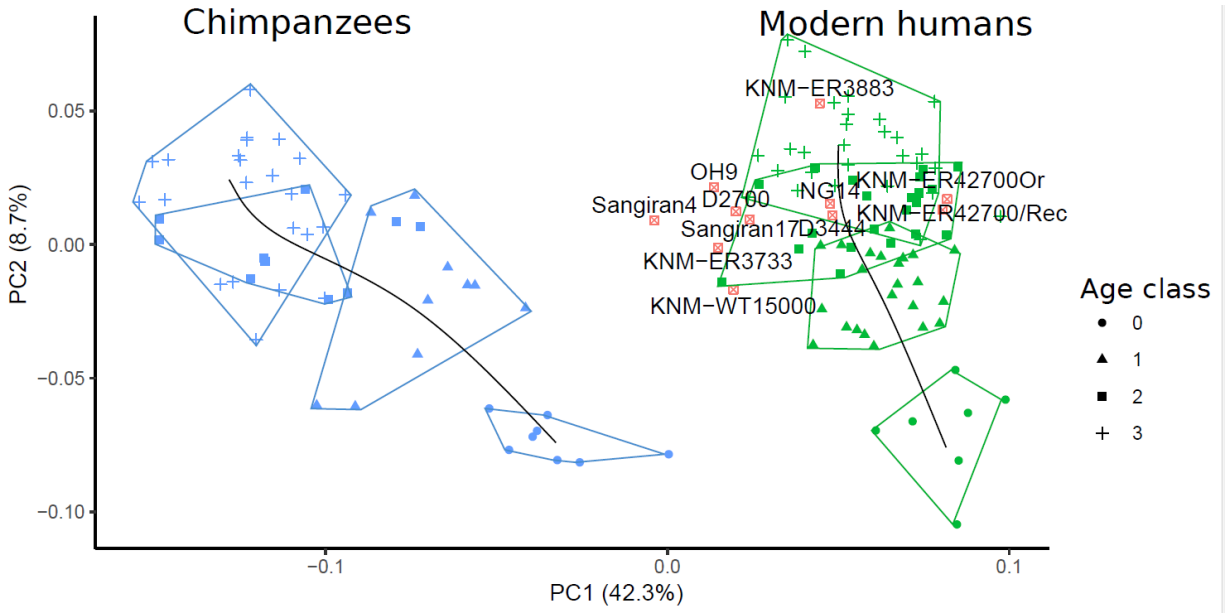

FIGURE 2. Trajectories comparison in PC1 and PC2. Colors: Blue = Chimpanzees, Green= Modern Humans, Red = Projected *H. erectus* . Symbols: ● = Age category 0, ■ = Age category 1, ▲ = Age category 2, + =Age category 3. Trajectories in bold line.

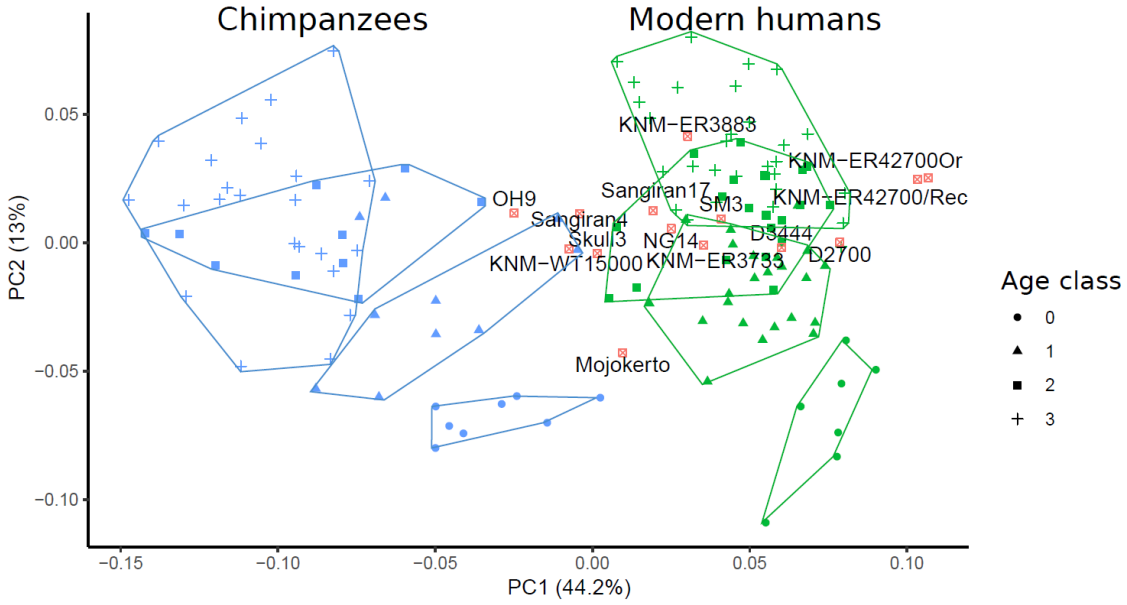

FIGURE 3. PCA plot for the Mojokerto dataset, PC1 and PC2. Colors: Blue = Chimpanzees, Green= Modern Humans, Red = Projected *H. erectus* . Symbols: ● = Age category 0, ■ = Age category 1, ▲ = Age category 2, + =Age category 3

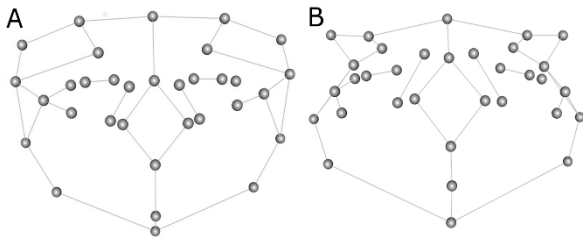

FIGURE 4. Shape change in inferior view along PC1. (a) Minimum PC1 values (chimpanzees), (b) maximum PC1 values (humans).

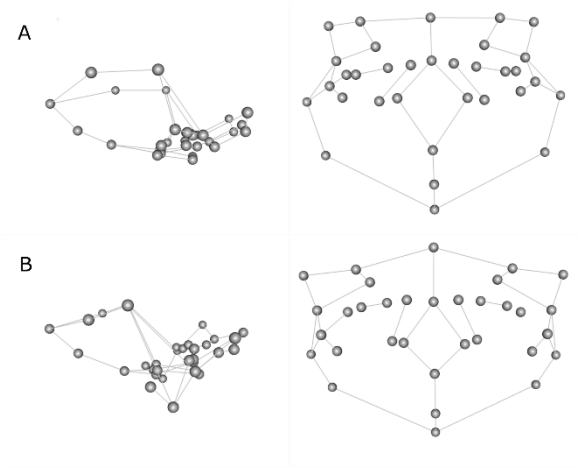

FIGURE 5. Shape change in lateral and inferior views along PC2. (a) Minimum PC2 values (infants), (b) maximum PC2 values (adults). In the lateral view, posterior side on the left, anterior side on the right.

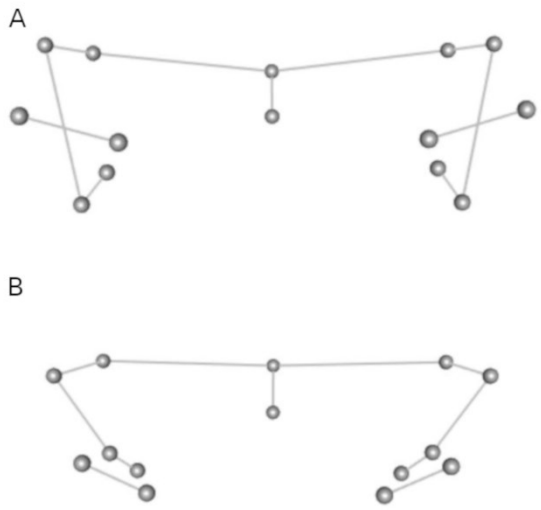

FIGURE 6. Shape change in frontal view along PC2 for the reduced dataset. (a) Maximum PC2 values, (b) minimum PC2 values.

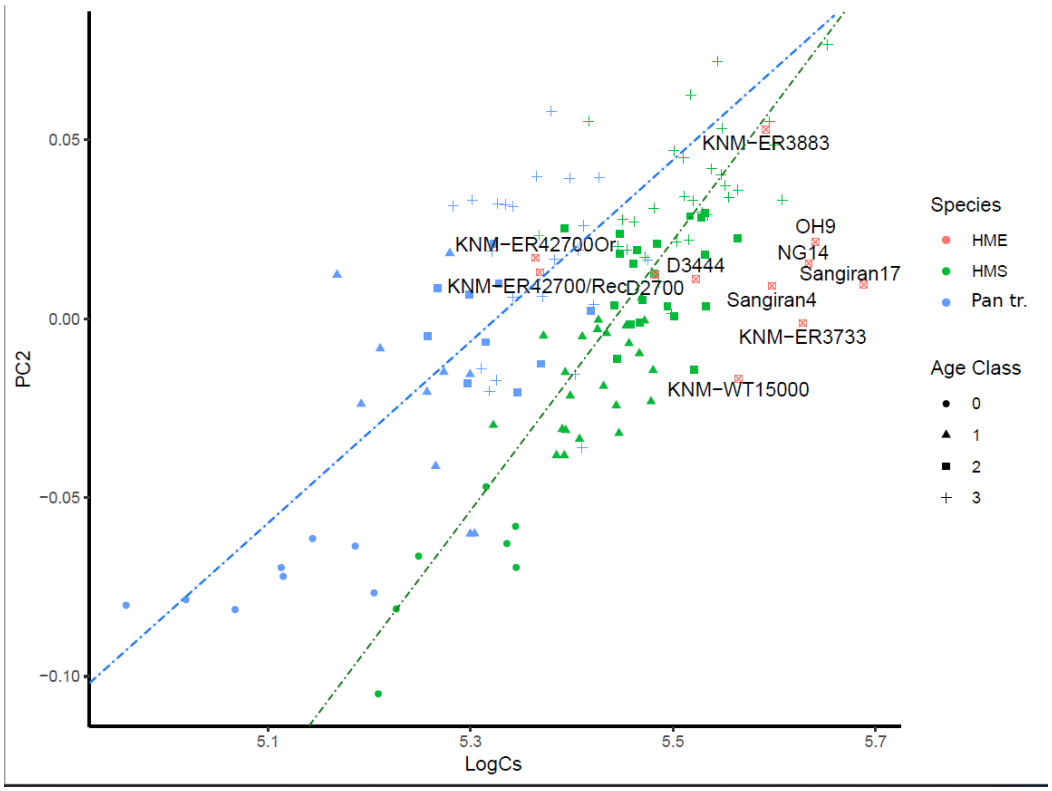

FIGURE 7. Plot LogCS/PC2 Colors: Blue = Chimpanzees, Green= Modern Humans, Red = *H. erectus s.l.*. Symbols: ● = Age category 0, ■ = Age category 1, ▲ = Age category 2, + =Age category 3, ◙=*H. erectus s.l.* Dashed lines represent specific regression line of LogCS onto PC2 (Green=modern human, Blue= chimpanzees)

TABLES:

	TABLE 1. Ontogenetic sample used			
Age group	Dentition	Sex	Humans	Chimpanzees
0	No molar erupted		7	8
		Female	4	2
		Male	3	1
		Unknown		5
1	First upper Molar erupted		23	10
		Female	3	3
		Male	10	1

		Unknown	10	6
2	Second upper Molar erupted		21	10
		Female	7	4
		Male	3	2
		Unknown	11	4
3	Third upper Molar erupted		29	23
		Female	15	14
		Male	14	9
		Unknown		
Total			80	51

TABLE 2. Sample Origin		
	Age Class	Origin (*subspecies*)
Chimpanzee	0	Unknown= 3 Liberia= 5 (*P. t. verus*)
	1	Unknown= 2 Liberia= 5 (*P. t. verus*) Gabon= 2 (*P.t. troglodytes*) Uganda= 1 (*P.t. schweinfurthii*)
	2	Liberia= 8 (*P. t. verus*) Gabon=2 (*P.t. troglodytes*)
	3	Unknown= 3 Liberia= 2 (*P. t. verus*) Gabon= 10 (*P.t. troglodytes*) Equatorial Guinea= 2 (*P.t. troglodytes*) Cameroon=3 (*P.t. troglodytes*) Uganda=1 (*P.t. schweinfurthii*) Cote d'Ivoire=2 (*P. t. verus*)
Modern humans	0	Italy= 7
	1	Italy=13 Germany=10
	2	Italy = 13 Germany= 8
	3	Italy = 15 Germany= 14

TABLE 3. Fossil sample used					
Fossil specimen[1]	Original (O) or Cast (C)	33 landmarks dataset	Mojokerto dataset	Developmental stage: Adult(A), Juvenile(J), Child(C)	Geographic origin
KNM-ER3883	O	X	X	A	Africa
OH9	O	X	X	A	Africa
KNM-WT15000	O	X	X	J (Smith 2004)	Africa
KNM-ER42700	C	X	X		Africa

KNM-ER3733	O	X	X	A	Africa
NG14	C	X	X	A	Asia
D3444	C	X	X	A	Georgia
D2700	C	X	X	J (Rightmire et al. 2006)	Georgia
S17	C	X	X	A	Asia
S4	O	X	X	A	Asia
NG14	C	X	X	A	Asia
Skull3	C		X	J (Antón 2002)	Asia
SM3	C		X	A	Asia
Mojokerto	C		X	C (Coqueugniot et al. 2004)	Asia

[1]Abbreviations: KNM-ER=Kenya National Museum East Rudolf; KNM-WT= Kenya National museum West Turkana; OH= Olduvai Hominin, S= Sangiran; NG= Ngandong; D= Dmanisi; Skull= Zhoukoutien, SM= Sambungmacan.

TABLE 4. Landmarks numbers and definitions		Mojokerto dataset
Landmark N*	Definition (Harvati and Weaver 2006; von Cramon-Taubadel and Smith 2012)	
1. Inion inf.	Point at which the inferior nuchal lines merge in the midline	X
2.Inion	Point at which the superior nuchal lines merge in the midline	X
3-4. Asterion R/L	Meeting point of the temporal, parietal, and occipital bones	X
5-6.Lateral Foramen magnum L/R	The most lateral point on the margin of the foramen magnum	
7. Opisthion	Midline point at the posterior margin of the foramen magnum	
8. Basion	Midline point at the anterior border of the foramen magnum	
9-11. Occipital condyle R. Anterior/L. Anterior	Most anterior point on long axis of the condyle, taken on the condyle	
10-12. Occipital Condyle R. Posterior / L. Posterior	Most posterior point on long axis of occipital condyle, taken on condyle	
13-24. Stylomastoid For. R/L	Middle of stylomastoid foramen (on temporal), at the level of surrounding bone	
14-25. Jugular For. R Anterior /L.Anterior	Most antero-medial point of the jugular fossa taken on occipital	
15-26. Jugular For. R. Post/L Post.	Most postero-lateral point of the jugular fossa take	
16-27. Parietal Notch R/L	Point on the posterosuperior border of the temporal where the squamosal and parietomastoid sutures meet	X
17-28. Mastoidiale R/L	Most inferior point on the mastoid process	X
18-29. Occipitomastoid crest R/L	Most inferior point on the juxtamastoid eminence	X
19-30. Medial petrotympanic crest R/L	Most medial point of petrotympanic crest at level of carotid canal	
20-31. Lateral petrotympanic crest R/L	Most lateral point of petrotympanic crest	
21-32. Inferior entoglenoid R/L	Most inferior point on the entoglenoid pyramid	X
22-33. Lateral articular fossa R/L	Deepest point on the lateral margin of the mandibular fossa	X
23 Sphenobasion	The midline point on the spheno-occipital suture	
*Abbreviation: R= Right, L= Left		

TABLE 5. Statistical assessment of differences in ontogenetic trajectories size ($MD_{H,P}$) , direction ($\Theta_{H,P}$), and shape (D_{Shape}) between modern human (H) and chimpanzees (P). Observed significant levels (P-values) were empirically generated from 9999 random permutations.

Comparison	$MD_{H,P}$	P_{Size}	$\Theta_{H,P}$	P_{θ}	D_{Shape}	P_{Shape}
H,P	0.043	0.02	45.94	0.0001	0.132	0.49

TABLE 6. Pairwise comparison with permutation test on PC2 scores per age category in the two taxa (p-value of each comparison)

		Modern Humans				Chimpanzees			
	Age	0	1	2	3	0	1	2	3
Modern humans	0		<0.0001	<0.0001	<0.0001	n.s.	<0.001	<0.0001	<0.0001
	1			<0.0001	<0.0001	<0.0001	n.s.	<0.001	<0.0001
	2				<0.0001	<0.0001	<0.01	n.s.	n.s.
	3					<0.0001	<0.0001	<0.0001	<0.01
Chimpanzees	0						<0.001	<0.0001	<0.0001
	1							n.s.	<0.01
	2								n.s.
n.s. = not significant									

Reference

Antón SC. 2002. Cranial growth in Homo erectus. Human evolution through developmental change:349-380.

Harvati K, and Weaver TD. 2006. Human cranial anatomy and the differential preservation of population history and climate signatures. The Anatomical Record Part A: Discoveries in Molecular, Cellular, and Evolutionary Biology 288A(12):1225-1233.

von Cramon-Taubadel N, and Smith HF. 2012. The relative congruence of cranial and genetic estimates of hominoid taxon relationships: Implications for the reconstruction of hominin phylogeny. Journal of Human Evolution 62(5):640-653.

Appendix II

This is the original article:

Mori, T., Profico, A., Reyes-Centeno, H., & Harvati, K. (2020). Frontal bone virtual reconstruction and geometric morphometric analysis of the mid-Pleistocene hominin KNM-OG 45500 (Olorgesailie, Kenya). *Journal of Anthropological Sciences*, *98*, 49-72.

doi 10.4436/jass.98022

JASs Reports
Journal of Anthropological Sciences
Vol. 98 (2020), pp. 49-72

Frontal bone virtual reconstruction and geometric morphometric analysis of the mid-Pleistocene hominin KNM-OG 45500 (Olorgesailie, Kenya)

Tommaso Mori[1,2], Antonio Profico[3,4], Hugo Reyes-Centeno[5,6,7] & Katerina Harvati[1,5]

1) Paleoanthropology, Department of Geosciences, Senckenberg Centre for Human Evolution and Palaeoenvironment, University of Tübingen, Tübingen 72070, Germany

e-mail: tommaso.mori@ifu.uni-Tübingen.de

2) Anthropology laboratory, Department of Biology, University of Florence, Via del Proconsolo 12, Florence, Italy

3) Dipartimento di Biologia Ambientale, Sapienza Università di Roma, Rome, Italy

4) PalaeoHub, Department of Archaeology, University of York, York, United Kingdom

5) DFG Center for Advanced Studies "Words, Bones, Genes, Tools", University of Tübingen, Rümelinstrasse 23,D-72070 Tübingen, Germany

6) Department of Anthropology, University of Kentucky, 211 Lafferty Hall, Lexington, KY 40506 USA

7) William S. Webb Museum of Anthropology, University of Kentucky, 1020 Export St, Lexington, KY 40504,KY USA

Summary - *KNM-OG 45500 is a hominin fossil composed of parts of a frontal bone, left temporal bone, and cranial vault pieces. Since its discovery along the Olorgesailie Formation (Kenya) in 2003, it hasbeen associated with the* Homo erectus *hypodigm. The specimen, derived from a geological context datedto ca. 900 Ka BP, has been described as a very small individual of probable female sex. However, despite its status as an important hominin specimen, it has not been used in a quantitative comparative frameworkbecause of its fragmentary condition. Here, we undertake a virtual reconstruction of the better-preserved fragment, the frontal bone. We additionally apply geometric morphometric analyses, using a geographically diverse fossil and modern human sample, in order to investigate the morphological affinities of KNM-OG 45500. Our results show that the frontal shape of KNM-OG 45500 exhibits similarities with EarlyPleistocene fossils from Eurasia and Africa that are assigned to H. erectus sensu lato (s.l.). Its size, on the other hand, is notably smaller than most other* Homo erectus *fossils and modern humans and similar to the specimens from Dmanisi (Georgia) and to* Homo naledi*. Taken together, our analyses of the frontal bone suggest a taxonomic attribution of KNM-OG 45500 to H. erectus s.l. and extend even further the range of size variability associated with this taxon around 900 Ka BP.*

Keywords - Homo erectus*, Shape analysis, Frontal bone, Geometric morphometrics, Virtual anthropology.*

Introduction

The taxonomic attribution of Pleistocene (following Gibbard *et al.,* 2010) fossils to *Homoerectus* has been highly debated by paleoanthro- pologists in the last decades. No full consensus exists among scientists regarding the definition of the *erectus* hypodigm (Stringer, 1984; Wood, 1984; Rightmire, 1990; Tattersall, 1992; Wolpoff *et al.*, 1994; Schwartz & Tattersall, 2000; Wood & Richmond, 2000; Antón, 2003; Schwartz, 2004; Antón, 2007; Terhune *et al*., 2007; Baab,2008b, 2016; Lordkipanidze *et al.*, 2013; Antón *et al*., 2014; Bauer & Harvati, 2015; Mori & Harvati, 2019). The most restricted conceptionof *H. erectus* (*sensu stricto*) limits the species to specimens from the Asian fossil record, which include the holotype from Trinil, while African

specimens are often attributed to *H. ergaster* (Dubois, 1894; Stringer, 1984; Wood, 1991; Wolpoff *et al.*, 1994; Schwartz & Tattersall, 2000). On the other hand, a commonly accepted definition of *H. erectus (sensu lato)* puts togetherspecimens from Africa and Eurasia, unifying Pleistocene fossils otherwise attributed to differ- ent *Homo* taxa, including *ergaster*, *georgicus*, and *soloensis* (Antón, 2003; Rightmire *et al*., 2006; Zeitoun *et al.*, 2010; Lordkipanidze *et al.*, 2013; Rightmire, 2013; Baab, 2015).

Different authors have tried to investigate the patterns of variation between geographicor chronological groups within the broadly defined *H. erectus* hypodigm (Rightmire, 1981, 1990; Stringer, 1984; Wood, 1992; Kidder & Durband, 2004; Terhune *et al.*, 2007; Baab, 2008b, 2016; Zeitoun *et al.*, 2010). Some of the recent studies have interpreted the fossil record as reflecting a single lineage (e.g. Suwa *et al.*, 2007; Lordkipanidze *et al.*, 2013) while others proposea view of species diversity in the Early Pleistocene (e.g. Baab, 2008a; Leakey *et al.*, 2012; Antón,Potts & Aiello, 2014; Spoor *et al.*, 2015). A recent reconstruction and analysis of Olduvai Hominin 7 (OH 7) from Olduvai Gorge (Tanzania), the holotype specimen of *H. habilis* (Spoor *et al.*, 2015), seemingly confirmed the latter hypoth- esis. However, whereas Spoor and colleagues (2015) highlighted from this reconstruction that early *Homo* groups were distinct also on the basisof different brain sizes, Antón *et al.* (2014) had rejected size as a defining feature of "early *Homo*" groups. Spoor *et al.* (2015) also suggested that, given the dissimilarities between both *H. habilis* and other "early *Homo*" specimens, these early Pleistocene eastern African fossils comprised multiple species. This is particularly important in light of recently described *Homo species novo*in the Middle and Late Pleistocene, including *H. naledi* (Berger *et al.*, 2015), *H. luzonensis* (Détroit *et al.*, 2019), and *H. floresiensis* (Brown*et al.*, 2004). Similarly, taxonomic diversity in later fossils dated between 1.8 MA BP and 900Ka BP from Africa and Eurasia is highly debated (Wood, 1994; Schwartz & Tattersall, 2000; Vekua *et al.*, 2002; Antón, 2003; Potts *et al.*, 2004; Schwartz, 2004; Gilbert & Asfaw, 2008;Baab, 2016). While the fragmentary fossil recordremains a limitation, what has become clear isthat the pattern of within-sample variation in Pleistocene hominin groups is often complex andunderstanding whether this variability represents multiple taxa or not is hotly debated. The small specimens from Dmanisi (Georgia), for example,have shown the existence of high morphological variability in what is considered by most scholars a single paleodeme (Howell, 1999; Vekua *et al.*, 2002; Rightmire *et al*., 2006; Lordkipanidze *et al.*, 2013). Given the fragmentary status of other fossils, however, some specimens are rarely stud- ied or included as comparative material, thus reducing the possibility to have a more complete picture regarding the evolutionary relationship between different geographic and temporal fossilgroups. This is the case for KNM-OG 45500,a hominin fossil recovered from the Olorgesailie formation, Kenya (Potts *et al.*, 2004).

The KNM-OG 45500 (also referred to as KNM-OL 45500 in the literature) fossil was recovered *in situ* in 2003 in a stratigraphic layer rich with Acheulean handaxes (Potts *et al.*2004). Volcanic layers underlying and overlying KNM-OG 45500 have been dated using the sin- gle-crystal $^{40}Ar/^{39}Ar$ method to between ca. 974 and 747 ka. Because of its close association to the lower layer, a geological age between 970 and 900 ka has been proposed for this specimen (Potts *et al.*, 2004). KNM-OG 45500 has been described as one of the smallest African *Homo erectus s.l.*, alongside the recently published DAN5/P1 fossilfrom the Dana Anoule North site of the Busidima Formation (Gona, Ethiopia) (Semaw *et al.* 2020) and the KNM-ER 42700 specimen fromthe Koobi Fora Formation (Spoor *et al.*, 2007;Neubauer *et al.*, 2018; Mori & Harvati, 2019), dated to ca. 1.6-1.5 Ma. KNM-OG 45500's frontal bone shows midline keeling, a shelf-like morphology of the post-toral sulcus, a lack of torsion in the toral anterior surface, and double-arched supraorbital shape (Potts *et al.*, 2004). Its endocranial volume (ECV) is estimated to be lessthan 800 cm^3, similar in size to the DAN5/P1 fossil (Semaw *et al.* 2020), as well as to the D2282

and D2280 specimens from Dmanisi (Georgia), which date to ca. 1.8 Ma and are assigned by most authors to *Homo erectus s.l.* (Vekua *et al.*, 2002; Antón, 2004; Potts *et al.*, 2004; Rightmire *et al.*, 2006, 2019; Lordkipanidze *et al.*, 2013). KNM-OG 45500 exhibits an overall smaller size than Early Pleistocene fossils from Kenya (e.g. KNM-ER3733 and KNM-WT15000, dated to between 1.8-1.5 Ma), but closer to the later OH12 fossil from Olduvai (dated to ca. 1.2-1.1 Ma) (Rightmire, 1979; Tamrat *et al.*, 1995)1995. In contrast, the morphology of the double-arched supraorbital torus is considered similar in shape to other African fossils, such as the Early Pleistocene specimen Daka BOU-VP-2/66 (Ethiopia) and KNM-ER3733 (Kenya)(Potts *et al.*, 2004).

The frontal bone, especially the morphology of the supraorbital torus, has been used to distinguish between different morphs of *H. erectus s.l.* (Stringer, 1984; Wood, 1984; Rightmire, 1990; Antón, 2003; Schwartz, 2004; Baab, 2015, 2016). More generally, the frontal bone is considered useful in reconstructing hominin phylogeny and population history in modern humans (Weidenreich, 1940; Smith, 2009; von Cramon-Taubadel, 2009; Athreya, 2012; Freidline *et al.*, 2012; von Cramon-Taubadel & Smith, 2012). Many of the morphological characters that are used to define *H. erectus s.l.* involve cranial superstructures: localized hypertrophies of the bones in the form of tori, crests, and keels. These features, however, are not always easy to quantify. The grade of frontal keeling, supraorbital morphology, and frontal profile are difficult to capture with standard morphometric approaches (Weidenreich, 1940; Athreya, 2012). Geometric morphometric (GM) methods, on the other hand, can help quantify such morphologies and provide the possibility to quantitatively compare different fossils in order to better evaluate the morphological differences and similarities between them (Rohlf & Slice, 1990; Bookstein, 1991; Slice, 2007; Mitteroecker & Gunz, 2009; Freidline *et al.*, 2012; Aytek & Harvati, 2016). In this framework, we aim to analyze the morphology of the more complete frontal fragment belonging to KNM-OG 45500.

Our primary objectives are (1) to undertake a reconstruction of the frontal bone of KNM-OG45500 and (2) to apply GM methods for the comparative analysis of this reconstruction, in order to assess the morphological affinities of this specimen with other African, Asian, and European early and mid-Pleistocene hominin fossils. Furthermore, we aim to address the ques-tion of intra-specific morphological variation in the Pleistocene human fossil record by compar-ing the range of variation in form (shape and size) within *H. erectus s.l.* to that observed withina broad geographic sample of modern humans.

Materials and methods

Frontal bone reconstruction

The frontal bone reconstruction of KNM-OG 45500 aims to account for possible taphonomic deformation and fragmentation. While the KNM-OG 45500 frontal bone pre- sents an almost complete supraorbital torus, the left margin of the supraorbital region is broken and the left part of the frontal squama is missing two fragments posteriorly. The right part of the supraorbital torus is abraded due to taphonomic processes, but laterally it is more complete than the left side and it reaches close to the frontozy- gomatic suture. Posteriorly, the coronal suture seems to be preserved only in the lateral part of the right side, with a preserved sphenofrontalis suture and stephanion. While bregma is missing,Potts *et al.* (2004) suggested that the squama is broken roughly 10 mm anterior to it.

The reconstruction was performed via mirroring of the preserved left structures on the right side and *vice versa,* a commonly applied procedure in virtual reconstruction (Gunz *et al.*, 2009; Bauer & Harvati, 2015; Weber, 2015; Harvati *et al.*, 2019), using the Avizo software(version 9.1, Thermo Fischer Scientific) and the transform function in the Meshlab software (v2016.12) (Cignoni *et al.*, 2008). The speci- men was mirrored using the transform flip axisfunction in the Meshlab software (v2016.12) (Cignoni *et al.*, 2008). We manually aligned,

Tab. 1 - Modern humans' populations origin.

POPULATION	N (M/F/U)	COLLECTIONS
Australia (Aborigines)	6 (3/3/0)	American Museum of Natural History, New York
Europe (Italy)	5 (2/3/0)	Museo di Storia Naturale, Florence
Chile (Tierra del Fuego)	2 (0/2/0)	Naturhistorisches Museum,Vienna
Sri Lanka	4 (0/0/4)	University Museum, Tübingen
China	5 (0/0/5)	Musee de l'Homme, Paris
Philippines	5 (0/0/5)	Musee de l'Homme, Paris
Tanzania (Masai)	2 (0/0/2)	University Museum, Tübingen

in Avizo software (version 9.1, Thermo Fischer Scientific) the mirrored version to the original one using both homologous anatomical struc- tures and the midsagittal plane as reference. The midsagittal plane is defined by a landmark approximating bregma (the midline point on the posterior edge), glabella, and the mid-toral sulcus. The mirrored specimen aligned well withthe original specimen along the orbital roof, the supraorbital region, and the medial portionof the frontal squama. We used the mirrored version of KNM-OG 45500 to reconstruct the missing portions of the left lateral frontal squama and lateral supraorbital region and theabraded right supraorbital torus.

Reference sample

Our comparative sample comprises 30 recent modern human adults. The sampling strategy was designed to capture as much variation as possible in recent human populations via world- wide coverage, the inclusion of both sexes, and groups known for their relatively smaller body size. The samples are derived from museum col-lections and are no older than a few hundred years (see Table 1 for specific geographic origin, sex, and housing institution information). One population, from the Philippines, comprises individuals of short stature (Reyes-Centeno *et al.*, 2014). 3D surface models of the specimens were obtained from medical computed tomog- raphy (CT) scans or micro-CT scans using the Avizo software (Noback & Harvati, 2014, 2015; Bosman *et al.*, 2019; Bosman, Reyes-Centeno &Harvati, 2020).

The fossil comparative sample comprises 20 specimens from different chronological periods and geographical areas. The 3D surface mod- els were derived from CT scans of the original specimens or optical surface scans of high-qual- ity casts (Tab. 2). Our sample comprises several *H. erectus s.l.* fossils spanning the Pleistocene, other Middle to Late Pleistocene *Homo* speci- mens sometimes attributed to *H. rhodesiensis*/ *heidelbergensis* (Broken Hill, Bodo, Petralona, Dali) and early *H. sapiens* (Jebel Irhoud 1, Skhūl V), as well as two other small-sized hominins:the Early Pleistocene MH 1 *A. sediba* type speci- men and the composite cranial reconstruction of *H. naledi* based on the DH1 holotype & DH3 paratype specimens named "naledi" in all fol- lowing analyses and text (Berger *et al.*, 2015; Schroeder *et al.*, 2017). While the mix of optical and tomographic scans from both original fos-sils and fossil casts could represent a source ofmeasurement error, previous work has shown that maximum surface deviations between original fossils and high-quality hominin fossil casts are minimal (Ponce De Leon & Zollikofer, 1999). Moreover, concerns over possible tech-nical and data source errors were mitigated in our study by the relatively dense landmark cov-erage and the sliding procedure of the surface semi-landmarks. We note that two of the fossil comparative specimens (M.H. 1 and D 2700) are sub-adults. In M.H. 1, third molars have not erupted but second molars are in occlusion,whereas D2700 exhibits an erupted M3 that is not in occlusion (Vekua *et al.*, 2002; Berger *etal.*, 2010). Furthermore, D2282 is described asa near-adult due to the lower M3 being "newly" erupted in terms of dental wear (Rightmire *et al.*, 2006).

Tab. 2 - Fossil sample used. Abbreviations: MH= Malapa Hominin, D= Dmanisi, KNM= Kenya NationalMuseums, ER=East Rudolf, OG= Olorgesailie, DH= Dinaledi Hominin, AMNH=American Museum of Natural History

FOSSIL SPECIMEN	CAST/ ORIGINAL	INSTITUTION	CHRONOLOGICAL AGE
Au. sediba			
MH 1[1]	C	AMNH	1.97 Ma (Pickering *et al.*, 2011)
H. erectus s.l.			
D 2280	C	AMNH	1.77 Ma (Garcia *et al.*, 2010)
D 2700[1]	C	AMNH	1.77 Ma (Garcia *et al.* 2010)
D 3444	C	AMNH	1.77 Ma (Garcia *et al.* 2010)
D 2282[1]	C	AMNH	1.77 Ma (Garcia *et al.* 2010)
Daka BOU-VP-2/66	O	National Museum of Ethiopia	1 Ma – 780 Ka (Asfaw *et al.*, 2002)
KNM-ER 3733	O	Kenya National Museum	1.63 Ma (Lepre & Kent, 2015)
KNM-ER 3883	O	Kenya National Museum	1.53 Ma (McDougall *et al.*, 2012)
Ngandong 14	C	AMNH	118-108 Ka (Rizal *et al.*, 2020)
Sangiran 17	C	AMNH	1.2 Ma/900 Ka (Larick *et al.*, 2001; Matsu'ura *et al.*, 2020)
Sambungmacan 3	C	AMNH	60-70 Ka (Yokoyama *et al.*, 2008)
Zhoukoudian I	C	AMNH	700-400 ka (Shen *et al.*, 2009)
Zhoukoudian 12	C	AMNH	700-400 ka (Shen *et al.* 2009b)
Middle-Pleistocene *Homo* (MPH)			
Bodo	O	National Museum of Ethiopia	640-550 Ka (Rightmire, 1996)
Broken Hill 1 (Kabwe)	C	AMNH	700 - 200 ka (Buck & Stringer, 2015)
Petralona	O	Aristotle University of Thessaloniki	700-150 Ka (Grün, 1996)
Dali	C	AMNH	270-180 Ka (Xiao, Jin & Zhu, 2002)
H. naledi			
H. naledi (DH1 & DH3 composite reconstruction)	C	University of the Witwatersrand	200-300 Ka (Dirks *et al.*, 2017)
Early *H. sapiens* (EHS)			
Jebel Irhoud 1	C	AMNH	300-90Ka (Grün & Stringer, 1991; Richter *et al.*, 2017)
Skhūl V	O	Peabody Museum, Harvard University	120-80 Ka (Grün, 2006)
Unknown			
KNM-OG 45500[2]	O	National Museums of Kenya	900 Ka (Potts *et al.*, 2004)

[1] Sub-adult specimens

[2] Also published as KNM-OL 45500. KNM-OG 45500 follows the accession number at the National Museums of Kenya.

Tab. 3 - Landmark number and definition.

	DEFINITION (BAAB, 2016)
1. Bregma	Posterior border of the frontal bone along the midsagittal plane.
2. Midline post-toral sulcus	Minima of concavity on midline post-toral frontal squama.
3. Glabella	Anterior-most point on frontal bone in Frankfort horizontal in the midsagittal plane.
4/6 Mid-torus inferior R/L	Inferior margin of superior margin of orbit roughly at the middle of the orbital margin.
5/7 Mid-orbital superior R/L	Superior point on the supraorbital torus at the middle of the orbital margin.
8/9 Frontotemporale R/L	Point where the temporal line reaches its most anteromedial position on the frontal.
10/11 Stephanion R/L	Point where the temporal line reaches the coronal suture.

Landmark and semilandmark configurations
We collected a total of 80 landmarks on thefrontal bone. Of these, 11 correspond to com- mon osteometric points (i.e. Type 1-3 landmarks*sensu* Weber & Bookstein, 2011). A list and definition of these are presented in Table 3. Twosemi-landmark curves (i.e. Type 4 landmarks, *sensu* Weber & Bookstein, 2011) along each superior temporal muscle line were digitized from *stephanion* to the frontozygomatic suture. A total of 14 evenly-spaced semilandmarks were placed on each curve. In order to fully investigatethe shape of the frontal squama and the supraor- bital torus, we used a patch of 41 surface semilan- dmarks defined on KNM-OG 45500 (i.e. Type 6 landmarks, *sensu* Weber & Bookstein, 2011)encompassing the space between the identifiedlandmarks (i.e. between the superior temporal muscle line and the supraorbital region).
In KNM-OG 45500, bregma is the only missing landmark. The estimation was per- formed by using anatomical landmarks and the semilandmark configurations mentioned above (Gunz *et al.*, 2009). The template (digi- tized on KNM-OG 45500) without bregma was projected onto the specimens (for a total of 10 landmarks, 28 curves semilandmarks and 41 sur-face semilandmarks). Projection of the template semilandmarks was performed using the place- Patch function from the R package "Morpho" (Schlager, 2017). This projection proceduredeforms the template onto every specimen target by thin-plate-spline (TPS) interpolation based on the target's landmarks and curve semiland- marks (Bookstein, 1989; Slice, 2007). After this step, the deformed coordinates are projected onto the target mesh. After projection, we slid the surface semilandmarks using the minimum bending energy criterion to guarantee landmarkcorrespondence across specimens (Gunz *et al*., 2005). Then, we reintroduced bregma taken onthe complete specimens and estimated the posi-tion of bregma on KNM-OG 45500. To estimate bregma in KNM-OG 45500, we used the ThinPlate Spline (TPS) algorithm (Bookstein, 1989) choosing as reference fossil the specimens with close shape affinity. Specifically, we performed four different estimations of bregma by calcu- lating the weighted mean using, respectively: i) the two closest specimens to KNM-OG 45500 in Procrustes distance, followed by ii) the fourclosest specimens, iii) the six closest, and iv) the eight closest specimens. In addition to the four estimated landmark configurations, we included a parsimonious fifth landmark configuration without reference specimens, instead defining the position of bregma as the most posterior point on the KNM-OG 45500 frontal squama along the midsagittal plane, as in the mirroring reconstruction procedure. TPS substitution was used because it performs better in estimation when the same taxon reference or closely relatedtaxon reference samples are available (Neeser *et al*., 2009).

The Euclidean distance between the reconstructed and unreconstructed bregma is 8 mm in 3 reconstructions and 12 mm in one reconstruction. Finally, we included all the five landmark configurations of KNM-OG 45500 as individual specimens in the subsequent statistical analyses.

The complete landmark configuration for subsequent analyses was obtained by projecting surface semilandmarks from a template onto each specimen using the same method described above. The template used was KNM-OG 45500's configuration with bregma defined as the midline point at the posterior edge of the frontal squama. The choice of the template does not influence the final results in the analyses (Mitteroecker & Gunz, 2009) because ultimately we guarantee correspondence among landmarks thanks to the sliding procedure (Gunz *et al.*, 2005). The position of all landmarks is presented in Figure 1. All landmarks were digitized by the same observer (T.M.). To estimate the measurement error of fixed landmark acquisition, we digitized the same specimen 10 times in 10 different days for the 11 Type 1-3 landmark configurations. Subsequently, intra-observer error was evaluated for each landmark based on a relative standard deviation threshold of 5%. For all 11 landmarks, the error was between 2-3.5% relative standard deviations and thus all landmarks were used for subsequent analysis.

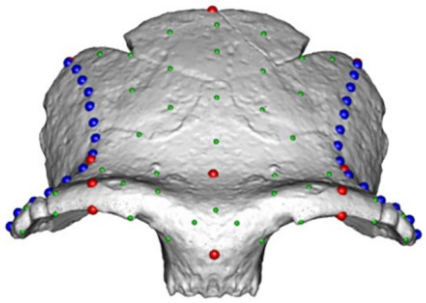

Fig. 1 - Landmark (red dots) and semilandmark (curves= blue, surface= green) configuration shown on the reconstructed Olorgesailie homi-nin KNM-OG 45500. [Image adapted from scan courtesy of the National Museums of Kenya]. The colour version of this figure is available at the JASs website.

Shape and form analysis

To explore variation in frontal bone shape in our sample, we conducted two analyses: one thatused both our fossil and modern human groupsand a subsequent one that used only the fossil specimens. In each case, curve semilandmarks and the projected surface semilandmarks were slid using the minimum bending energy criterion in order to guarantee landmark correspondence across specimens (Gunz *et al*., 2005). Thereafter, the landmark configurations of the comparative sample were superimposed with generalized Procrustes analysis (GPA) (Gower, 1975; Rohlf & Slice, 1990; Bookstein, 1991), in which the sum of squared distances between corresponding landmarks is minimized by rotation, translation, and scaling. After GPA superimposition, a prin- cipal component analysis (PCA) on the covari-ance matrix of the Procrustes coordinates was used to visualize and explore the shape space. The KNM-OG 45500 configurations (four with bregma estimated via TPS and one without bregma estimation) were then projected in the shape space. The landmark configurations of the five reconstructions were superimposed via GPA on the Procrustes mean shape of the reference sample. In this way, neither the PCA axes nor the Procrustes coordinates of our reference sam- ple were influenced by KNM-OG 45500 itself,therefore treating it as an unknown. PCA doesnot use *a priori* group categorization. Group variation along major PC axes of variation was visualized *a posteriori* by applying convex hulls (Mitteroecker & Bookstein, 2011). Shape vari- ation along PCA was visualized as a deforma- tion of a 3D surface mesh derived from the mean GPA landmark configuration. Vertices of the 3D surface mesh are the landmarks and semilandmarks used in the analysis. The mean surface was transformed via TPS interpolation (Bookstein, 1989) along 2 standard deviations (std. dev.) of a given PC axis.

Following GPA, two variables useful for assessing form variation and specimen affinities

are generated: centroid size and Procrustes dis-tance. Centroid size, calculated as the square root of the summed squared distances of the landmark coordinates from their centroid, is an indicator of relative size differences between individuals in a sample (Rohlf & Slice, 1990; Bookstein, 1991; Slice, 2007; Mitteroecker & Gunz, 2009). In this study, the size of the frontalbone is expressed by the logarithm of centroidsize (logCS). Size variability (range of logCS) in modern humans was used as a proxy to compare size variability in our fossil sample.

Procrustes distance, calculated as the square root of the sum of squared differences between two superimposed landmark configurations, is a measure of overall shape similarity between two landmark configurations, and therefore between two specimens. Following our second analysis, the pairwise Procrustes distance matrix between all fossil specimens in our sample was used to perform a cluster analysis with the unweighted pair group method using arithmetic averages (UPGMA) (Sokal, 1958). This approach itera-tively quantifies the similarity between two fos-sils and generates clusters of all sampled speci- mens in a rooted dendrogram, where all tips are of equal distance to the root. In this analysis, the four reconstruced specimens were reduced to a single individual by calculating the mean pair-wise Procrustes distances of their configurations to other specimens.

Finally, following the second analysis with the fossil subset, we applied a Spearman cor- relation test between each PC and logCS to evaluate whether the PCs had an allometric component. We performed this test twice, the first time using all the fossil comparative sam-ple without KNM-OG 45500 and then using only the fossil sample grouped as *H. erectus s.l.,* removing KNM-OG 45500 from the analy-sis. All of the procedures described above were conducted in R (R Core Team, 2018) using the "Morpho," "Arothron," and "Phangorn" pack- ages (Schliep, 2010; Schlager, 2017; Profico *et al.*, 2018). The raw dataset and R code used can be provided by the corresponding author upon request.

Results

The KNM-OG 45500 reconstruction is presented in Figure 2. The reconstructed parts, shown in grey, are the right supraciliary arch and left margin of the supraorbital torus at the height of the zygomatic process of the frontal bone. This part of the bone, however, is abraded and not restored in its thickness, which could be slightly reduced compared to its likely original condition. The abraded part extends for ca 1,2 cm laterally. The abrasion removed very little of the bone material in this area, as shown in Figure 2. The left side of the frontal squama was also restored based on the right morphology, which appears undistorted. The overlap of the fron- tal squama between the original and mirrored specimens (mixed gray and red color in Fig. 2)suggests a symmetric, undistorted medial por- tion of the frontal bone. The original lateral left portion, instead, is taphonomically fractured and probably placed in a lower position compared to its original morphology. Laterally the left side of the frontal squama has therefore been recon- structed using the posterolateral coronal margin of the right side (Fig. 2).

A plot of the first two principal components, accounting for over 80% of the total variance, resulting from the first PCA performed on the entire comparative sample is shown in Figure 3. It shows a clear separation between the recent modern humans and the fossil specimens, mostly along PC1. PC2, on the other hand, dif-ferentiates the Middle Pleistocene *Homo* speci- mens (Bodo, Dali, Petralona, and Broken Hill/ Kabwe) from the *Homo erectus* and *Homo sapi- ens* samples. Fossils in this plot show a degree of temporal clustering along PC1 and PC2. Early Pleistocene *H. erectus s.l.* specimens tend to have lower PC1 scores than Middle and late Pleistocene fossils. D2280 and KNM-ER 3733 exhibit the lowest PC1 among *H. erectus s.l.* andSambungmacan 3 the highest score. The DH1 & DH3 composite reconstruction of the *H. nal-edi* specimen plots outside the variation of other fossils, with low PC1 and PC2 scores. Shape variation associated with positive PC1 scores is

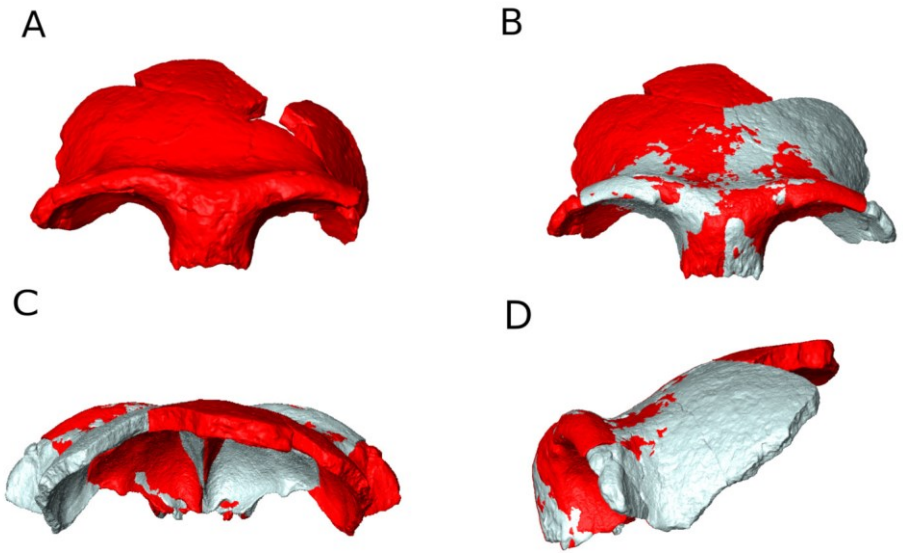

Fig. 2 - KNM-OG 45500 Reconstruction: (A) Original specimen (dark red); (B) frontal view of super-imposition of the mirrored specimen (light grey) on the original one in order to reconstruct the missing areas; (C) posterior view; (D) lateral view. [Image scan courtesy of the National Museumsof Kenya]. The colour version of this figure is available at the JASs website.

linked to a more globular frontal squama with a much higher bregma position. At negative PC1 scores, the frontal morphology exhibits a "shelf-like" condition, with a projected glabellar region and a clear supraorbital torus with an evident post-toral sulcus. In addition, temporal lines are more medially displaced and relatively longer along negative PC1 scores than in positive PC1 values, while positive PC1 exhibits a more latero-inferiorly placed and more arched temporal line. The lateral supraorbital region shows a flexion inferior to the frontozygomatic area for positive PC1. PC2 scores are linked to the supraorbital morphology and the relative size of the frontal squama. Positive scores of PC2 are related to a more robust, thicker, and laterally wider supraor-bital torus with a relatively bigger supraorbital region compared to the shorter frontal squama. Negative values of PC2 show a more posteriorly elongated temporal line and relatively elongated frontal squama compared to the supraorbital region. The five reconstructions of KNM-OG 45500 plot in different positions of shape space, though all fall within or closest to the *H. erec-tus s.l.* convex hull. Overall, they all fall with the Early Pleistocene *H. erectus s.l.* fossils. The configuration where bregma was taken on the posterior margin of the frontal squama (labeled "KNM-OG 45500" in Fig. 3) plots well withinthe *H. erectus s.l.* convex hull of the group; while those where bregma was reconstructed (labeled "KNM-OG 45500 rec" in Fig. 3) plot on the margin of the *H. erectus s.l.* convex hull, associ- ated with lower PC2 scores.

The second analysis was performed only on the fossil samples. Results are presented in thePCA plot in Figure 4 and closely mirror those of the first analysis. Here, PC1 and PC2 account for ca. 64% of the total variance. Similar to thefirst analysis, D2280 and KNM-ER 3733 exhibitthe lowest PC1 scores in the *H. erectus s.l.* group, while Sambungmacan 3 has the highest PC score. Shape variations associated with this component are similar to PC1 shape variation from the first analysis, albeit exhibiting a notably lower degreeof frontal bone globularization in the absence of

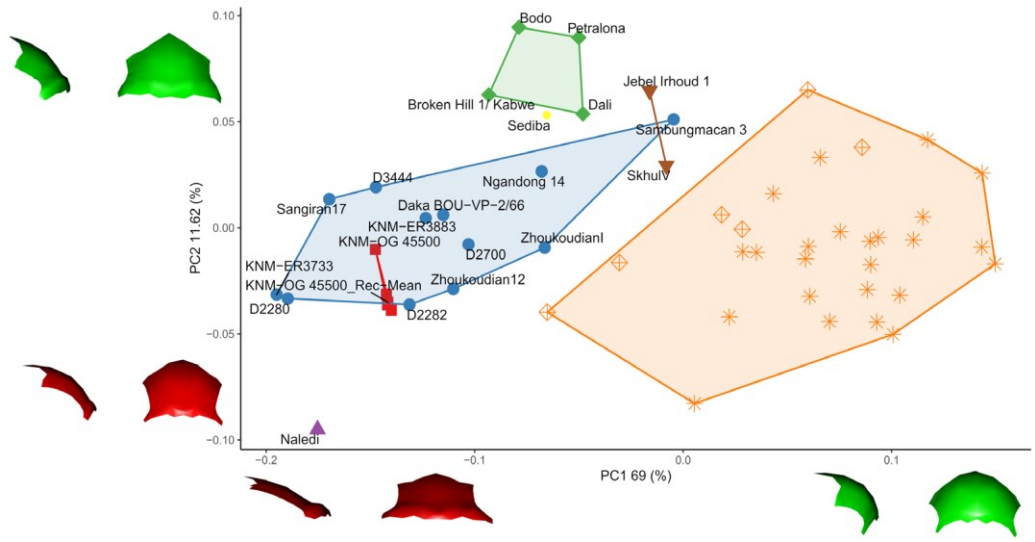

Fig. 3 - PCA plot of fossil specimens and recent modern humans. Convex hulls based on group attribu- tion from Table 2. Colors and shape: orange symbols = recent modern humans (Australian in crossed diamond); blue circle*= H. erectus s.l.*; green diamond= Middle-Pleistocene Homo; brown downward triangle= early* H. sapiens*; yellow small circle*= Au. sediba*; purple triangle*= H. naledi*; red square = KNM-OG 45500. Surfaces (frontal and lateral view) are shape transformations along +/-2 std. dev. from mean along PC axes. The colour version of this figure is available at the JASs website.

the modern human sample. Along PC2, MiddlePleistocene *Homo* fossils tend to have higher values while early *Homo sapiens* and later Asian
H. erectus s.l. have lower PC2 scores. *H. erectus*
s.l. show both high and low values, with Early Pleistocene specimens toward the positive end and Middle-Late Pleistocene fossils toward the negative end. Positive scores of PC2 are associ- ated with a thicker morphology of the supraor-bital torus, an overall more robust structure, and a proportionally smaller frontal squama. Again, KNM-OG 45500 with the unreconstructed bregma plots well within the *H. erectus s.l.* con- vex hull and the reconstructed specimens fall on the border of the convex hull. This second analysis highlights more the degree of temporal differentiation seen in the first PCA between our sampled *H. erectus s.l.* specimens. Similarly to the first analysis, Middle to Late Pleistocene East and Southeast Asian specimens tend to have higher PC1 and lower PC2 scores, closer to fossil
H. sapiens. By contrast, Early Pleistocene African and Eurasian fossils have lower PC1 and higherPC2 scores distributions.
Results of pairwise Procrustes distances between all the specimens included in the second analysis are presented in the Supplemental online Material. The individuals closest in overall shape to KNM-OG 45500 are D3444, KNM-ER 3733, Zhoukoudian12, and KNM-ER 3883, respectively, all *H. erectus s.l.* The individuals clos-est in overall shape to the mean configuration of the reconstructed bregma specimens (KNM-OG 45500 rec) are Zhoukoudian12, D2282, the naledi composite reconstruction (DNH1 and DNH3), and KNM-ER 3733. The phenogram generated from the UPGMA cluster analysis, presented in Figure 5, shows two main clusters. One cluster includes the more recent, Middle- Late Pleistocene fossils, and the other includes the older specimens, with the exception of the *Au. sediba* and *H. naledi* specimens. KNM-OG 45500 clusters closest to the African KNM-ER3733 and the *H. naledi* specimens.

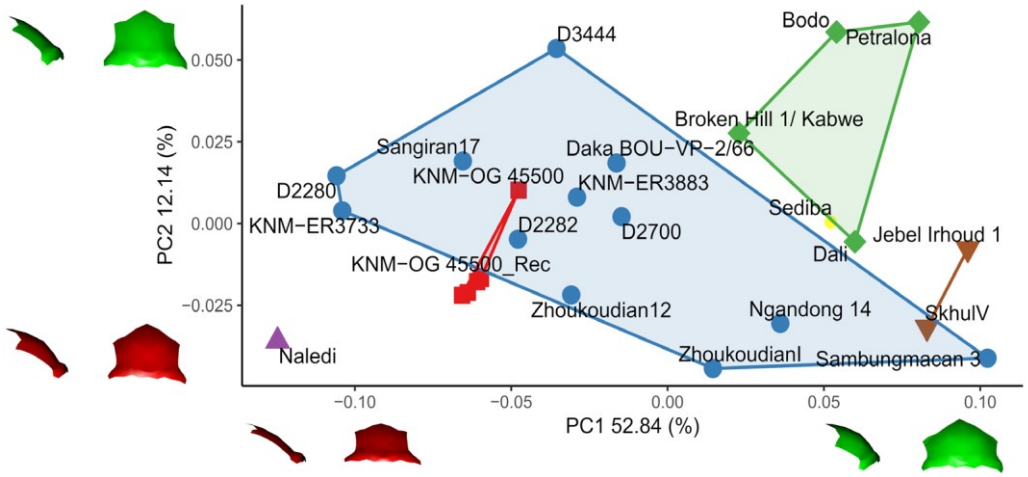

Fig. 4 - PCA plot of fossil specimens. Convex hull based on group attribution from Table 2. Colors and shape: blue circle =* H. erectus s.l.*; green diamond = Middle-Pleistocene Homo; brown down- ward triangle = early* H. sapiens*; yellow small circle=* Au. sediba*; purple triangle =* H. naledi*; red square = KNM-OG 45500. Frontal bone (in lateral and frontal views) shape variation corresponds to +/-2 std. dev. from mean PC values along each axis. The colour version of this figure is availableat the JASs website.

LogCS distribution in our sample is presentedin Figure 6. KNM-OG 45500 shows smaller size values compared to the *H. erectus s.l.* distribution and is broadly similar to the Dmanisi specimens. It is also evident that *H. erectus s.l.* specimens display a much higher degree of size variability compared to our sample of modern humans. The Daka fossil, geographically proximate and pene-contemporaneous to KNM-OG 45500, has a much higher logCS than KNM-OG 45500. There is a moderate, positive association between logCS and PC1 when the full fossil sample is considered, which is statistically significant (Spearman's rho= 0.58, r^2= 0.34, p-value=0.007), indicating that approximately 34% of the shape variation associated with the first component is explained by logCS. However, when consider-ing only the *H. erectus s.l.* group, the association between logCS and PC1 is weaker and not sta-tistically significant (Spearman's rho= 0.29, r^2= 0.084, p-value= 0.35). PC2 does not correlate to logCS in either of the two analyses.

Discussion

Our reconstruction of the KNM-OG 45500 frontal bone has allowed for a comprehensive, quantitative analysis of its form (size and shape) in comparison to other fossil specimens and diverse modern humans. In both of our shape analyses, the KNM-OG 45500 reconstruction with bregma taken on the posterior margin of the frontal squama plots squarely within the *H. erectus s.l.* convex hull and shows the lowest Procrustes distances to members of this taxon – irrespective of similarities or differences in overall size. In this regard, our results agree with previous interpreta-tions by Potts *et al.* (2004), who highlighted its particularly small size and morphological affini- ties to *H. erectus s.l.*. However, all the estimations of bregma in our other four KNM-OG 45500 reconstructions indicated that originally bregma was probably more posterior than the posterior-most sagittal point on the frontal squama takenon the original specimen. Our reconstruction

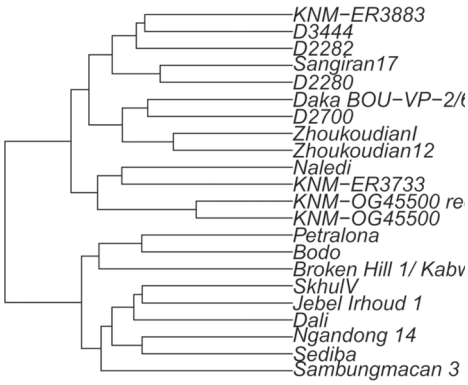

Fig. 5 - UPGMA cluster analysis based on pair- wise Procrustes distances between individuals. The colour version of this figure is available at the JASs website.

results are thus in agreement with Potts and col-leagues (Potts *et al.*, 2004) confirming that theoriginal squama was probably about 8mm longer. This elongated squama, as well as its relatively thin supraorbital torus, place these reconstruc- tions near the margin of the *H. erectus s.l.* con-vex hull and closer to the early specimens from Dmanisi and Kenya. Given the results of multipleestimations of bregma and the result of the unre- constructed bregma, we are confident that the original shape of KNM-OG 45500 most likelywould fall inside the convex hull of all KNM-OG 45500 estimations used in the analyses.

Our reconstructions and the applica-tion of geometric morphometric comparative approaches add to previous observations in twoimportant ways. First, we found that the first two shape components (PCs) were not strongly associated with frontal bone size (logCS) within

H. erectus s.l., suggesting that variation of the supraorbital morphology and frontal squama is not entirely size-dependent. Second, our rigor- ous data sampling approach allowed us to iden-tify affinities in both size and shape that have not been previously described. We discuss these results below and their implications for under-standing the evolution of Pleistocene *Homo*, par- ticularly with regard to taxonomic diversity and temporal variation.

Size and allometry

While our results show that the frontal bone shape of Pleistocene *Homo* has a mod- est, significant allometric component, it is not significant within the sampled *H. erectus s.l.* group. The KNM-OG 45500 shape follows the expected allometric trend along PC1 (low score) when considering the full sample. If KNM-OG45500 is accepted as a member of *H. erectus s.l,* we must then also accept greater size variability during this time period (ca. 900 Ka BP) in the taxon than hitherto understood. In fact, within the *H. erectus s.l.* sample only the much older specimens from Dmanisi show a logCS similarto KNM-OG 45500. In this regard, KNM-OG 45500's small size, together with its geological age, is contrary to the general trend of an increasein cranial/brain size over time often described for human evolution and for the evolution of *Homo erectus* specifically (Rightmire, 2004, 2013; Antón, 2007; Lieberman, 2011; Plavcan, 2012;Lordkipanidze *et al.*, 2013;)

KNM-OG 45500's endocranial volume (ECV) has been estimated to between 622 cm^3 and <800 cm^3 (Potts *et al.*, 2004; Baab, 2016).We consider the lower range to be more plau- sible given our logCS result for KNM-OG 45500, which is similar to the Dmanisi speci- mens, where the ECV spans from 601 cm^3(D2700) to 730 cm^3 (D2280) (Rightmire *etal*., 2019). The pene-contemporaneous Daka BOU-VP-2/66 (Ethiopia) and Buia UA 31 (Eritrea) specimens, by comparison, have ECV values of 986 cm^3 (Gilbert & Asfaw, 2008) and995 cm^3 (Bruner *et al.*, 2016), respectively — more than 1/3 larger than the expected cranial capacity of KNM-OG 45500. The difference in frontal bone size between Daka BOU-VP-2/66and KNM-OG 45500 (Fig. 6) is larger thanthe size range observed among the modernhumans or Middle Pleistocene *Homo* sampled in our study. It is worth noting that our modern human sample comprises small-sized individu- als from the Philippines (Reyes-Centeno *et al.*, 2014). Although relatively small, our modern human sample thus allows us to place the size difference between KNM-OG 45500 and Daka

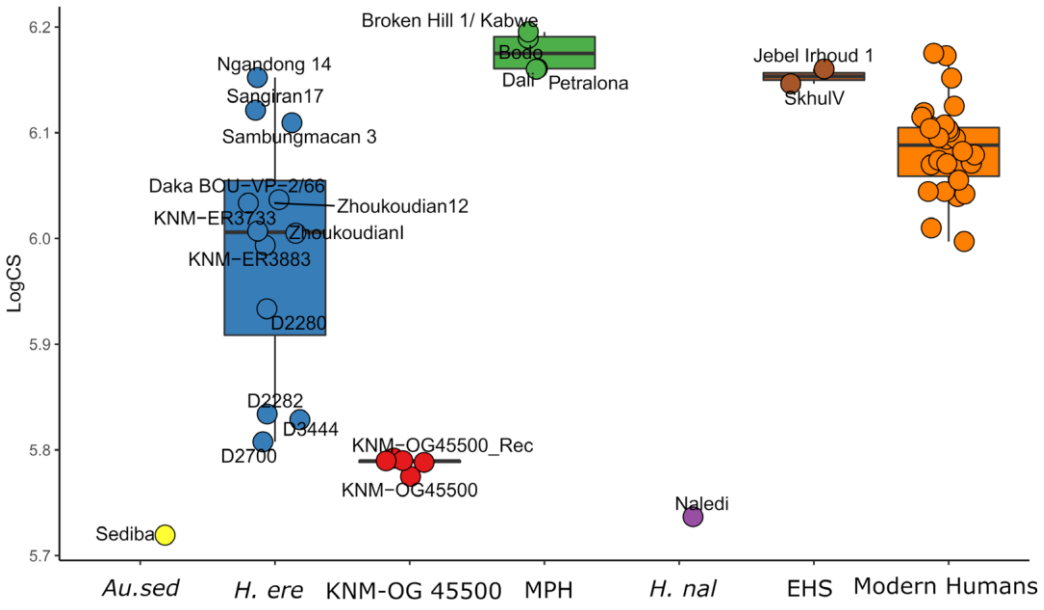

Fig. 6 - Boxplot with the distribution of LogCS values from each specimen. Groups based on Table 2definitions. The colour version of this figure is available at the JASs website.

BOU-VP-2/66 in the context of size variation among modern humans. While in other cases the differences between KNM-OG 45500 and other fossils can be related to large chronologic and geographic ranges, the comparison with Daka can be assumed to be less influenced by those factors. Size variation is affected by many factors: resource abundance, geographical differences, ecological response, sexual dimorphism, and others. It is, however, difficult to correctly identify one factor or the synergy of different ones in the paleontological context (Plavcan, 2012). Here, we consider three aspects that can be related to KNM-OG 45500's size: ontogenetic stage, sexual dimorphism and taxonomic diversity.

Ontogenetic variation and sexual dimorphism

It might be hypothesized that KNM-OG 45500 could represent a sub-adult individual and, as such, its small size could be a result of its immature ontogenetic stage (Potts *et al.*, 2004). In our analyses, high PC1 scores are associated with a "modern human" shape. Ontogenetic GM studies of cranial and endocranial shape var- iation show that juveniles of extant *Hominina*etend to plot closer to modern humans compared to adult individuals of the same taxon along thefirst principal component of a PCA (Gunz *et al.*, 2010; Neubauer *et al.*, 2010; Terhune *et al.*, 2013; Scott *et al.*, 2014; Mori & Harvati, 2019). Such a tendency can be reasonably associated also to fossil hominins. Our results inform thishypothesis to the extent that they likely reflectthe ontogenetic status of other fossil specimens, at least to some degree. For example, in the PCA analyses, the D 2700 sub-adult specimen plots toward higher PC 1 values in compari- son to the other Dmanisi fossils, which are of an adult or near-adult ontogeny. Similarly, the MH1 *Au. sediba* subadult, which is younger in dental development than D 2700 (Berger *et al.*,2010; Rightmire *et al.*, 2019), also plots toward higher PC 1 values, where frontal bone shape

is characterized by a less anteriorly projected supraorbital morphology and a rounder frontal squama. In contrast, KNM-OG 45500 plots far from modern humans along PC 1 and is closer to the adult Georgian specimens than to the D 2700 subadult. Given the limited nature of oursample and the small number of adult and sub- adult individuals from the same paleodeme (*i.e.* the sediba specimen is the only representative of its taxon), this result alone does not fully rejectthe hypothesis of a subadult stage for KNM-OG 45500. Qualitatively, however, the develop- ment of superstructures, such as the supraorbital torus, suggest an adult or near-adult ontogeny for KNM-OG 45500 (Potts *et al.*, 2004). The only suture preserved is the sphenotemporal suture on the temporal bone, which is closed but not completely obliterated. While this evi- dence alone is not sufficient to estimate the age of death, comparison to modern human suture closure patterns suggests that KNM-OG 45500 was either at a late stage of adolescence or already in adulthood (Meindl & Lovejoy, 1985).

Another factor that could account for the small size of KNM-OG 45500 can be related to sexual dimorphism. It has recently been pro- posed that *H. erectus* from Africa around 1.5 MaBP was more dimorphic than modern humans but less so than other highly dimorphic great apes (Villmoare *et al.*, 2019). Assuming common tax-onomic attribution, it is reasonable to considerthat KNM-OG 45500's small size relative to the larger dimensions of the pene-contemporaneous and geographically contiguous Daka and Buiafossils supports high sexual dimorphism in this taxon. This is consistent with the interpretations for the *H. erectus* crania at Dmanisi, Georgia (Rightmire *et al*., 2019), the footprint evidencefrom Ileret, Kenya (Villmoare *et al.*, 2019), andthe interpretation of the fossil crania from Gona, Ethiopia (Semaw *et al.* 2020). However, skull 5from Dmanisi and OH 12 also suggest the possi-ble existence of different sexual dimorphism pat- terns. Both specimens are small but robust, thus commonly considered to be male (Antón, 2004; Rightmire *et al*., 2019). Because KNM-OG45500 does not reflect robust superstructures, but only a small cranial size, we might hypothe- size that KNM-OG 45500 was probably a small-bodied gracile individual, probably of female sex(Potts *et al.*, 2004). Given KNM-OG 45500's geological age our results seem to confirm high sexual dimorphism in *H. erectus s.l.* until ca. 900 Ka BP. It has been proposed that sexual dimor- phism would have been reduced in our lineage,passing from more dimorphic to less dimor- phic taxa associated with a relative increase infemale size (Arsuaga *et al.*, 1997; Plavcan, 2012;Grabowski *et al.*, 2015), such a high level of sizedimorphism around 900 Ka BP implies that this reduction in sexual size dimorphism happened in less than a million year. Nevertheless, the rela- tionship between sexual dimorphism and fron- tal bone robusticity, shape, and size in *H. erectus s.l.* is currently not well understood and shouldbe further investigated. Moreover, it is possible that other factors could influence the small size of KNM-OG 45500, including a combination of subadult ontogenetic status sex, or taxonomy (see below).

Taxonomic considerations

With the caveats of ontogeny and sex in mind, we found some previously undescribed fossil affinities to KNM-OG 45500. Potts *et al.* (2004) considered KNM-OG 45500 to be mostsimilar to the Dmanisi D2282 near-adult and D2280 adult specimens. In our study, we con- firm this similarity in shape (Procrustes distance)to D2282, in addition to affinity to D2700 in size (logCS). We also found that the shape affini- ties of KNM-OG 45500 to other *H. erectus s.l.*specimens are closer than previously reported in a preceding GM study of the unreconstructed frontal bone (Baab, 2016 Supplement Material). Whereas Baab (2016) found that KNM-OG45500 was an outlier in shape space in com- parison to other Pleistocene *Homo* samples, our results place KNM-OG 45500 within or close to the variation of our sampled *H. erectus s.l.* group. The difference in results with Baab (2016)is likely due, at least in part, to differences in variables used in the analysis, the comparative sample used, and methodological approaches.

Baab (2016) sampled 17 landmarks on the unreconstructed frontal bone, estimating some bilateral landmarks using reflected relabeling (Mardia *et al*., 2000) of the better-preserved side. However, some landmarks were digitized on the left side, which appears deformed on the lateral posterior margin, while the position of the mid-torus landmark taken on the right side was likely somewhat influenced by the abra-sion of the surface. Our reconstruction allowed for greater landmark coverage and accounted for taphonomic distortion of the left side of the frontal squama by using the better preserved right side. However, similar to Baab's results though to a lesser degree, our KNM-OG 45500 reconstructions fell on the margin of *H. erectus s.l.* variability.

Pending more robust attributions of sex and ontogeny for KNM-OG 45500, it is pos- sible that the observed variation in frontal bone form can be linked to taxonomic diversity. Other small-sized *H. erectus s.l.* within Africa are known from the fossil record (Antón, 2004; Rightmire, 2004; Bruner *et al.*, 2015; Semaw *et al.*, 2020). Taxonomic diversity based on differ-ences in cranial size, among other features, has been suggested for early *Homo* groups (Spoor *et al.*, 2015). As a result, Berger *et al.* (2017) have hypothesized that KNM-OG 45500 and OH 12 represent a diverse small-bodied subequatorial hominin lineage culminating in the more recent *H. naledi* specimens in South Africa. Our results support this hypothesis only to the extent that both our cluster analysis and the logCS values highlight similar morphology and size between KNM-OG 45500 and H. *naledi*. Moreover, KNM-OG 45500 and Daka BOU-VP-2/66, which are close in both chronology and geog-raphy (Asfaw *et al.*, 2002; Potts *et al.*, 2004; Gilbert & Asfaw, 2008) are different not only in their size, but also in shape when we consider all the reconstructions made with the estimation of bregma. KNM-OG 45500 has a more shelf-like morphology compared to Daka BOU-VP-2/66 and a thin supraorbital torus. Despite this evi-dence, our overall results do not support a dif-ferent taxonomic attribution of KNM-OG 45500 from the one proposed by Potts and col- leagues (2004). Both in terms of its positioning in shape space and pairwise Procrustes distance, KNM-OG 45500 is more distant from the *H. naledi* specimen than from other *H. erectus s.l.* fossils, especially the early Pleistocene African and Georgian specimens. For this reason, we cannot reject the hypothesis that KNM-OG 45500 belongs to the *H. erectu*s hypodigm. Future work in eastern Africa and the inclusion of newly discovered hominin remains excavated at Olorgesaile could shed light on local patterns of cranial form evolution and allow further comparison with other Pleistocene *Homo* fossils across Africa.

Patterns of variation in H. erectus s.l.

Another aspect that is important to note is the presence of continuity of frontal bone shape in Africa. This continuum in frontal bone mor- phology presumably appeared with the emer- gence of *Homo erectus s.l.* diagnostic features, expressed in specimens like KNM-ER 3733, and lasted up to about 1 Ma, represented in our study by KNM-OG 45500. Beginning in the Middle Pleistocene, some fossils then show a more derived morphology. Our results show this to the extent that Middle to Late Pleistocene fos- sils across Africa and Eurasia are distinct from the Early Pleistocene fossils along the major axis of variation in shape space (i.e. along PC1 in Fig. 4), consistent with previous GM stud- ies on cranial form (Manzi *et al*., 2003; Baab, 2015, 2016; Manzi, 2016; Profico *et al.*, 2016). The UPGMA phenogram (Fig. 5) also shows two temporal clusters that split our fossil sample primarily by chronology, from early specimens dated to between ca. 1.77 to 0.7 Ma BP to more derived specimens dated to between the Middle and Late Pleistocene. The Early Pleistocene *Au. sediba* and Middle Pleistocene *H. naledi* speci- mens seem to contradict the pattern seen in the shape analysis. Whereas the positioning of *Au.sediba* is likely associated in part to its sub-adult stage, the positioning of the *H. naledi* specimen might indeed be indicative of distinct taxonomy or greater anatomical variation in Pleistocene

Homo than previously considered (Berger *et al.*, 2017; Schroeder *et al.*, 2017). However, we cau-tion that our observations might be biased by the composite reconstruction, which includes both the *H. naledi* DH1 holotype & DH3 paratype.

Looking at the *H. erectus s.l.* fossils, our results seem to cluster specimens in different paleodemes (Howell, 1999). In this sense, the African early Pleistocene Nariokotome pale- odeme (Howell, 1999) seems to be relatively homogeneous until ca. 1 Ma, comprising also KNM-OG 45500 and Daka BOU-VP-2/66. In Eurasia, the Dmanisi paleodeme is not very dif-ferent in frontal morphology from the African Nariokotome paleodeme. Asian paleodemes from Sangiran, Zhoukoutien, and Ngandong seem to express a morphological trajectory that is initially similar to the Early Pleistocene African Eurasian morphology (Sangiran 17, associ- ated with a low PC1 score in Fig. 4) and sub- sequently becomes more derived (Zhoukoutien and Ngandong, associated with higher PC1 val-ues in Fig. 4) later in time. However, caution is required in drawing such conclusions since we are only sampling one or two specimens for each paleodeme. Moreover, no full consensus exists about the relationships among these paleodemes (Openoorth, 1932; Weidenreich, 1951; Stringer, 1984; Wolpoff *et al.*, 1994; Delson *et al.*, 2001;Widianto & Zeitoun, 2003; Zeitoun *et al.*, 2010; Schwartz & Tattersall, 2015; Tattersall, 2015; Rightmire *et al*., 2019). Nevertheless, the highvariability expressed by *H. erectus s.l.* is often linked to the great geochronological and asso- ciated paleoenvironmental spread of the taxon, spanning from the Early to Late Pleistocene of Africa and Southeast Asia (Antón *et al.* 2014).

The Sambungmacan 3 specimen is of par-ticular interest in the context of our results. Dated from a context possibly as late as 70-40 ka(Yokoyama *et al.*, 2008), it shows a more derived frontal morphology compared to the Ngandong specimen, which comes from a context dated to ca. 118-108 ka (Rizal *et al.*, 2020). Despite their close origin and chronology, Sambungmacan 3 shows closer morphological affinities to the JebelIrhoud 1 and Skhul V specimens. Consistent with previous observations (Delson *et al.*, 2001), our results show that Sambungmacan 3 has a relatively rounded frontal squama (i.e. high PC1 scores in Figs. 3,4), distinct from other *H. erectus s.l.* fossils. These results might indicate a taxo- nomic difference between earlier *H. erectus* and Sambungmacan 3, which might be interpreted asan "evolved lineage" of *H. erectus.* Previous works have found that this specimen, as well as other late Javan individuals from Ngandong, are at the extreme of *H. erectus* variability (Weidenreich, 1951; Delson *et al.*, 2001; Widianto & Zeitoun,2003; Zeitoun *et al.*, 2010; Baab, 2016), sothat some authors proposed that they might represent a different taxon, *H. sapiens soloensis* or *H. soloensis* (Openoorth, 1932; Widianto & Zeitoun, 2003; Zeitoun *et al.*, 2010). This viewis analogous to the debate on taxonomic diversity in eastern Africa *H. erectus s.l.* fossils. Comparedto Zeitoun *et al.* (2010), our analysis did not include the full fossil series from Ngandong and Sambungmacan, nor the full available morphol- ogy of these specimens. Our results, therefore, might differ from theirs for this reason. Similarto that study, however, we found Sambungmacan 3 to be closer to Jebel Irhoud 1 in our PCA plotand to Skhul V in terms of Procrustes distance. Future analysis should investigate further the relationship between all the fossils from Java in order to better assess morphological variation in that series.

Interestingly, Sambungmacan 3 is also close to the Aboriginal Australian individuals from thecomparative modern human sample in our study.Genomic research on recent Southeast Asian and Aboriginal Australian populations have found evidence of genetic introgression from Pleistocene populations, including Denisovans, Neanderthals, and possibly a third hominin group (Malaspinas *et al.*, 2016; Jacobs *et al.*, 2019; Mondal *et al.*, 2019). Moreover, some evidence suggests that Aboriginal Australians may descend from the first modern humans who dispersed into Oceania between 70 and 50 ka (Rasmussen *et al.*, 2011; Reyes-Centeno*et al.*, 2014). In light of this, it is interesting to note that the Australian individuals sampled

in our analysis plot closer to the hominin fossils along PC1 and PC2 (crossed diamond in Fig. 3) compared to the other modern humans sampled. Moreover, Australians are particularly close in Procrustes distances to Sambungmacan 3 and to other fossils. Although these similarities could be due to bias in our sampling strategy, the cranial phenotype is known to be linked to the genotype such that genetic introgression events may influence cranial morphology of modern humans (Reyes-Centeno *et al.*, 2014; Gunz *et al.*, 2019). Therefore, future work should aim to test the hypothesis that Sambungmacan 3 might represent evidence of admixture between hominin groups. The implication is that gene flow is an important factor to consider in the high morphological variation of *H. erectus s.l.*, both in the Early Pleistocene of eastern Africa at one extreme and in the Late Pleistocene of Southeast Asia and Oceania at the other extreme.

Limitations and future research directions

Our analyses are limited by two main fac- tors. The first is that analysis of the frontal bone shape alone might not be sufficient to capture the phylogenetic relationships between different fossil groups (Terhune *et al*., 2007; Baab, 2016; Schroeder *et al.*, 2017). Future work should therefore also analyze KNM-OG 45500's temporal bone fragment in order to evaluate differences and similarities to other fossils and to further test the conclusions drawn from our analyses. We note that while temporal bone morphology has been suggested to be particularly important in tracing population history in both modern humans (Harvati & Weaver, 2006a; Smith *et al*., 2007; Reyes-Centeno *et al*., 2017) and hominins (Lockwood *et al*., 2004, 2005; Harvati & Weaver, 2006b; Terhune *et al*., 2007), the frontal bone has been suggested to better reflect phylogenetic relationships across hominoid taxa (von Cramon-Taubadel & Smith, 2012). Second,we were unable to include a number of impor-tant specimens in our study, such as the penecontemporaneous Buia UA 31 specimen from Eritrea (Macchiarelli *et al.*, 2004; Bruner *et al.*, 2016) or the later OH 12 specimen from Kenya (Leakey, 1971). In addition, we were unable toinclude the small-sized specimens from eastern Africa (e.g. DAN5/P1 and KNM-ER 42700) or from Southeast Asia (e.g. Ngandong and LiangBua 1 (Brown *et al.*, 2004)), variably assignedto *H. erectus s.l.* or to distinct taxa. The frontalbones of all of these specimens either require fur-ther reconstruction for appropriate comparison or they were not available for this study. Future work should therefore focus on a broader com- parison, aiming for the comprehensive analysis of incomplete specimens.

Conclusions

In summary, our results show that the KNM-OG 45500 frontal bone exhibits affinities to Early Pleistocene fossils from both Africa andEurasia in its form. In both its shape and size,it is most similar to Early Pleistocene specimens taxonomically assigned to *H. erectus/ergaster.* Overall, our results concur with the original attribution of KNM-OG 45500 to *H. erectus s.l.* and similarly highlight how KNM-OG 45500 extends the taxon's range of size variation for this time period. Based on its small size, KNM-OG 45500 might be considered female, although the relationship of size, shape, and sexual dimorphismin *H. erectus s.l.* must be explored further. Finally, the possibility that this specimen is part of a lineage culminating in the South African *H. naledi*remains open. It is therefore important to consider KNM-OG 45500 in future research on the evolu- tion of Pleistocene *Homo*, and the reconstruction introduced here will allow its inclusion in futurestudies. We expect that additional work with the KNM-OG 45500 temporal bone, including more comprehensive cranial reconstruction efforts, will further shed light on the diversity of Pleistocenehominins and clarify the *H. erectus* hypodigm.

Data sharing

The raw dataset and R code used can be provided by the corresponding author upon request.

3D surfaces used cannot be provided due to copyright restriction and license agreement with institutions.

Acknowledgments

We thank the following institutions and col- leagues for access to fossil comparative material: Richard Potts and colleagues at the Smithsonian Institution, as well as Fredrick Manthi, Timo- thy Gichunge, and the members of the Depart- ment of Earth Science, National Museums of Kenya for access to the KNM-OG 45500 sur- face scan and CT scans of KNM-ER 3733 and KNM-ER 3883; Gen Suwa, the Authority for Research and Conservation of Cultural Heritage (ARCCH), and the National Museum of Ethio- pia for providing the Daka calvarium (BOU- VP-2/66) external mesh reconstruction; Sabine Eggers for access to CT scan from the Depart- ment of Anthropology of the Naturhistorisches Museum in Vienna; Giselle Garcia and Eric Delson, American Museum of Natural History; Monica Zavattaro and Jacopo Moggi-Cecchi for access to the CT scans from the Anthropological Collection at the Museo di Storia Naturale dell' Università di Firenze; Antoine Balzeau, Mar- tin Friess, and Dominique Grimaud-Hervé for access to the CT scans from the Muséum national d'Histoire naturelle, Paris. The Skhūl V fossil scan was downloaded from the Peabody Museum, Harvard University, while the H. naledi (DH1& DH3) and A. sediba (MH1) scans were down- loaded from the MorphoSource database, Duke University (media number: M7300-8170). We thank Marlijn Noback for providing access to scans of the modern human comparative sample, as well as Yonatan Sahle for facilitating access to the Daka CT scan and for helpful discussion on this project. Finally, we thank Hannes Rath- mann for his help in the figures' production. This work was funded in part by the German Research Foundation (DFG-INST-37/706-1 FUGG and DFG-FOR-2237: "Words, Bones, Genes, Tools: Tracking Linguistic, Cultural, and Biological Trajectories of the Human Past").

Author contributions

KH and TM conceptualized and designed the study. TM collected the data. TM and AP ana-lyzed the data. TM, AP, HRC, KH interpreted and commented on the results of the analyses. TM drafted the manuscript. HRC, KH, AP revised and edited extensively the whole manu- script. All authors read, provided feedback and approved the manuscript.

References

Antón S.C. 2003. Natural history of *Homo* erec- tus. *Am. J. Phys. Anthropol.*, 122: 126-170.

Antón S.C. 2004. The face of Olduvai hominid12. *J. Hum. Evol.*, 46: 335-345.

Antón S.C. 2007. Defining Homo erectus: size considered. *Handbook of Paleoanthropology*, 3: Chapter 11.

Antón S.C., Potts R. & Aiello L.C. 2014. Evolution of early Homo: An integrated bio- logical perspective. *Science*, 345: 1236828.

Arsuaga J.L., Carretero J.M., Lorenzo C. *et al.* 1997. Size Variation in Middle Pleistocene Humans. *Science*, 277: 1086-1088.

Asfaw B., Gilbert W.H., Beyene Y. *et al.* 2002.Remains of Homo erectus from Bouri, MiddleAwash, Ethiopia. *Nature*, 416: 317.

Athreya S. 2012. The frontal bone in the genusHomo: a survey of functional and phyloge- netic sources of variation. *J. Anthropol. Sci.*, 90: 1-22.

Aytek A.İ. & Harvati K. 2016. The human fossil record from Turkey. In K. Harvati &
M. Roksandic (eds): *Paleoanthropology of the Balkans and Anatolia*, pp. 79-91. Springer, Dordrecht.

Baab K.L. 2008a. A re-evaluation of the taxo- nomic affinities of the early Homo cranium KNM-ER 42700. *J. Hum. Evol.*, 55: 741-746.

Baab K.L. 2008b. The taxonomic implications of cranial shape variation in Homo erectus. *J.Hum. Evol.*, 54: 827-847.

Baab K.L. 2015. Defining Homo erectus. In W. Henke & I. Tattersall (eds): *Handbook of*

paleoanthropology, pp. 2189-2219. Springer, Berlin, Heidelberg.
Baab K.L. 2016. The role of neurocranial shape indefining the boundaries of an expanded Homoerectus hypodigm. *J. Hum. Evol.*, 92: 1-21.
Bauer C.C. & Harvati K. 2015. A virtual re- construction and comparative analysis of theKNM-ER 42700 cranium. *Anthrop. Anz.*, 72:
129-140.
Berger L.R., de Ruiter D.J., Churchill S.E. *et al.* 2010. *Australopithecus sediba*: A New Species of *Homo*-Like Australopith from South Africa.*Science*, 328: 195-204.
Berger L.R., Hawks J., de Ruiter D.J. *et al.* 2015. Homo naledi, a new species of the genus Homo from the Dinaledi Chamber, South Africa. *Elife*, 4: e09560.
Berger L.R., Hawks J., Dirks P.H. *et al.* 2017.Homo naledi and Pleistocene hominin evolu- tion in subequatorial Africa. *Elife*, 6: e24234. Bookstein F.L. 1989. Principal warps: Thin-plate splines and the decomposition of defor- mations. *IEEE Transactions on pattern analysis and machine intelligence*, 11: 567-585. Bookstein F.L. 1991. *Morphometric tools for land-*
mark data: geometry and biology. Cambridge University Press, Cambridge.
Bosman A., Buck L., Reyes-Centeno H. *etal.* 2019. The Kabua I cranium: Virtual anatomical reconstructions In Y. Sahle, H. Reyes-Centeno & C. Bentz (eds): *Modern Human Origins and Dispersal*. Kerns Verlag, Tübingen.
Bosman A.M., Reyes-Centeno H. & Harvati K.2020. A virtual assessment of the suprainiac depressions on the Eyasi I (Tanzania) and Aduma ADU-VP-1/3 (Ethiopia) Pleistocene hominin crania. *J. Hum. Evol.*, 145: 102815.
Brown P., Sutikna T., Morwood M.J. *et al.* 2004.A new small-bodied hominin from the Late Pleistocene of Flores, Indonesia. *Nature*, 431: 1055. Bruner E., Bondioli L., Coppa A. *et al.* 2016.The endocast of the one-million-year-old hu- man cranium from Buia (UA 31), Danakil Eritrea. *Am. J. Phys. Anthropol.*, 160: 458-468. Bruner E., Grimaud-Hervé D., Wu X. *et al.*2015. A paleoneurological survey of Homo erectus endocranial metrics. *Quat. Int.*, 368:80-87.
Buck L.T. & Stringer C.B. 2015. A rich local-ity in South Kensington: the fossil hominin collection of the Natural History Museum, London. *Geological Journal*, 50: 321-337.
Cignoni P., Callieri M., Corsini M. *et al.* 2008.Meshlab: an open-source mesh processing tool. In: *Eurographics Italian chapter confer- ence*, p. 129-136.
Delson E., Harvati K., Reddy D. *et al.* 2001. The Sambungmacan 3 Homo erectus calvaria: a comparative morphometric and morpho- logical analysis. *Anat. Rec. (Hoboken)*, 262: 380-397.
Détroit F., Mijares A.S., Corny J. *et al.* 2019. A new species of Homo from the Late Pleistoceneof the Philippines. *Nature*, 568: 181.
Dirks P.H., Roberts E.M., Hilbert-Wolf H. *et al.* 2017. The age of Homo naledi and associ- ated sediments in the Rising Star Cave, South Africa. *Elife*, 6: e24231.
Dubois M.E.F.T. 1894. *Pithecanthropus erectus: eine menschenähnliche Übergangsform aus Java.*Landesdruckerei.
Freidline S.E., Gunz P., Janković I. *et al.* 2012. A comprehensive morphometric analysis of the frontal and zygomatic bone of the Zuttiyehfossil from Israel. *J. Hum. Evol.*, 62: 225-241. Garcia T., Féraud G., Falguères C. *et al.* 2010.Earliest human remains in Eurasia: New 40Ar/39Ar dating of the Dmanisi hominid-bearing levels, Georgia. *Quat. Geochronol.*, 5:
443-451.
Gibbard P.L., Head M.J., Walker M.J. *et al.* 2010. Formal ratification of the Quaternary System/Period and the Pleistocene Series/Epoch with a base at 2.58 Ma. *J. Quat. Sci.*, 25: 96-102.
Gilbert W.H. & Asfaw B. 2008. *Homo erectus:Pleistocene Evidence from the Middle Awash, Ethiopia.* University of California Press, Berkeley and Los Angeles, California.
Gower J.C. 1975. Generalized procrustes analy- sis. *Psychometrika*, 40: 33-51.
Grabowski M., Hatala K.G., Jungers W.L. *et al.* 2015. Body mass estimates of hominin fossils

and the evolution of human body size. *J. Hum. Evol.*, 85: 75-93.
Grün R. 1996. A re-analysis of electron spin resonance dating results associated with the Petralona hominid. *J. Hum. Evol.*, 30: 227-241.
Grün R. 2006. Direct dating of human fossils.
Am. J. Phys. Anthropol., 131: 2-48.
Grün R. & Stringer C.B. 1991. Electron spin resonance dating and the evolution of modern humans. *Archaeometry*, 33: 153-199.
Gunz P., Mitteroecker P. & Bookstein F.L. 2005. Semilandmarks in three dimensions. In D.E. Slice (ed): *Modern morphometrics in physical anthropology*, pp. 73-98. Springer, Boston, MA.
Gunz P., Mitteroecker P., Neubauer S. *et al.* 2009. Principles for the virtual reconstruction of hominin crania. *J. Hum. Evol.*, 57: 48-62.
Gunz P., Neubauer S., Maureille B. *et al.* 2010. Brain development after birth differs between Neanderthals and modern humans. *Curr. Biol.*, 20: R921-R922.
Gunz P., Tilot A.K., Wittfeld K. *et al.* 2019. Neandertal introgression sheds light on mod- ern human endocranial globularity. *Curr. Biol.*, 29: 120-127. e125.
Harvati K., Röding C., Bosman A.M. *et al.* 2019. Apidima Cave fossils provide earliest evidence of Homo sapiens in Eurasia. *Nature*, 571: 500-504.
Harvati K. & Weaver T.D. 2006a. Human cra-nial anatomy and the differential preservation of population history and climate signatures.*Anat. Rec. (Hoboken)*, 288A: 1225-1233.
Harvati K. & Weaver T.D. 2006b. Reliability of cranial morphology in reconstructing Neanderthal phylogeny. In J.J. Hublin, K. Harvati & T. Harrison (eds): *Neanderthals revisited: new approaches and perspectives*, pp. 239-254. Springer, Dordrecht.
Howell F.C. 1999. Paleo-Demes, Species Clades, and Extinctions in the Pleistocene Hominin Record. *J. Anthrop. Res.*, 55: 191-243.
Jacobs G.S., Hudjashov G., Saag L. *et al.* 2019. Multiple Deeply Divergent Denisovan Ancestriesin Papuans. *Cell*, 177: 1010-1021.e1032.
Kidder J.H. & Durband A.C. 2004. A re-eval- uation of the metric diversity within Homo erectus. *J. Hum. Evol.*, 46: 297-313.
Larick R., Ciochon R.L., Zaim Y. *et al.* 2001. Early Pleistocene 40Ar/39Ar ages for Bapang formation hominins, central Jawa, Indonesia.*Proc. Natl. Acad. Sci. USA*, 98: 4866-4871.
Leakey M.D. 1971. *Olduvai Gorge: Volume 3, excavations in beds I and II, 1960-1963.* Cambridge University Press, Cambridge.
Leakey M.G., Spoor F., Dean M.C. *et al.* 2012.New fossils from Koobi Fora in northern Kenya confirm taxonomic diversity in early Homo. *Nature*, 488: 201.
Lepre C.J. & Kent D.V. 2015. Chronostratigraphy of KNM-ER 3733 and other Area 104 hominins from Koobi Fora. *J. Hum. Evol.*, 86: 99-111.
Lieberman D.E. 2011. *The evolution of the hu-man head.* The belknap press of Harvard University Press.
Lockwood C.A., Kimbel W.H. & Lynch J.M. 2004. Morphometrics and hominoid phy- logeny: Support for a chimpanzee–human clade and differentiation among great ape subspecies. *Proc. Natl. Acad. Sci. USA*, 101: 4356-4360.
Lockwood C.A., Kimbel W.H. & Lynch J.M.2005. Variation in early hominin temporal bone morphology and its implications for spe- cies diversity. *Trans. R. Soc. S. Afr.*, 60: 73-77. Lordkipanidze D., Ponce de León M.S.,Margvelashvili A. *et al.* 2013. A CompleteSkull from Dmanisi, Georgia, and the Evolutionary Biology of Early *Homo*. *Science*, 342: 326-331.
Macchiarelli R., Bondioli L., Chech M. *et al.* 2004. The late early Pleistocene human re- mains from Buia, Danakil depression, Eritrea. *Rivista Italiana di Paleontologia e Stratigrafia (Research In Paleontology and Stratigraphy)*, 110.
Malaspinas A.-S., Westaway M.C., Muller C. *et al.* 2016. A genomic history of Aboriginal Australia. *Nature*, 538: 207-214.
Manzi G. 2016. Humans of the MiddlePleistocene: The controversial calvarium from

Ceprano (Italy) and its significance for the or- igin and variability of Homo heidelbergensis. *Quat. Int.*, 411: 254-261.
Manzi G., Bruner E. & Passarello P. 2003. The one-million-year-old Homo cranium from Bouri (Ethiopia): a reconsideration of its *H. erectus* affinities. *J. Hum. Evol.*, 44: 731-736.
Mardia K.V., Bookstein F.L. & Moreton I.J. 2000. Statistical assessment of bilateral sym- metry of shapes. *Biometrika*, 87: 285-300.
Matsu'ura S., Kondo M., Danhara T. *et al.* 2020.Age control of the first appearance datum forJavanese Homo erectus in the Sangiran area.*Science*, 367: 210-214.
McDougall I., Brown F.H., Vasconcelos P.M. *et al.* 2012. New single crystal 40Ar/39Ar ages improve time scale for deposition of the Omo Group, Omo–Turkana Basin, East Africa. *J Geol. Soc. London*, 169: 213-226.
Meindl R.S. & Lovejoy C.O. 1985. Ectocranial suture closure: a revised method for the de- termination of skeletal age at death basedon the lateral-anterior sutures. *Am. J. Phys. Anthropol.*, 68: 57-66.
Mitteroecker P. & Bookstein F. 2011. Linear discrimination, ordination, and the visuali- zation of selection gradients in modern mor-phometrics. *Evol. Biol.*, 38: 100-114.
Mitteroecker P. & Gunz P. 2009. Advances in Geometric Morphometrics. *Evol. Biol.*, 36: 235-247.
Mondal M., Bertranpetit J. & Lao O. 2019. Approximate Bayesian computation with deep learning supports a third archaic introgression in Asia and Oceania. *Nat. Comm.*, 10: 1-9.
Mori T. & Harvati K. 2019. Basicranial ontog- eny comparison in Pan troglodytes and Homo sapiens and its use for developmental stage definition of KNM-ER 42700. *Am. J. Phys. Anthropol.,* 170: 579-594
Neeser R., Ackermann R.R. & Gain J. 2009.Comparing the accuracy and precision of three techniques used for estimating missing landmarks when reconstructing fossil homi-nin crania. *Am. J. Phys. Anthropol.*, 140: 1-18.
Neubauer S., Gunz P. & Hublin J.-J. 2010.Endocranial shape changes during growth in chimpanzees and humans: A morphometric analysis of unique and shared aspects. *J. Hum.Evol.*, 59: 555-566.
Neubauer S., Gunz P., Leakey L. *et al.* 2018. Reconstruction, endocranial form and taxo- nomic affinity of the early Homo calvaria KNM-ER 42700. *J. Hum. Evol.,* 121: 25-39.
Noback M.L. & Harvati K. 2014. Covariation in the Human Masticatory Apparatus. *Anat. Rec. (Hoboken)*, 298: 64-84.
Noback M.L. & Harvati K. 2015. The contri- bution of subsistence to global human cranial variation. *J. Hum. Evol.*, 80: 34-50.
Openoorth W. 1932. Homo (Javanthropus) soloensis, een pleistoceene mensch van Java. *Wetesch Mededee. Dienst Mijnbauw NederlIndie*, 20: 49-74.
Pickering R., Dirks P.H., Jinnah Z. *et al.* 2011. Australopithecus sediba at 1.977 Ma and im-plications for the origins of the genus Homo.*Science*, 333: 1421-1423.
Plavcan J.M. 2012. Body size, size variation, andsexual size dimorphism in early Homo. *Curr. Anthropol.*, 53: S409-S423.
Ponce De Leon M.S. & Zollikofer C.P. 1999.New evidence from Le Moustier 1: Computer- assisted reconstruction and morphometry ofthe skull. *Anat. Rec. (Hoboken)*, 254: 474-489. Potts R., Behrensmeyer A.K., Deino A. *etal.* 2004. Small Mid-Pleistocene Hominin Associated with East African Acheulean Technology. *Science*, 305: 75-78.
Profico A., Di Vincenzo F., Gagliardi L. *et al.* 2016. Filling the gap. Human cranial remainsfrom Gombore II (Melka Kunture, Ethiopia; ca. 850 ka) and the origin of Homo heidelber- gensis. *J. Anthropol. Sci.*, 94: 1-24.
Profico A., Schlager S., Valoriani V. *et al.* 2018.Reproducing the internal and external anato-my of fossil bones: Two new automatic digitaltools. *Am. J. Phys. Anthropol.*, 166: 979-986.
R Core Team. 2018. *R: A language and environ-ment for statistical computing.*
Rasmussen M., Guo X., Wang Y. *et al.* 2011. AnAboriginal Australian genome reveals sepa-rate human dispersals into Asia. *Science*, 334: 94-98.

Reyes-Centeno H., Ghirotto S., Détroit F. *et al.* 2014. Genomic and cranial phenotype data support multiple modern human dispersals from Africa and a southern route into Asia**.** *Proc. Natl. Acad. Sci. USA***,** 111: 7248-7253.
Reyes-Centeno H., Ghirotto S. & Harvati K. 2017. Genomic validation of the differential preservation of population history in mod- ern human cranial anatomy. *Am. J. Phys. Anthropol.*, 162: 170-179.
Richter D., Grün R., Joannes-Boyau R. *et al.* 2017. The age of the hominin fossils from Jebel Irhoud, Morocco, and the origins of theMiddle Stone Age. *Nature*, 546: 293.
Rightmire G.P. 1979. Cranial remains of Homoerectus from Beds II and IV, Olduvai Gorge, Tanzania. *Am. J. Phys. Anthropol.*, 51: 99-115.
Rightmire G.P. 1981. Patterns in the evolutionof Homo erectus. *Paleobiology*, 7: 241-246. Rightmire G.P. 1990. *The Evolution of Homo*
Erectus: Comparative Anatomical Studies of an Extinct Human Species. Cambridge UniversityPress, Cambridge.
Rightmire G.P. 2004. Brain size and encephali- zation in early to mid-Pleistocene Homo. *Am.*
J. Phys. Anthropol., 124: 109-123.
Rightmire G.P. 2013. Homo erectus and Middle Pleistocene hominins: brain size, skull form,and species recognition. *J. Hum. Evol.*, 65: 223-252.
Rightmire G.P., Lordkipanidze D. & Vekua A. 2006. Anatomical descriptions, comparative studies and evolutionary significance of the hominin skulls from Dmanisi, Republic of Georgia. *J. Hum. Evol.*, 50: 115-141.
Rightmire G.P., Margvelashvili A. & Lordkipanidze D. 2019. Variation among theDmanisi hominins: Multiple taxa or one spe-cies? *Am. J. Phys. Anthropol.*, 168: 481-495.
Rightmire P.G. 1996. The human cranium fromBodo, Ethiopia: evidence for speciation in the Middle Pleistocene? *J. Hum. Evol.*, 31: 21-39. Rizal Y., Westaway K.E., Zaim Y. *et al.* 2020. Lastappearance of Homo erectus at Ngandong, Java, 117,000–108,000 years ago. *Nature*, 577: 381-385. Rohlf F.J. & Slice D. 1990. Extensions ofthe Procrustes Method for the Optimal Superimposition of Landmarks. *Syst. Biol.*, 39: 40-59.
Schlager S. 2017. Morpho and Rvcg–Shape Analysis in R: R-Packages for geometric mor-phometrics, shape analysis and surface ma- nipulations. In G. Zheng, S. Li & G. Székely(eds): *Statistical shape and deformation analysis*,pp. 217-256. Academic Press, Cambridge.
Schliep K.P. 2010. phangorn: phylogenetic anal-ysis in R. *Bioinformatics*, 27: 592-593.
Schroeder L., Scott J.E., Garvin H.M. *et al.* 2017. Skull diversity in the Homo lineage and the relative position of Homo naledi. *J. Hum.Evol.*, 104: 124-135.
Schwartz J.H. 2004. Getting to Know Homo erectus. *Science*, 305: 53.
Schwartz J.H. & Tattersall I. 2000. What con- stitutes Homo erectus. *Acta Anthropol. Sin.*,19: 18-22.
Schwartz J.H. & Tattersall I. 2015. Defining the genus *Homo*. *Science*, 349: 931-932.
Scott N., Neubauer S., Hublin J.-J. *et al.* 2014. A Shared Pattern of Postnatal Endocranial Development in Extant Hominoids. *Evol. Biol.*, 41: 572-594.
Semaw S., Rogers M.J., Simpson S.W. *et al.* 2020. Co-occurrence of Acheulian and Oldowan artifacts with Homo erectus cranial fossils from Gona, Afar, Ethiopia. *Sci. Adv.*, 6:eaaw4694.
Shen G., Gao X., Gao B. *et al.* 2009. Age of Zhoukoudian Homo erectus determined with 26Al/10Be burial dating. *Nature*, 458: 198-200.
Slice D.E. 2007. Geometric Morphometrics.
Annu. Rev. Anthrop., 36: 261-281.
Smith H.F. 2009. Which cranial regions re- flect molecular distances reliably in humans? Evidence from three-dimensional morphol- ogy. *Am. J. Hum. Biol.*, 21: 36-47.
Smith H.F., Terhune C.E. & Lockwood C.A. 2007. Genetic, geographic, and environmen-tal correlates of human temporal bone varia- tion. *Am. J. Phys. Anthropol.*, 134: 312-322.
Sokal R.R. 1958. A statistical method for evalu- ating systematic relationships. *Univ. Kansas, Sci. Bull.*, 38: 1409-1438.

Spoor F., Gunz P., Neubauer S. *et al.* 2015. Reconstructed Homo habilis type OH 7 sug- gests deep-rooted species diversity in early Homo. *Nature*, 519: 83.

Spoor F., Leakey M.G., Gathogo P.N. *et al.* 2007. Implications of new early Homo fos- sils from Ileret, east of Lake Turkana, Kenya. *Nature*, 448: 688.

Stringer C.B. 1984. The definition of Homoerectus and the existence of the speciesin Africa and Europe. *Cour. Forsch. Inst. Senckenberg, Frankfurt am Main*, 69: 131-143. Suwa G.E.N., Asfaw B., Haile-Selassie Y. *et al.* 2007. Early Pleistocene *Homo erectus* fossils from Konso, southern Ethiopia. *Anthropol. Sci.*, 115: 133-151.

Tamrat E., Thouveny N., Tai M. *et al.* 1995. Revised magnetostratigraphy of the Plio- Pleistocene sedimentary sequence of the Olduvai Formation (Tanzania). *Palaeogeogr., Palaeoclimatol., Palaeoecol.*, 114: 273-283.

Tattersall I. 1992. Species concepts and species identification in human evolution. *J. Hum. Evol.*, 22: 341-349.

Tattersall I. 2015. Homo ergaster and Its Contemporaries. In W. Henke & I. Tattersall (eds): *Handbook of Paleoanthropology*, pp. 2167-2187. Springer Berlin Heidelberg,

Terhune C.E., Kimbel W.H. & Lockwood C.A.2007. Variation and diversity in Homo erec- tus: a 3D geometric morphometric analysis of the temporal bone. *J. Hum. Evol.*, 53: 41-60. Terhune C.E., Kimbel W.H. & Lockwood C.A. 2013. Postnatal temporal bone on- togeny in Pan, Gorilla, and Homo, and the implications for temporal bone ontogeny in Australopithecus afarensis. *Am. J. Phys. Anthropol.*, 151: 630-642.

Vekua A., Lordkipanidze D., Rightmire G.P. *etal.* 2002. A New Skull of Early Homo from Dmanisi, Georgia. *Science*, 297: 85-89.

Villmoare B., Hatala K.G. & Jungers W. 2019. Sexual dimorphism in Homo erectus inferredfrom 1.5 Ma footprints near Ileret, Kenya. *Sci.Rep.*, 9: 7687.

von Cramon-Taubadel N. 2009. Congruenceof individual cranial bone morphology and neutral molecular affinity patterns in mod- ern humans. *Am. J. Phys. Anthropol.*, 140: 205-215.

von Cramon-Taubadel N. & Smith H.F. 2012. The relative congruence of cranial and genetic estimates of hominoid taxon relationships: Implications for the reconstruction of homi-nin phylogeny. *J. Hum. Evol.*, 62: 640-653.

Weber G.W. 2015. Virtual anthropology. *Am. J. Phys. Anthropol.*, 156: 22-42.

Weber G.W. & Bookstein F.L. 2011. *Virtual anthropology: a guide to a new interdisciplinary field.* Springer, NewYork, Wien.

Weidenreich F. 1940. *The torus occipitalis and related structures and their transformations in the course of human evolution.* Geological Soc.of China.

Weidenreich F. 1951. Morphology of Solo man. *Anthropological Paper of the American Museum of Natural History*, 43: 205-290.

Widianto H. & Zeitoun V. 2003. Morphological description, biometry and phylogenetic po- sition of the skull of Ngawi 1 (east Java, Indonesia). *Int. J. Osteoarch.*, 13: 339-351.

Wolpoff M.H., Thorne A.G., Jelinek J. *et al.* 1994. The case for sinking Homo erectus: 100 years of Pithecanthropus is enough. *Cour.Forschungsinst. Senckenb.*, 171: 341-361.

Wood B. 1991. *Koobi Fora research project: Hominid cranial remains.* Oxford University Press, USA.

Wood B. 1992. Origin and evolution of the ge-nus Homo. *Nature*, 355: 783.

Wood B. 1994. Taxonomy and evolution- ary relationships of Homo erectus. *Cour. Forschungsinst. Senckenb.*, 171: 159-165.

Wood B. & Richmond B.G. 2000. Human evo- lution: taxonomy and paleobiology. *J. Anat.*,197: 19-60.

Wood B.A. 1984. The origin of Homo erectus.

Cour. Forsch. Inst. Senckenberg, 69: 99-111. Xiao J., Jin C. & Zhu Y. 2002. Age of the fos-

sil Dali Man in north-central China deduced from chronostratigraphy of the loess–paleosol sequence. *Quat. Sci. Rev.*, 21: 2191-2198.

Yokoyama Y., Falguères C., Sémah F. *et al.* 2008. Gamma-ray spectrometric dating of

late *Homo erectus* skulls from Ngandong and Sambungmacan, Central Java, Indonesia. *J. Hum. Evol.*, 55: 274-277.
Zeitoun V., Détroit F., Grimaud-Hervé D. *et al.* 2010. Solo man in question: Convergent views to split Indonesian *Homo erectus* in twocategories. *Quat. Int.*, 223-224: 281-292.

Editor, Giovanni Destro Bisol

Appendix III

This is the manuscript redy for submission:

Mori, T.; Riga, A.; Ahmet Ihsan, A.; Harvati, K. (To be submitted) “A new virtual reconstruction and geometric morphometric analysis of Kocabaş hominin fossil from Turkey”

A NEW VIRTUAL RECONSTRUCTION AND GEOMETRIC MORPHOMETRIC ANALYSIS OF KOCABAŞ HOMININ FOSSIL FROM TURKEY

Tommaso Mori[1,2*], Alessandro Riga[2], Ahmet Ihsan Aytek[3], Katerina Harvati[1,4]

[1] Paleoanthropology, Department of Geosciences, Senckenberg Centre for Human Evolution and Palaeoenvironment, University of Tübingen, Tübingen 72070, Germany.

[2] Anthropology Laboratory, Department of Biology, University of Florence, Via del Proconsolo 12, Florence, Italy.

[3]Burdur Mehmet Akif Ersoy University, Department of Anthropology, Faculty of Arts and Science, TR-15030 Burdur – TURKEY

[4] DFG Centre for Advanced Studies "Words, Bones, Genes, Tools", Eberhard Karls University of Tübingen, Tübingen, Germany

*tommaso.mori@uni-tuebingen.de

ABSTRACT

The Kocabaş specimen comes from a travertine quarry near the homonymous village in the Denizli basin (Turkey). The specimen comprises three main fragments: portions of the right and left parietal and left and right part of the frontal bone. The fossil was assumed to belong to the *Homo erectus s.l.* hypodigm by some authors, while others see similarities with middle Pleistocene fossils such as Kabwe and Bodo or Ceprano and Arago. However, a geometric morphometric (GM) analysis of a fully reconstructed specimen is still lacking. Here, we present the first attempt to make a complete reconstruction of the missing medial portion of the frontal bone and a comprehensive GM analysis.

We restored the calotte by aligning and mirroring the three preserved fragments. Afterward, we restored the missing portion by applying the Thin Plate Spline (TPS) interpolation algorithm of target fossils onto the reconstructed Kocabaş specimen. For the GM analyses, we collected a total of 80 landmarks on the frontal bone (11 osteometric points, 14 bilateral curve semilandmarks, and 41 surface semilandmarks). The comparative sample includes 21 fossils from different chronological periods and geographical areas and 30 adult modern humans from different populations.

Shape analyses highlighted the presence in Kocabaş of some features usually related to middle Pleistocene humans, such as a big supraorbital torus associated with a relatively short frontal squama and absent post-toral sulcus. Cluster analysis and linear discriminant analysis classification procedure suggest Kocabaş be part of the same taxonomic unit of Eurasian and African specimens

usually described as *H. heidelbergensis s.l.*. In light of our results, we consider that an attribution of the Kocabaş hominin to *H. erectus s.l.* is unwarranted. The results of our analyses are compatible with different evolutionary scenarios, but a more precise chronological framework is needed for a thorough discussion of the evolutionary significance of this specimen. Future work should clarify its geological age, given uncertainties regarding its stratigraphic provenance.

Keywords: *Homo erectus*; *Homo heidelbergensis*; middle Pleistocene; virtual anthropology

Introduction:

Human dispersal and the human route "out of Africa" played a major role in the early phases of human evolution. The earliest human remains outside the African continent currently known are dated to 1.77 Ma at the site of Dmanisi, Georgia [111]. However, early and early middle Pleistocene human fossils from Eurasia are scarce and a gap in paleoanthropology between this early dispersal and the more recent and relatively abundant middle Pleistocene human fossil record. The fossil hominin from Kocabaş from the Denizli Basin in Turkey, recovered in 2002 from a travertine quarry near the Kocabaş village, can help shed light on early human presence in Eurasia.

The Kocabaş remains were discovered by workers during the processing of the travertine blocks brought from the travertine area to the factory (Dalmersan), as reported by Prof. Dr Mehmet Cihak Alçiçek [73]. There, the blocks were sliced at *ca* 35 cm of thickness. The partial calotte was embedded in one of the blocks, and unfortunately was cut by the saw used in the factory. The process only left 3 fragments of the skullcap: a large fragment of the right parietal, a fragment of the right frontal preserving part of the supraorbital torus, and a partial left parietal articulated with a fragment of the left frontal bone (not preserving the supraorbital torus). The exact provenance of the hominin find is not known. Nevertheless, it is considered that it likely derives from the Upper Travertine level, which was the only one exploited at the time of discovery in 2002 [74, 75]. This level also yielded various Pleistocene faunal remains, such as *Equus, Dama, Stephanorinus sp., Bison sp., Bos, Testudo sp.* [74, 112]. Based on the thermoluminescence dating of the sediments at the specimen's presumed location a first geological age of 510,000 ± 50,000 to 330,000 ± 30,000 years was suggested for the travertines (Kappelman et al. 2008). However, since Thermoluminescence has an upper limit of ca. 500 ka, a Turkish-French team carried on a paleomagnetic study of a sequence of travertine sediments (Vialet and Alçiçek 2012). The authors proposed an older age of more than 780 ka for the fossil-bearing sediments. Lastly, a more detailed paleomagnetic and

cosmogenic analysis on the sequence of travertine sediments conducted by Lebatard et al. (2014) showed that the levels exhibited reverse polarity. The authors therefore suggested that they were deposited before the Cobb Mountain sub-chron (between 1.22 and ca. 1.5 Ma). Lebatard et al. (2014) concluded that the Kocabaş specimen has a chronological age most likely between 1.1 and 1.3 Ma BP. This older chronology was supported by Khatib et al. [113], who in their stratigraphic, sedimentological, and paleomagnetic study of the region also proposed an age between 1.2 and 1.6 Ma for the Upper Travertine of Kocabaş. The Kocabaş skullcap, therefore, potentially fills a paleoanthropological gap between 1.6 and 1 Ma, observed in both the African and the Eurasian human fossil record. Indeed, this record is scarce in the time period between ca. 1.6 Ma (OH9 from Olduvai, Tanzania) and ca. 1 Ma (*Homo erectus*-like hominins from East Africa: KNM-OL 45500, Daka-Bouri BouVP2/66, BuiaUA 31). In Eurasia among the already cited specimens from Dmanisi, specimens found in the european continent are few: apart from the deciduous tooth from the Orce Basin dated to ca. 1.4 Ma (Toro-Moyano et al., 2013) the oldest human fossils are the Atapuerca–Sima del Elefante highly fragementary remains, dated to ca. 1.2 Ma (Carbonell et al., 2008). In east Asia oldest paleoanthropological evidence were recovered from the Sangiran dome and dated probably around 1.3 Ma [114]. The geographical provenance and proposed early chronology of the Kocabaş individual, therefore, makes this specimen pivotal for our understanding of the transition and relationship between early Pleistocene *H. erectus s.l.* and later middle Pleistocene human populations.

A preliminary description and comparative analysis on the Kocabaş specimen were conducted by Kappelman et al. (2008). These authors provisionally attributed Kocabaş to *Homo erectus sensu lato* on the basis of non-metric features and a few linear measurements. Important traits include the prominent supraorbital torus, which Kappelman et al. (2008) found to resemble Javan and African, rather than Chinese, *H. erectus*, and a distinct post-toral sulcus, commonly considered as a typical *H. erectus* condition (Kappelman et al. 2008). This first conclusion was supported by several subsequent studies [75-78]. Linear measurement analysis and cladistic approach supported the conclusion that Kocabaş belonged to *H. erectus s.l.* hypodigm [75, 78]. However, works based on a geometric morphometric (GM) approach did not convincingly support such a taxonomic affiliation. Only two GM comparative shape analyses have been published to date [56, 77], both showing that the Kocabaş frontal morphology is similar both to *H. erectus s.l.* and to middle Pleistocene African (Broken Hill 1 and Bodo; [77] or Eurasian fossils (Ceprano and Arago; [56]. Furthermore, the GM analysis performed by Vialet et al. [77] has been questioned on several

poins by Aytek and Harvati [56]. Some of the problematic issues pointed out were that Vialet et al. (2014) did not include a measure of supraorbital torus thickness, thus removing a critical feature in the characterization of frontal shape from their GM analysis. Second, Vialet et al. (2014) proposed a morphological similarity between OH9 and Kocabaş, but do not present any information on how OH9 (which is missing the upper part of the frontal bone, including bregma) was reconstructed. Finally, and perhaps most importantly, the taxonomic groupings used by Vialet et al. (2014), are do not comform to commonly accepted taxonomic attributions of the Pleistocene fossil record, potentially influencing their interpretation of the results: Middle Pleistocene specimens like Bodo and Broken Hill 1, commonly attributed to *H. heidelbergensis sensu lato* [115, 116] or *H. rhodesiensis* (e.g. Hublin 2009; Harvati et al. 2010), were instead assigned by Vialet et al. (2014) to African *H. erectus* and thus grouped together with much older specimens, such as KNM-ER 3733 and 3883. Even though their analysis showed similarities between Kocabaş and these middle Pleistocene African specimens (with Bodo and Broken Hill 1 plotting very close to Kocabaş in their PCA), this result was not discussed in the conclusions of Vialet et al. (2014), who instead proposed strong morphological affinities to early *H. erectus*.

Given these problems, the analysis performed by Aytek and Harvati [56] focused on the supraorbital torus shape, in order to include this important feature, as well as fragmentary specimens such as OH9, in their shape analysis. Their results showed no clear affinity of Kocabaş to OH9 specimen. Rather, they found similarities to the later Chinese *H. erectus s.l.* and middle Pleistocene samples. In 2018 a new work was published where Vialet and colleagues [78] performed a metric and cladistic analysis, concluding again that Kocabaş belonged to *H. erectus s.l.* However, this most recent analysis also shows some shortcomings: The metric analysis performed only comprised 4 linear measurements. After the data collection, no size correction was performed and the 4 measurements were analyzed through principal component analysis (PCA). However, such an analysis reflects only size differences along the first component, an expected result given the nature of PCA, an exploratory method looking for the greater source of variation, which, in this case, is size differences. No other clear pattern or separation between the different samples used was found. The cladistic analysis showed closer relation to the late early Pleistocene fossil (ca. 1 Ma BP) Buia, Daka, KNM-OG 45500). However, in this latter analysis, the authors did not include any middle Pleistocene fossils. Therefore, it was not possible to test any relationship between Kocabaş and later hominin specieslater hominin taxa. The taxonomic status of this important specimen, therefore, remains controversial.

Here, we use virtual anthropology and semilandmark-based GM surface analysis, to reconstruct and investigate the morphology of the Kocabaş frontal bone in a comparative framework, which includes *H. erectus s.l.* from Africa and Asia, as well as middle Pleistocene *Homo* from both Eurasia and Africa. In this framework we also present a new reconstruction of the skullcap with a complete restoration of the frontal squama using state-of-the-art techniques in virtual anthropology [54].

Material and Methods

Frontal bone virtual reconstruction

Reconstruction of the frontal bone was conducted digitally using Avizo software (version 9.1) (Thermo Fisher Scientific). The original fossil was scanned using a NextEngine 3D surface scanner (Camera resolution 3Mp and accuracy 125 µm) by AIA in the Hierapolis Museum, Pamukkale, Denizli. Afterward, the 3D meshes of the fragments were used for the virtual reconstruction. The reconstruction followed three main steps: i)Alignment of original preserved morphology, ii) Reconstruction and alignment of bilateral structures based on mirroring of existing morphology and iii) Reconstruction of missing structures by interpolation from reference specimens.

i) First the two fragments of the right parietal and left parieto-frontal element were articulated following the sagittal suture and aligned using the cut plane as a reference plane to get the original curvature. After this step, to align the frontal fragment we mirrored the previously articulated elements along the sagittal plane [53]. The mirrored specimen preserved the articulation between parietal and frontal bone at the level of stephanion along the coronal suture; this mirrored specimen was used only as a guide to align better the original right frontal fragment to the right parietal bone. Once the right frontal fragment was aligned, the previously mirrored left frontal fragment was discarded and the three original fragments were merged to form a complete 3D model (see Figure 1).

[Figure 1 here]

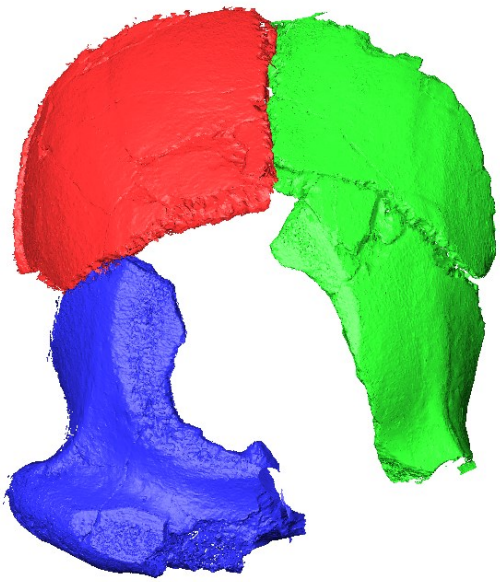

Figure 1. Alignment of the fragments.

In order to test the reconstruction accuracy, we performed a second alignment of the original fragments at a different time.

ii) The two 3D meshes composed of the three fragments (left fronto-parietal fragment, right frontal fragment, and right parietal fragment) derived from the two alignment processes were mirrored to reconstruct the left portion of the orbital missing part. The mirrored version of the 3D mesh was aligned using two different approaches. The first was done manually in a virtual environment (resulting in Kocabaş 1) following homologous anatomical structures. The second in a semiautomatic way using Thin Plate Spline Algorithm (TPS) [38, 53, 54, 117] (resulting in Kocabaş 2). The alignment based on TPS algorithm was performed *via* registration of 5 landmarks (Bregma, Stephanion L/R, and Frontotemporale L/R) on both specimens (the original and the mirrored version) and 80 semilandmarks digitized on the preserved portion of the skullcap of the original reconstructed specimen. The patch of 80 semilandmarks was projected onto the mirrored specimen and slid using the minimum bending energy algorithm to guarantee landmark correspondence across specimens [45]. Subsequently, the 85 landmarks and semi-landmarks of the reference (original specimen) and the target (mirrored specimen) were used to perform TPS interpolation [38]; the surface of the target was warped onto the reference specimen according to its landmarks and semi-landmarks. This mode guarantees that the target surface will be transformed exactly to the corresponding

landmarks of the reference, applying nearest-neighbor interpolation. This approach to reconstruct the missing side was tested by Benazzi and Senck [117] to have better accuracy compared to a simple mirroring and aligning method and to closely match the original morphology of the missing part. After these steps we had two slightly different 3D models (see Figure 2). To avoid confusion, in all subsequent analyses, we referred in the plot to Kocabaş 1 and Kocabaş 2 which, in turn, referred to the 2 alignments made from the original fragments. Kocabaş 1 was made using a manual alignment of the mirrored aspect, Kocabaş 2 used the TPS methodology described above.

[Figure 2 here]

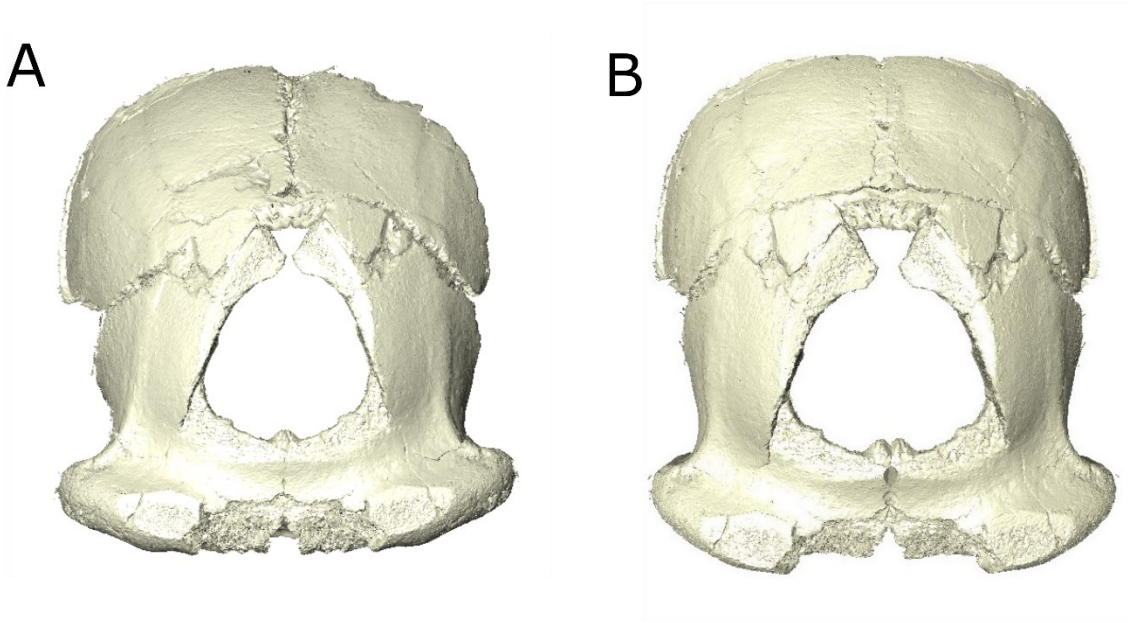

Figure 2. A – Kocabaş 2 made using TPS method (see above). B – Kocabaş 1 made using manual alignment of mirrored better preserved bilateral structures.

iii) In order to fully reconstruct the frontal squama and the medial aspect of the supraorbital torus, we used TPS interpolation of reference fossils onto the reconstructed Kocabaş specimen (Table 2). We used six different fossils for each of the two alignments. On both reconstructions (Kocabaş 1 and Kocabaş 2), we could collect 8 landmarks (nr. 1-2-4-6-8-9-10-11 from Table 1), 14 equally distant curves semilandmark for each temporal line and we placed 250 surface semilandmark as a template on the preserved aspect of Kocabaş skullcap. The template was projected on all the reference fossils used for the reconstruction. After projection semilandmarks were allowed to slide using the minimum bending energy algorithm

[45]. Subsequently, we warped each fossil to the landmarks and semilandmarks configuration of Kocabaş. In conclusion, we had two different alignments Kocabaş 1 and Kocabaş 2, on each one of these alignments we warped six different fossils (see Tab. 2 for a list) resulting in twelve different reconstructions of the frontal squama and the medial portion of the supraorbital torus (see figure 3 for an example). The twelve reconstructions as well as the mean of the two sets of reconstructions based on different alignmetns, were used as individual specimens in our shape analyses(see, e.g. Harvati et al. 2019; Mori et al. 2020).

[Figure 3 here]

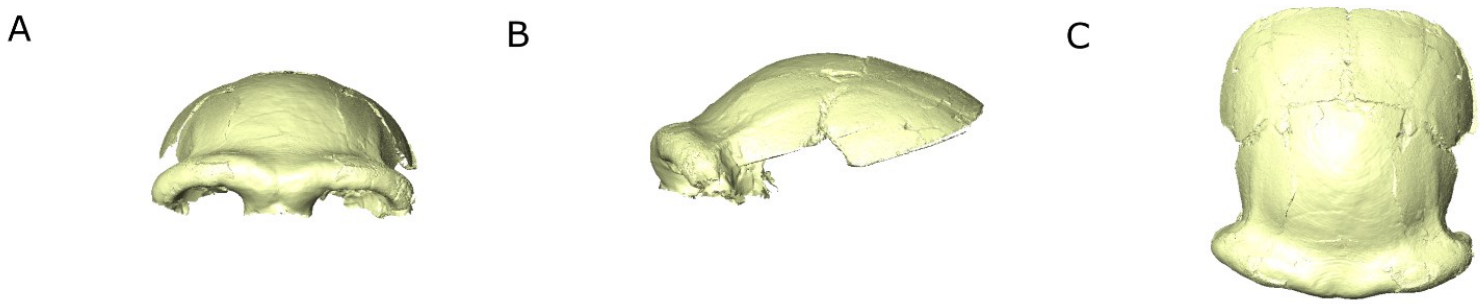

Figure 3 Full reconstruction of the medial portion of the frontal bone. Reconstruction based on Petralona specimen. A - Frontal view; B - Lateral view; C - Superior view.

Reference sample

The comparative sample comprises 30 recent adult modern humans from different populations of various geographical backgrounds. The sampling strategy was designed to capture maximum variation in recent human populations, with worldwide coverage and the inclusion of both sexes. The comparative samples are derived from ethnographic museum collections no older than a few hundred years (see Table 1 for specific geographic origin, sex, and housing institution information). 3D surface models of the specimens were obtained from medical computed tomography (CT) scans or microCT scans using the Avizo software. The majority of these were taken from previous studies [118-122].

Table 1. Modern humans populations origin

Population	N (M/F/U)	Collections
Australia	6 (3/3/0)	American Museum of Natural History, New York
Europe (Italy)	5 (2/3/0)	Museo di Storia Naturale, Florence
Chile (Tierra del Fuego)	2 (0/2/0)	Naturhistorisches Museum,Vienna

Sri Lanka	4 (0/0/4)	University of Tübingen
China	5 (0/0/5)	Musee de l'Homme, Paris
Philippines	5 (0/0/5)	Musee de l'Homme, Paris
Tanzania	2 (0/0/2)	University of Tübingen

The fossil comparative sample comprises 21 specimens from different chronological periods and geographical areas. The 3D surface models are derived from CT scans of the original specimens or optical surface scans of high resolutions casts (Table 2). We included several *H. erectus s.l.* fossils spanning the Pleistocene, as well as other Middle to Late Pleistocene *Homo* specimens attributed to *H. rhodesiensis*/*heidelbergensis* and to early *H. sapiens* (Jebel Irhoud 1, Skhūl V).

Table 2. Fossil sample used[1]

Fossil Specimen	Frontal reconstruction	Cast/Original	Institution	Chronological Age
H. erectus s.l.				
D 2280		C	AMNH	1.77 Ma [123]
D 2700[2]		C	AMNH	1.77 Ma (Garcia et al. 2010)
D 3444	X	C	AMNH	1.77 Ma (Garcia et al. 2010)
D 2282[2]		C	AMNH	1.77 Ma (Garcia et al. 2010)
KNM-OG 45500[3]		O	National Museums of Kenya	900 Ka [70]
Daka BOU-VP-2/66	X	O	National Museum of Ethiopia	1 Ma – 780 Ka [124]
KNM-ER 3733		O	Kenya National Museum	1.63 Ma [125]
KNM-ER 3883	X	O	Kenya National Museum	1.53 Ma [126]
Ngandong 14		C	AMNH	60-70 Ka/130Ka [127, 128]
Sangiran 17	X	C	AMNH	1.2 Ma [129]
Sambungmacan 3	X	C	AMNH	60-70 Ka [127]
Zhoukoudian I		C	AMNH	700-400 ka [130]
Zhoukoudian 12		C	AMNH	700-400 ka (Shen et al. 2009b)
Middle-Pleistocene *Homo* (MPH)				
Ceprano		C	AMNH	430 - 385 ka [131, 132]
Arago		O	University of Tübingen	438 ± 31 ka [133]
Bodo		O	National Museum of Ethiopia	640-550 Ka [134]
Broken Hill 1 (Kabwe)		C	AMNH	700 - 200 ka [135]
Petralona	X	O	Aristotle University of Thessaloniki	700-150 Ka [136]
Dali		C	AMNH	270-180 Ka [137]
Early *H. sapiens* (EHS)				
Jebel Irhoud 1		C	AMNH	300-90Ka [138, 139]
Skhūl V		O	Peabody Museum, Harvard University	120-80 Ka [140]
Unknown				
Kocabaş		O	Hierapolis Museum	1.2Ma-500ka [74, 75]
	[1]Abbreviations: D= Dmanisi, KNM= Kenya National Museums, ER=East Rudolf, OG= Olorgesailie, AMNH= American Museum of Natural History [2]sub-adult specimens [3]also published as KNM-OL 45500. KNM-OG 45500 follows the accession number at the National Museums of Kenya			

Landmark digitization

We collected a total of 80 landmarks on the frontal bone. Of these, 11 correspond to common osteometric points (i.e. Type 1-3 landmarks *sensu* Weber & Bookstein, 2011). A list and definition of the landmarks used are presented in Table 3. Two semi-landmark curves (i.e. Type 4 landmarks, *sensu* Weber and Bookstein, 2011) along each superior temporal muscle line were digitized from *stephanion* to the frontozygomatic suture. A total of fourteen evenly-spaced semilandmarks were placed on each curve. To fully investigate the shape of the frontal squama and the supraorbital torus, we used a patch of forty one surface semilandmarks (i.e. Type 6 landmarks, *sensu* Weber and Bookstein, 2011) encompassing the space between the previously identified landmarks (i.e. between the superior temporal muscle line and the supraorbital region). The patch was first digitized on KNM-OG 45500 and later projected on each specimen. The patch comprised eighteen symmetrical semilandmarks and five sagittal semilandmarks. The position of all landmarks is presented in Figure 4.

Table 3. Landmark number and definition

Full configuration	Definition [61]	Preserved configuration	OH9 Configuration
1. Bregma	Posterior border of the frontal bone along the midsagittal plane	X	
2. Midline post-toral sulcus	Minima of concavity on midline post-toral frontal squama	X	X
3. Glabella	Anterior-most point on frontal bone in Frankfort horizontal in the midsagittal plane		X
4/6 Mid-torus inferior R/L	Inferior margin of superior margin of orbit roughly at the middle of the orbital margin	X	X
5/7 Mid-orbital superior R/L	Superior point on the supraorbital torus at the middle of the orbital margin		X
8/9 Frontotemporale R/L	Where the temporal line reaches its most anteromedial position on the frontal	X	X
10/11 Stephanion R/L	Where the temporal line reaches the coronal suture.	X	X (only L)

All landmarks were digitized by the same user (T.M.). To estimate the measurement error of fixed landmark acquisition, we digitized the same specimen 10 times in 10 different days for the 11 Type 1-3 landmark configuration. Subsequently, intra-observer error was evaluated for each landmark based on a relative standard deviation threshold of 5%. Error assessment for these landmarks is important, as they are used as delimiting the placement of semilandmarks. For all 11 landmarks, the error was between 2-3.5% relative std. dev. and thus all landmarks were used for subsequent analysis.

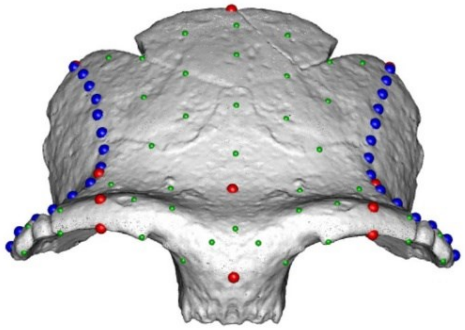

Figure 4 Landmark (red dots) and semilandmark (curves= blue, surface= green) configuration shown on the reconstructed Olorgesailie hominin KNM-OG 45500. [Image adapted from scan courtesy of the National Museums of Kenya]

Shape and statistical analysis

To explore variation in frontal bone shape in our sample, we conducted multiple analyses with different sample distribution and landmark sets.

The first analysis used the full sample, which comprised all fossils and modern humans, and the full landmarks and semilandmarks datasets.

The second analysis was conducted on a reduced landmark dataset comprising only the landmarks preserved on the original specimen, which therefore did not have to be estimated. This dataset included eight landmarks and the two temporal curves semilandmarks, and was termed “Preserved configuration” dataset.

The third analysis included only the landmarks / curves preserved on the specimen OH9, which made it possible to include this important individual in our comparative sample. This dataset comprised nine landmarks and only the left temporal curve and was termed the “OH9 configuration” dataset.

The fourth analysis used the full landmarks and semilandmarks dataset, but was limited to the fossil sample only.

In the first, third andfourth analyses, we used multiple reconstructions of Kocabaş derived by multiple estimations of the frontal bone morphology. In this case, we named Kocabaş 1 and Kocabaş 2 the mean landmarks / semilandmarks configuration of the six different reconstructions (based on different reference specimens) made for the two different alignments, where Kocabaş 1 refers to the manual alignment and Kocabaş 2 to the TPS based alignment.

In each case, we used the following procedure: a patch of Surface semilandmarks (when present) were projected on each specimen. The patch was first digitized on KNM-OG 45500, we assured to have perfectly symmetrical patch using the symmetrize fuction from the R package "Morpho" [141]. Bilateral landmark of the patch were reflected and relabeled then both configurations are averaged to obtain a perfectly symmetric one.. Curve semilandmarks and the projected surface semilandmarks (when present) were slid using the minimum bending energy criterion to guarantee landmark homology across specimens [45]. Thereafter, landmark configurations were superimposed using generalized Procrustes analysis (GPA) (removing all Kocabaş reconstructions) [37, 40, 69], in which the sum of squared distances between corresponding landmarks is minimized by rotation, translation, and scaling. After GPA superimposition, principal component analysis (PCA) of the Procrustes coordinates was used to visualize and explore each shape space. The landmark configurations of the Kocabaş reconstructions were superimposed via GPA on the Procrustes mean shape of the reference sample in each GPA made. The variance-covariance matrixes of these PCAs were used to project the different reconstructions in every analysis. In this way, neither the PCA axes nor the Procrustes coordinates of our reference sample were influenced by Kocabaş itself, therefore treating it as an unknown. While PCA was performed without *a priori* group categorization, group variation along major PC axes of variation was visualized *a posteriori* by applying convex hulls [142]. Shape variation along PCs was visualized as a deformation of a 3D surface mesh derived from the mean GPA landmark configuration or directly as modification of landmarks position. Vertices of the 3D surface mesh are the landmarks and semilandmarks used in the analysis. The mean surface and landmarks configuration was transformed via TPS interpolation [36] along 2 standard deviations (std. dev.) of a given PC axis.

UPGMA Cluster analysis

Procrustes distance, calculated as the square root of the sum of squared differences between two superimposed landmark configurations, was used as a quantitative measure for assessing overall shape affinities between specimens, with low values indicating greater shape similarity. Following the fourth analysis, the pairwise Procrustes distance matrix between all the fossils was used to perform a cluster analysis with the unweighted pair group method using arithmetic averages (UPGMA) [143]. We calculated the Procrustes distances for the Kocabaş reconstructions taking the mean configuration of all the different reconstructions made. This approach iteratively quantifies the similarity between two fossils and generates clusters of all sampled specimens in a rooted tree dendrogram, where all branch tips are of equal distance to the root.

Linear discriminant analysis

Linear discriminant analysis (LDA) and classification analyses based on PC scores from the fourth analysis were used to classify group affiliation of all Kocabaş reconstructions. We decided to perform LDA based on PC scores from the fourth analysis because this PCA was conducted only on fossil specimens. Using PCs from previous analyses would have led the discriminant function to perform well in separating modern humans from other groups but it would not have had a good discriminant power in the separation between fossils. We used solely two groups: *H. erectus s.l.* and the generally defined Middle Pleistocene *Homo* because the inclusion of early *Homo sapiens* would have reduced the number of variables to only one in the analysis since LDA needs fewer variables than cases in each group [144]. Specimens used to calculate the function, therefore, were only fossils grouped as MPH and *H. erectus s.l.* We used the first four principal components as variables for the LDA, accounting for 84.04% of the total variance, and all reconstructions were treated as unknown. We calculate the posterior probability of classification with SPSS software package (IBM, version 24 for Windows). We investigated whether the dataset used met the assumption [145]. We used histograms and saphiro-wilks test to verify that all Principal Component scores showed an approximately normal distribution. Outlier detection through boxplots was performed [145]. Although Sambungmacan 3 was found to be an outlier in the PC1 scores for the *H. erectus s.l.* group and Dali an outlier in PC2 scores for the MPH, we decided to keep them given the limited number of fossils available, a common problem in paleontology. Finally, the covariance matrices were similar among groups in all analyses, and Box's M-tests showed that they were homogeneous for the samples (resulting p-value was 0.153). Given the small number of individuals and also the grouping

affiliation that could represent a source of error in the LDA, results need to be approached with caution.

All of the procedures described above were conducted in SPSS software package (IBM, version 24 for Windows) and R [146] using the "Morpho", "Arothron", and "Phangorn" packages [141, 147-149].

Results

Shape analyses

Figure 5 shows a plot of the first two components resulting from a PCA of the Procrustes coordinates including all the comparative samples. These components account for over 80% of the total variance. Together, they show a clear separation between the recent modern humans and the fossil specimens, mostly along PC1. PC2, instead, helps to differentiate the Middle Pleistocene *Homo* fossils from *H. erectus s.l.*. The distribution of PC1 values in the sample seems to reflect a temporal trend; Early Pleistocene specimens such as KNM-ER 3733 or D2280 exhibit the lowest PC1 scores with Sambungmacan 3 showing the highest PC1 scores among fossil samples, similar to those of the early *H. sapiens* specimens Jebel Irhoud 1 and Skhul 5. Shape variation associated with positive PC1 scores is linked to a more rounded frontal squama with a much higher bregma position, characterizing *H. sapiens*. At negative PC1 scores, the frontal morphology exhibits a "shelf-like" condition, with a projected glabellar region and a clear supraorbital torus with an evident post-toral sulcus and lateral constriction, features typical of the *H. erectus* s.l. frontal bone morphology. Furthermore, temporal lines are less laterally displaced and relatively longer along negative PC1 scores than in positive PC1 values, while positive PC1 exhibits more latero-inferiorly placed and more arched temporal lines. The supraorbital region laterally shows a flexion inferior to the frontozygomatic area for positive PC1, reflecting the reduced lateral segments of the superciliary arches in modern humans. PC2 scores are linked to the supraorbital morphology and the relative size of the frontal squama. Positive scores of PC2 are related to a more robust, thicker, and laterally wider supraorbital torus with a relatively bigger supraorbital region compared to the frontal squama and a less constricted frontal, morphology characteristic of Middle Pleistocene *Homo*. Negative values of PC2 show a more posteriorly elongated temporal line and proportionally more elongated frontal squama compared to the supraorbital region. All reconstructions of Kocabaş, including those based on *H. erectus* reference specimens fall outside the *H. erectus s.l.* range of variation. In contrast, they are all closer to the Middle Pleistocene *Homo* convex hull and closest to the African

specimens Kabwe and Bodo, although they tend to have lower PC 1 values compared to Middle Pleistocene *Homo,* indicating a somewhat more receding forehead than most members of this group.

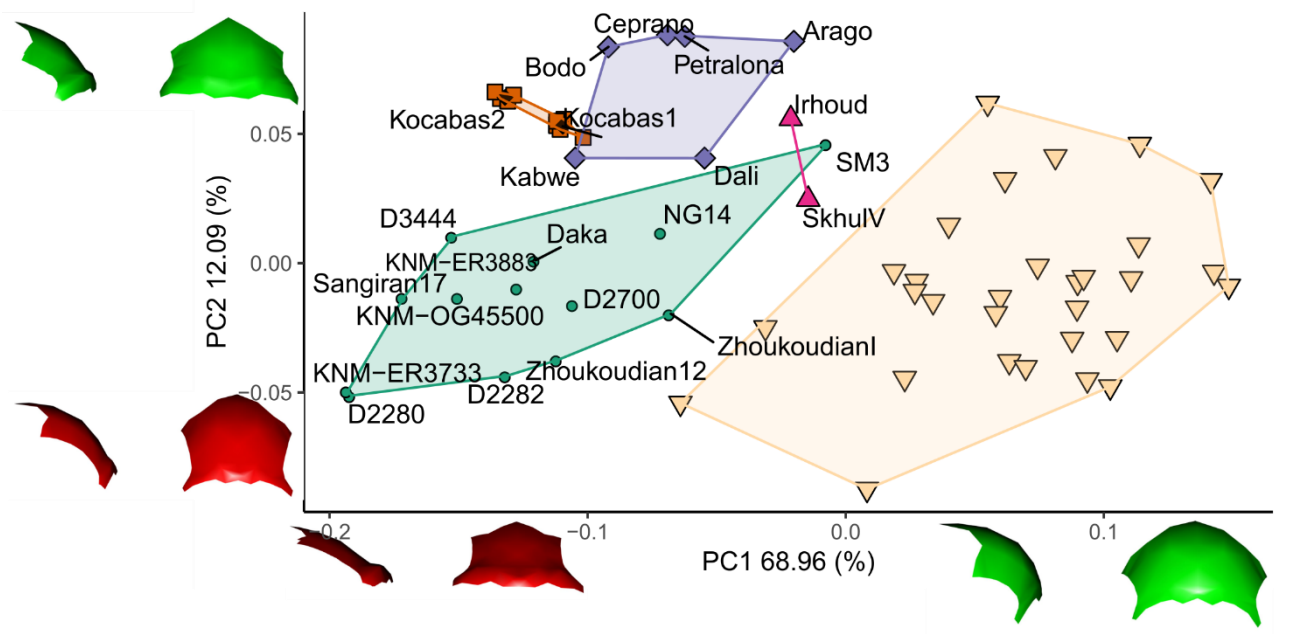

Figure 5. PCA plot of fossil specimens and recent modern humans. Convex hulls based on group attribution from Table 2. Symbols: yellow triangle = modern humans, green circle = *H. erectus s.l.*, purple diamond = Middle-Pleistocene *Homo,* pink triangle = early *H. sapiens*, brown square = Kocabaş reconstructions (black diamond = mean configuration of each reconstruction). Surface shape transformations along +/-2 std. dev. from mean along PC axes are shown below (PC1) and on the left side (PC2) of the plot.

In the second analysis, we used only the landmarks and curve semilandmarks that were obtained directly on the Kocabaş fossil after the mirroring steps of the fragments (see figure 2). Therefore, only two reconstructions were used, both comprising only the existing bone fragments after manual and TPS alignment (Kocabaş 1 / Kocabaş). Results of the PCA are presented in Figure 6. Here, PC1 and PC2 account for ca. 79% of the total variance. This reduced dataset still separates fossils and modern humans along with the first two components. However, the separation between fossil samples is less evident along PC2 compared to the previous analysis: the convex hulls of Middle Pleistocene *Homo* and *H. erectus* s.l. overlap somewhat, with Kabwe and Dali falling within

the latter samples variation. Nevertheless, specimens from the Middle Pleistocene *Homo* group still show the highest PC2 scores among all individuals. In this shape space, a positive PC1 score is linked to a higher vault with a higher bregma position, temporal lines are lower and more curved projecting latero-posteriorly. The orbital landmarks are almost on the same plane as the mid-toral sulcus and the anterior part of the temporal line in the top view. Low PC1 values are linked to a flatter frontal vault, a straight temporal line with more anteriorly projecting orbital landmarks. The mid-toral sulcus and the anterior portion of the temporal line are not on the same plane as the orbital landmarks for negative PC1 scores. Low PC2 is linked to a relatively longer frontal squama compared to positive PC2. The temporal lines, for positive PC2, are more laterally placed with a greater distance between temporal lines and the orbital region. Negative values of PC2 are related to a narrower post-orbital constriction. As in analysis 1, Kocabaş is closer to the Middle Pleistocene *Homo* convex hull than to the *H. erectus s.l.* one, falling closest to African specimens like Bodo and Kabwe. However, its PC1 score is more negative than those of the former sample, indicating, again, a somewhat flatter frontal in Kocabaş than in the Middle Pleistocene *Homo* specimens in included here.

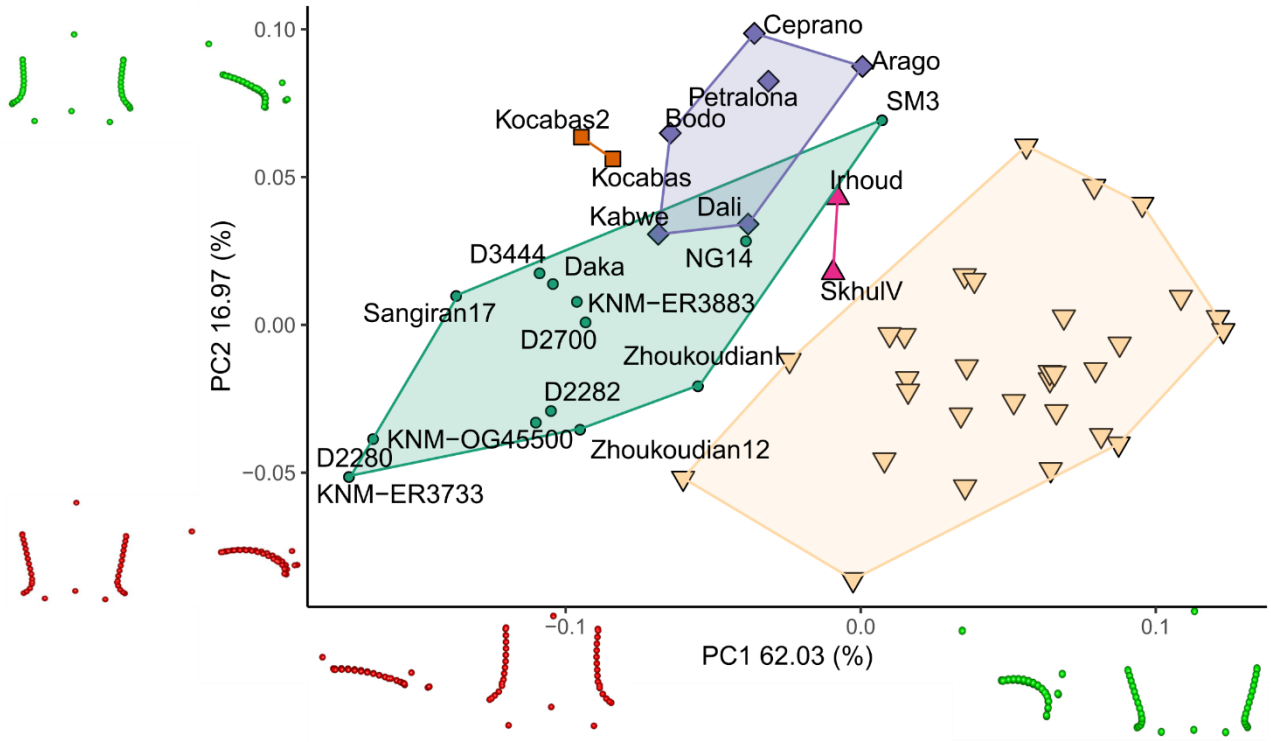

Figure 6 PCA plot "Preserved configuration". Samples and symbols as in Figure 5. Frontal landmarks (in lateral and upper views) shape variation corresponding to +/-2 std. dev. from mean PC values along each axis are shown below (PC1) and to the left (PC2) of the plot.

Analysis 3 was based only on the limited number of landmarks / curve semilandmarks preserved on OH9, and was conducted in oder to include this important specimen. Resutls are presented in Figure 7. PC1 and 2 together account for ca. 70% of the total variance. This limited dataset still separates fossil and modern humans along PC1, similar to the previous two analyses, however, as in Analysis 2, the covex hulls of Middle Pleistocene *Homo* and *H. erectus* s.l. overlap, with Kabwe, Bodo and Dali falling within the range of *H. erectus* s.l. variation. Shape changes associated with PC1 for positive scores are a vertically positioned mid toral sulcus relative to bregma, a reduced thickness of the supraciliary region, and a rounder and more arched temporal line, negative values are related to a more anteriorly projecting lower orbital landmarks compared to the temporal line and a flatter morphology (*i.e.* the difference in height between stephanion and bregma). In PC2 the temporal line is shorter and more distant to the orbital region for positive scores compared to the negative values. Positive PC2 shape changes are associated with a thicker supraorbital torus with a more anteriorly placed mid toral sulcus compare to negative PC2. Here, again, Kocabaş is closer in its plot position to the middle Pleistocene *Homo,* especially to the Kabwe and Bodo specimens from Africa. Interestingly, OH9 does not cluster with other African early Pleistocene *H. erectus s.l..* Although it also plots away from Kocabaş and the other middle Pleistocene *Homo* on PC1, it shows a similar PC2 score to Kocabaş and to the latter sample generally.

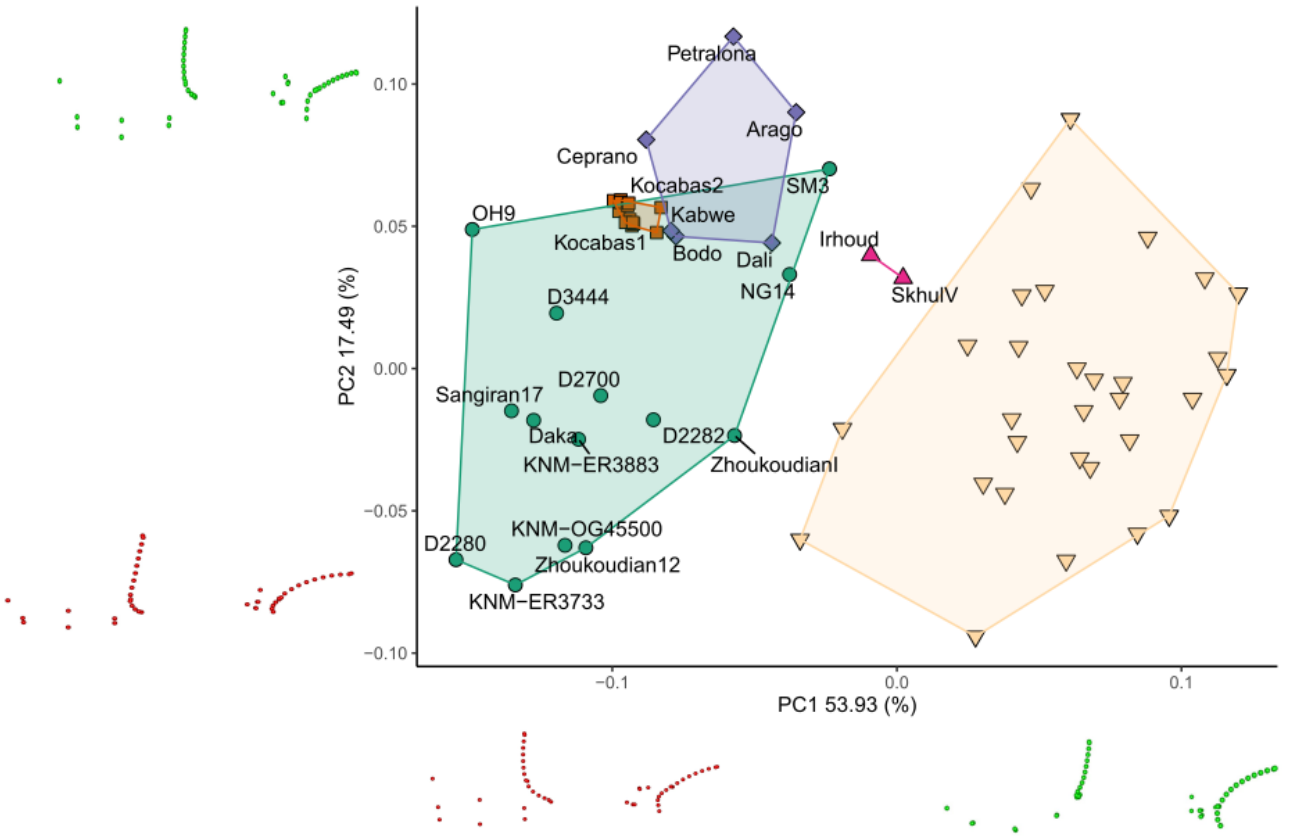

Figure 7 PCA plot "OH9 Configuration". Samples and symbols as in Figure 5. Frontal landmarks (in lateral and upper views) shape variation corresponding to +/-2 std. dev. from mean PC values along each axis is shown below (PC1) and to the left (PC2) of the plot.

In our last shape analysis (Analysis 4), we included only the fossil specimens but used all the landmark and semilandmarks also uses in Analysis 1 (Figure 8). This PCA mirrors the one in Analysis 1, in that the Middle Pleistocene Homo sample is well separated from that of the H. erectus s.l. with only one early H. sapiens specimen (Skhul 5) overlapping with the convex hull of the other, plotting close to the Sambungmachan 3 specimen. Shape variation associated with the first component includes a more rounded frontal squama for positive PC1 scores and a post-toral sulcus reduction with wider postorbital constriction and the frontal squama is relatively shortened antero-posteriorly. Negative PC1 scores are associated with a more anteriorly projecting glabellar region; in addition, the temporal lines are less curved and more medially displaced, and the frontal squama in between them shows a flatter morphology. Postorbital constriction, as well as a marked post-toral sulcus, is evident for negative PC1 scores. The supraorbital torus also projects more laterally for negative PC1 scores. Along PC2, Middle Pleistocene *Homo* fossils tend to have higher values while early *Homo sapiens* have lower PC2 scores. *H. erectus s.l.* show both high and low values, with Early Pleistocene specimens toward the positive end and Middle-Late Pleistocene fossils toward the

negative end. Positive scores of PC2 are associated with a thicker morphology of the supraorbital torus and an overall more robust structure. Positive PC2 is also associated with a reduction of the post-toral sulcus with the frontal squama that ends in the supraorbital torus with an almost uninterrupted shape. The frontal squama is reduced in size relative to the supraciliary region. Negative PC2 scores are associated with a weaker supraorbital torus compared to the relative size of the frontal squama. As in all other analyses, all reconstructions of the frontal bone of Kocabaş plot close to the middle Pleistocene *Homo* group. They all show a relatively rounded frontal profile with a thick supraorbital torus. One of the reconstructions, the Kocabaş 2 alignment, has among the highest PC2 scores in the plot. As before, Kocabaş is closer to the middle Pleistocene Bodo and Kabwe specimens. We observe a certain degree of geographical and temporal differentiation between our sampled *H. erectus s.l* also in this plot along PC1 from older to younger specimens. Middle to Late Pleistocene East and Southeast Asian specimens tend to have positive PC1 and negative PC2 scores, closer to fossil *H. sapiens*. By contrast, Early Pleistocene African and Middle Pleistocene African and Eurasian fossils have negative PC1 and positive PC2 distributions.

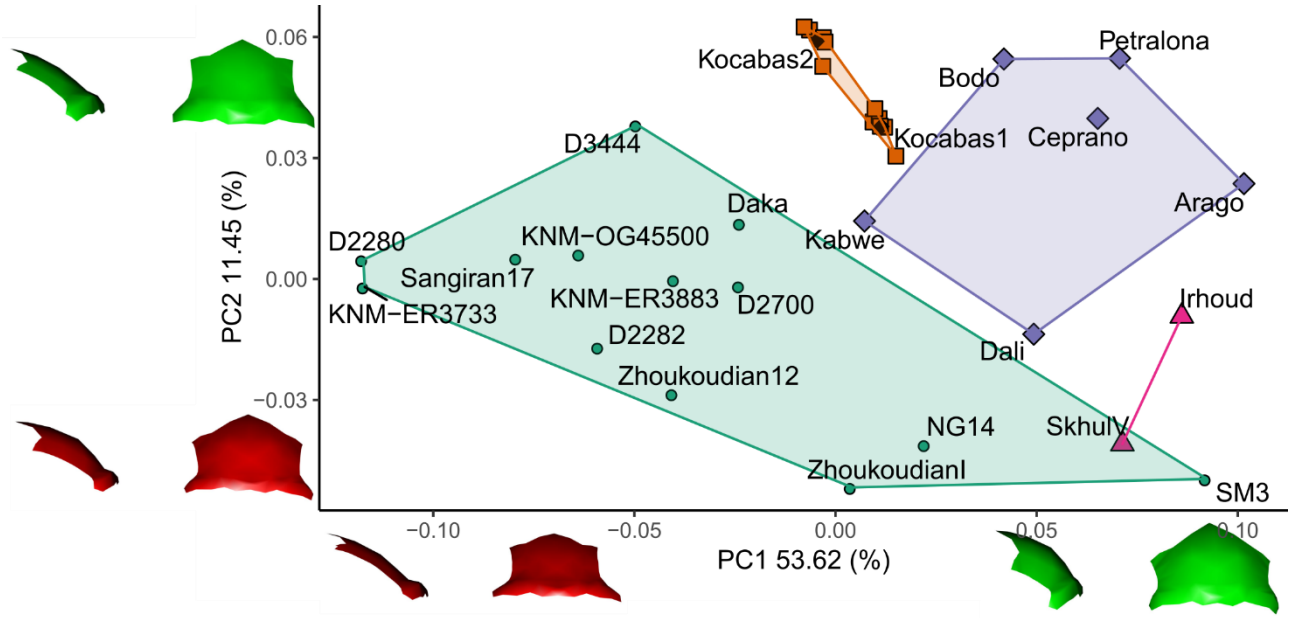

Figure 8 PCA plot only fossil sample, full configuration. Samples and symbols as in Figure 5. Frontal bone (in lateral and frontal views) shape variation corresponds to +/-2 std. dev. from mean PC values along each axis.

UPGMA Cluster analysis

Results of pairwise Procrustes distances between all the fossil specimens from the last analysis were used as the distance matrix for the cluster analysis. The tree generated from the

UPGMA cluster analysis (Figure 9) shows two main branches. One branch includes the more recent, Middle-Late Pleistocene fossils, and the other branch includes the older *H. erectus s.l.* specimens. Kocabaş's mean shape reconstruction clusters with the more recent Middle Pleistocene *Homo* specimens.

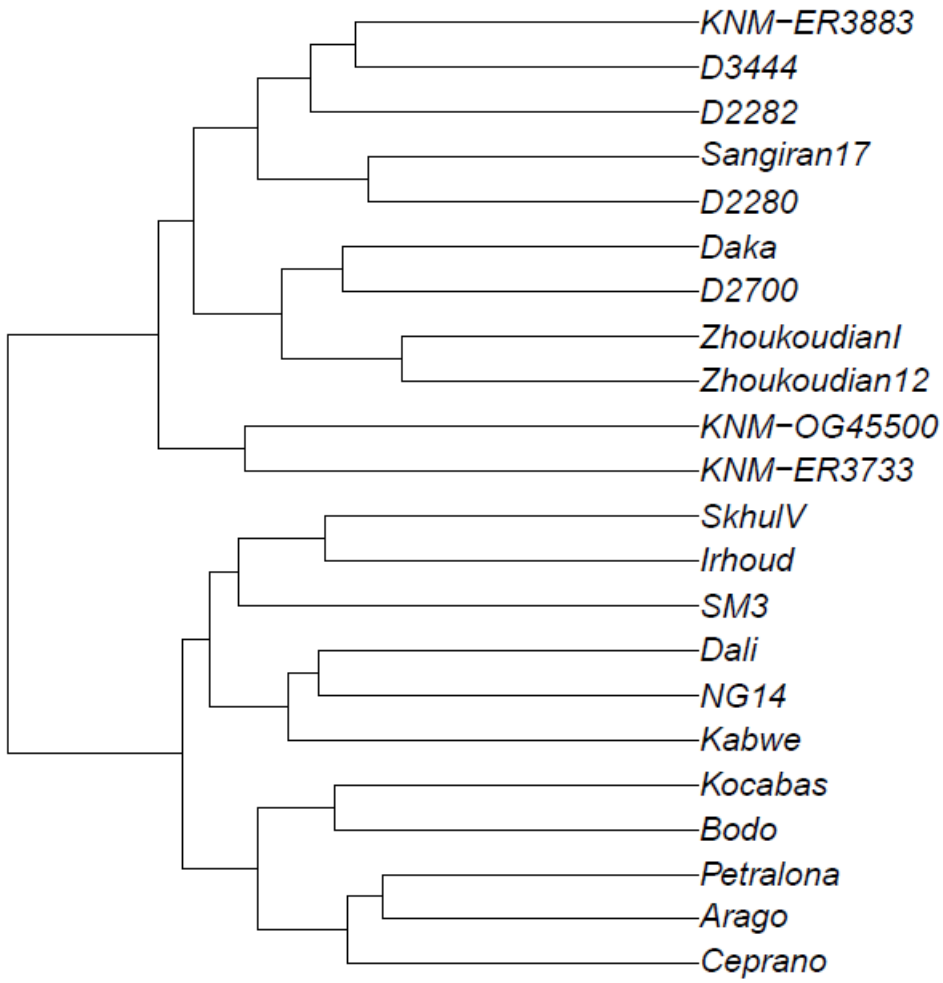

Figure 9. UPGMA cluster analysis based on pairwise Procrustes distances between individuals.

Linear Discriminant Analysis

The LDA classification used two groups, MPH and *H. erectus s.l.*. The Kocabaş reconstrcutions were treated as unknown. Our cross-validation analysis correctly classified 78,9% of the cases. We, therefore, consider that the results are robust. Only four specimens were misclassified: D3444, Sambungmacan 3, Dali, and Kabwe. These specimens had a posterior probability to belong to the

opposite group of: 0.59, 0.86, 0.81, and 0.52, respectively. All Kocabaş reconstructions were classified as middle Pleistocene *Homo* with a posterior probability between 0.990 and 1.000.

Discussion

Our reconstruction of the frontal bone of Kocabaş has allowed for a comprehensive, quantitative analysis of its morphology. All the reconstructions in all the analyses fall outside the convex hulls of our samples on PC1 and 2. Nevertheless, all reconstructions tend to plot closest to middle Pleistocene *Homo.* Together with results from the UPGMA cluster analysis and the classification from the LDA, Kocabaş seems to show morphological similarities to middle Pleistocene *Homo*. In this regard, our results disagree with previous works [73, 75-78], which concluded that Kocabaş was a representative of *H. erectus s.l.* with closer affinities to the Daka, Buia, and KNM-OG 45500 specimens [78].

Kocabaş shape analyses

Putting together results from different analyses, we report Kocabaş's morphological similarities to other fossils. In our reconstruction, Kocabaş shows a thick supraorbital torus with a large trigone area and a relatively short frontal squama compared to the supraorbital region, a relatively shallow post-toral sulcus and a more rounded frontal profile compared to the shelf-like morphology of African *H. erectus* such a KNM-ER3773 or KNM-OG 45500. In our PCA plots, Kocabaş falls between more derived MPH and archaic *H. erectus s.l.* Considering the cluster analysis results and the LDA classification, this specimen seems to have more affinities with MPH.

Kocabaş taxonomy and working hypothesis

Our study highlights the presence of continuity of frontal bone shape in Africa during the Early Pleistocene. This continuum in frontal bone morphology presumably appeared with the emergence of *Homo erectus s.l.* diagnostic features, expressed in specimens like KNM-ER 3733 and lasted up to about 1 Ma, represented in our study by KNM-OG 45500 and Daka specimens. Beginning in the Middle Pleistocene, some fossils then show a more derived morphology. Our results show this to the extent that Middle to Late Pleistocene fossils across Africa and Eurasia are distinct from the Early Pleistocene fossils along the major axis of variation in shape space (i.e. along PC1 in Fig. 8), consistent with previous GM studies on cranial forms [43, 49, 61, 91, 150, 151]. The UPGMA phenogram (Fig. 9) also shows two temporal clusters that split our fossil sample primarily chronologically, from early specimens dated to between ca. 1.77 to 0.7 Ma to more derived

specimens dated to between the Middle and Late Pleistocene. These observations suggest probably a taxonomic and phylogenetic discontinuity that ranges across the Matuyama/Brunhes reversal of 780 ka, in a possible relationship with the more general phenomenon known as the "Mid-Pleistocene revolution" [152] that, in turn, corresponds to the beginning of environmental changes of MIS 18-16. Phenetic differences between Early and Middle Pleistocene fossils might represent a distinction at the species level in our analyses. Unfortunately, a gap in fossil evidence between 1 Ma BP and 600ka makes it difficult to track evolutionary changes in the genus *Homo* in this period. However, after this time, more encephalized hominins were widespread in Africa and Eurasia. Today, the exact chronology and phylogenetic relationship related to the appearance of MPH, which we may call *H. heidelbergensis,* is still unclear[102, 103, 105, 116, 153]. As a matter of fact, we do not know when and where the humans that were ancestral to both the Neanderthals in Europe and Homo sapiens in Africa originated [103].

In this context, we introduce the first hypothesis about Kocabaş. This fossil may represent the earliest form of the same taxonomic unit of Bodo specimen. Kocabaş presents morphology consistent with but less derived than later specimens assigned to this taxon; it has a PC1 score and related morphology usually linked to more archaic specimens but a PC2 which is already derived as the other MPH specimens. The paleomagnetic and cosmogenic nucleotide study made on the travertine quarry, from which presumably the specimen comes, proposed age for Kocabaş between 1 Ma and 1.5 Ma BP [74], with the lower limit considered more plausible. Such results place it as a good candidate as the earliest representative of MPH taxonomic unit. Kocabaş demonstrates a morphology that is sufficiently distinct from *H. erectus s.l.*, despite the overlap of some features, and close to the early representatives of African and Eurasian MPH, particularly Bodo, Kabwe, and Ceprano. Kocabaş exhibits the occurrence of a stock of derived features that characterized MPH taxonomic unit and it presents a mosaic of morphological characteristics between *H. erectus s.l.* and MPH; such as a less rounder and partially more shelf-like frontal morphology, related to its low PC1 score, and more derived supraorbital morphology with an almost absent post-toral sulcus (high PC2 score).

Considering the later forms of humans: Neanderthals, Denisovans, and modern humans that presumably appeared respectively in Europe, Asia, and Africa, Turkey is almost a midpoint among these regions. At present, we have little evidence regarding other possible candidates representing early forms of MPH groups. Specifically *H. heidelbergensis s.l..* One candidate as a putative early form of *H. heidelbergensis s.l.* is gombore MK 1 and MK 2 specimens [49]. The chronology proposed

for this specimen is younger compared to the presumed datation of Kocabaş. However, taken together they can be representative of the earliest form of a new taxon that originates in the Levant and spread across Africa and Eurasia. Unfortunately, the preservation of Gombore specimen makes hard a direct comparison between the two specimens in our work.

A second working hypothesis may be that Kocabaş represents a geographical variety of *H. erectus s.l.* and differences from other *H. erectus s.l.* can be linked to differences in paleodemes that belonged to this widespread taxon. Testing such a hypothesis is difficult given the limited nature of fossils from this geographic area and timeframe. Our sample only comparable specimens in terms of time and space: OH9, Daka, KNM-OG 45500 [70, 124, 154] show some differences from Kocabaş frontal shape. Overall, Kocabaş is more similar in morphology to middle Pleistocene specimens, but similarities exist with specimens dated to the end of the Early Pleistocene. In comparison with OH9, they both show similar PC2 morphology but differ in shape along the PC1 axis, representing most of the variance in our analysis. Moreover, the analysis did not completely compare frontal morphology but only some preserved aspects of the frontal morphology. An important feature missing in the OH9 analysis is the overall frontal height, given the lack of bregma. Such region is fundamental when we want to evaluate more or less derived morphology, as shown from other results. Overall, this hypothesis might be true only when we extend the variability of *H. erectus s.l.* even further, but it implies that we might also include later fossils from Africa, such as Kabwe and Bodo, in this taxon. We, therefore, consider this hypothesis very unlikely.

As a third hypothesis, we might consider the possibility of a younger age for Kocabaş. The history of this specimen makes it hard to be certain about the stratigraphic and archeological context of its recovery [56, 74, 75]. Datation of this specimen has been a difficult task; the first dating placed it around 400Ka BP (U-Th analysis) and 500 Ka BP (thermoluminescence method) [73, 106]. A date of 1.1 Ma was proposed based on ESR technique [107]. The last dating based on paleomagnetic and cosmogenic nucleotide studies gave an age around 1 to 1.5 Ma BP [74]. All these different results, together with the history of the discovery of this specimen, led Muttoni and colleagues not to consider the hominin skull a well-dated specimen [108]. The paleontological remains are also scarce and poorly studied. Erten and colleagues [155] studied the paleontological materials, which they referred to as “insufficient to propose any reliable date” (pg. 276 Erten et al., 2005); however, they concluded that *Equus* specimens might agree with the previously proposed age of 400 Ka. Later, another study [112] referred to the tafocenosis as compatible with the villafranchian faunal assemblage concluding that it could be older than 1.2 Ma BP. As a matter of

fact, when we consider fossils without a certain chronology, it is easy to speculate about different evolutionary hypotheses as recently happened for*H. naledi* and its place in the hominin lineage [156, 157]. For this reason, it would be possible that Kocabaş could be younger than expected, if so, we might consider it as a specimens that could belong more probably to Bodo's taxonomic unit probably *H. heidelbergensis s.l.* and not to *H. erectus s.l.* as previously thought.

Despite the different Hypotheses depicted above, this hominin skull seems to be quite distinct from other *H. erectus s.l.* fossils and more similar in its frontal morphology to Middle Pleistocene hominin often referred as *H. heidelbergensis/rhodesiensis* (*H. heidelbergensis s.l.*).

Comparison with previous work and reconstruction bias

Differences between our and the results from Vialet and colleagues [78] could be related to differences in the reconstruction steps. The alignment of disarticulated fragments is difficult to reproduce, and it is prone to inter and intra-individual error [54]. For this reason, we performed two alignments and two mirroring procedures (using two different methods, see Material and Methods) and multiple reconstructions of the missing area to mitigate this source of error. TPS alignment of mirrored parts is less subjective than the manual alignment, and it is considered to represent better the morphology of the original specimen [117]. For this reason, we considered Kocabaş 1 reconstruction to be more precise or, at least, more reproducible. We could not directly test how much differ our reconstruction from the one made by Vialet and colleagues, but our results show that already two different alignments made by the same user (T.M.) give different results in the GM analysis (see PCA plots). Differences between the two alignments and the mirroring step are clearly shown in the second analysis (Fig. 6). Here, the dataset used derived only from the portion of fossils preserved, for that reason differences between the two reconstructions are mainly due to intra-observer error in the alignment since landmark accuracy tested positively in our sampling strategies. Reconstruction procedures of the frontal squama and the medial aspect of the supraorbital torus were substantial and results need to be taken under consideration in light of all the analyses together. Looking at the various results from different datasets, PCA plots show that Kocabaş had similar PC1 PC2 distribution. Full reconstruction of the missing part was obtained using different reference samples. We decided to use a wide geographical and temporal range of different *H. erectus s.l.* fossils and Petralona. The different fossils have different supraorbital torus morphology from extremely double-arched morphology such as Daka to more straight such as SM3. They are also different in the frontal squama from more elongated morphology to more rounded ones. Despite the difference in the reference sample, all the reconstructions of the missing area gave very

close results in the PCA plot. Thus, indicating that the reference specimen does not influence the results of the final reconstruction of Kocabaş.

Compared to Vialet and coauthor analyses [78], our work also differs from a methodological point of view in the dataset and data analyses. They used multivariate metric analysis that gives a different result from our geometric morphometric analysis. However, their PCA plots are highly influenced by the size of the specimen because they did not correct variables for the size difference. PCA is an ordination procedure that emphasizes variation in our sample [158]. In their case, without a size correction, the main difference between all fossils is the difference in size. Cladistic analysis is less affected by size differences, given the nature of the dataset used. However, it is dependent on the operational taxonomic units (OTU) chosen and the sample used. In their case, they did not comprise any Middle Pleistocene specimens although affinities between Kocabaş and MPH were reported in previous studies [56, 73, 77].

Compared to the earlier works on Kocabaş we found some similarities and differences in our results. Similar to the plot presented by Vialet and colleagues [77] from their GM analysis we also found Kocabaş to plot close to Broken Hill/Kabwe and Bodo. Compared to Aytek and Harvati [56], however, we did not find Kocabaş to be closer in shape space to Chinese *H. erectus,* but we confirm some of the differences between OH9 and Kocabaş. We also confirm the affinities they noted between Kocabaş and middle Pleistocene *Homo*. Aytek and Harvati [56] noted that in Vialet and coauthor analysis [77], results were influenced by a lack in the coverage of the supraorbital area in the landmark set. On the contrary, Vialet and colleagues (2018) argued that results from Aytek and Harvati (2016) were driven by a landmark configuration focused solely on the supraorbital region. Here, we quantify and analyze the morphology of the frontal bone in its totality, comprising information from the supraorbital torus and the frontal squama together. Our study shows that the distinction in shape between earlier *H. erectus* and middle Pleistocene *Homo* are related to the multivariate pattern of shape differences in supraorbital morphology and frontal squama relative size and shape.

Limitation and future direction

Kocabaş has a chronological age and a geographical position that might be linked with the period suggested for speciation in a taxon that presumably is ancestral to later hominin taxa. However, caution is needed, the specimen history is troubled, and it is difficult to be entirely sure about its original position in the sediment where it was recovered. Despite all the effort made and the excavation history of the travertine cave, there is a chance that this specimen is derived from

other travertine layers. At present, we cannot exclude this hypothesis. Moreover, all the reconstruction procedures introduce a level of uncertainty; we tried to reduce the bias from the reconstruction procedure by making multiple versions of the specimen and by analyzing Kocabaş using different datasets, reducing the analysis to the only preserved aspect of the fossil. At present, it is clear that the manual alignment of the fragments is difficult to replicate each time, and therefore is important to find new ways to do the alignment using automatic approaches [see 159]. Future studies should try to convincingly estimate the specimen's age to evaluate this specimen in the correct framework. Moreover, this study shows that a reassess of the status of *H. heidelbergensis s.l.* and probably *H. erectus s.l.* might need to be reconsidered [23, 32, 61, 90, 91, 102, 104, 105, 115, 116, 122, 124, 150, 160, 161] in light of local and temporal morphological differences also evidenced in our analyses.

Conclusion

Kocabaş specimen came from a travertine quarry located in the Denizli basin. The specimen comprises 3 main fragments: portions of the right and left parietal and part of the left and right frontal bone. Different authors have already studied the specimen [56, 75-78], but none of them performed a GM analysis on a fully reconstructed specimen. Here, we present the first attempt to fully reconstruct the missing medial portion of the frontal bone and a comprehensive GM analysis of the frontal squama. Our shape analyses highlighted the presence in Kocabaş of some features usually related to later middle Pleistocene humans, such as a big supraorbital torus associated with a relatively short frontal squama, a reduction of the post-toral constriction, and quite arched temporal lines. Together with cluster analysis and LDA classification procedure, Kocabaş seems to be part of the same taxonomic unit, which comprises Eurasian and African specimens usually described as *H. heidelbergensis s.l*. Results of our analyses suggest different evolutionary scenarios, but in conclusion, we consider Kocabaş not to belong to *H. erectus s.l.* Future work should aim to confirm the presumed geological age of this specimen. In conclusion, our results disagree with the previous analyses, which placed this specimen inside the *H. erectus s.l.* taxon.

Reference

1. von Koenigswald, G. and F. Weidenreich, *The relationship between Pithecanthropus and Sinanthropus.* Nature, 1939. **144**.
2. Weidenreich, F., *Some problems dealing with ancient man.* American Anthropologist, 1940. **42**(3): p. 375-383.
3. Mayr, E. *Taxonomic categories in fossil hominids*. in *Cold Spring Harbor Symposia on Quantitative Biology*. 1950. Cold Spring Harbor Laboratory Press.

4. Simonetta, A., *Catalogo e sinonimia annotata degli ominoidi fossili ed attuali (1758–1955).* Atti Soc. Toscana Sci. Nat., Pisa, Ser. B, 1957. **64**: p. 53-113.
5. Robinson, J.T., *The australopithecines and their bearing on the origin of man and of stone tool-making.* South African Journal of Science, 1961. **57**: p. 3-16.
6. Brown, F., et al., *Early Homo erectus skeleton from west lake Turkana, Kenya.* Nature, 1985. **316**(6031): p. 788-792.
7. Leakey, L.S., *New finds at Olduvai gorge.* Nature, 1961. **189**(4765): p. 649-650.
8. Leakey, R. and A.C. Walker, *Further hominids from the Plio-Pleistocene of Koobi Fora, Kenya.* American Journal of Physical Anthropology, 1985. **67**(2): p. 135-163.
9. Leakey, R.E., *New hominid fossils from the Koobi Fora formation in northern Kenya.* Nature, 1976. **261**(5561): p. 574-576.
10. Walker, A. and R.E. Leakey, *The hominids of east Turkana.* Scientific American, 1978. **239**(2): p. 54-67.
11. Antón, S.C., *Natural history of Homo erectus.* American Journal of Physical Anthropology, 2003. **122**(37): p. 126-170.
12. Baab, K.L., *The taxonomic implications of cranial shape variation in Homo erectus.* Journal of Human Evolution, 2008. **54**(6): p. 827-847.
13. Harrison, T., *Cladistic concepts and the species problem in hominoid evolution*, in *Species, species concepts and primate evolution*. 1993, Springer. p. 345-371.
14. Howell, F., *Evolution of African mammals.* Maglio VJ and Cooke HBS (eds), 1978: p. 154-248.
15. Howells, W.W., *Homo erectus—who, when and where: a survey.* American Journal of Physical Anthropology, 1980. **23**(S1): p. 1-23.
16. Rightmire, G.P., *Comparisons of Homo erectus from Africa and southeast Asia.* Courier Forschungsinstitut Senckenberg, 1984. **69**: p. 83-98.
17. Rightmire, G.P., *Species recognition and Homo erectus.* Journal of human evolution, 1986. **15**(8): p. 823-826.
18. Rightmire, G.P., *The Evolution of Homo Erectus: Comparative Anatomical Studies of an Extinct Human Species*. 1990, Cambridge: Cambridge University Press.
19. Rightmire, G.P., *Evidence from facial morphology for similarity of Asian and African representatives of Hhomo erectus.* American Journal of Physical Anthropology: The Official Publication of the American Association of Physical Anthropologists, 1998. **106**(1): p. 61-85.
20. Rightmire, G.P., D. Lordkipanidze, and A. Vekua, *Anatomical descriptions, comparative studies and evolutionary significance of the hominin skulls from Dmanisi, Republic of Georgia.* Journal of Human Evolution, 2006. **50**(2): p. 115-141.
21. Rightmire, G.P., A. Margvelashvili, and D. Lordkipanidze, *Variation among the Dmanisi hominins: Multiple taxa or one species?* American journal of physical anthropology, 2019. **168**(3): p. 481-495.
22. Andrews, P., *An alternative interpretation of the charac ters used to define Homo erectus. The Early Evolution of Man with Special Emphasis on Southeast Asia and Africa.* Cour. Forsch. Inst. Senckenberg, Frankfurt am Main, 1984. **69**: p. 167-175.
23. Stringer, C.B., *The definition of Homo erectus and the existence of the species in Africa and Europe.* Cour. Forsch. Inst. Senckenberg, Frankfurt am Main, 1984. **69**: p. 131-143.
24. Tattersall, I., *Species recognition in human paleontology.* Journal of Human Evolution, 1986. **15**(3): p. 165-175.
25. Wood, B., *Koobi Fora research project: Hominid cranial remains*. Vol. 4. 1991: Oxford University Press, USA.

26. Wood, B.A., *The origin of Homo erectus.* Cour. Forsch. Inst. Senckenberg, 1984. **69**: p. 99-111.
27. Wood, B., *Taxonomy and evolutionary relationships of Homo erectus.* Courier Forschungsinstitut Senckenberg, 1994. **171**: p. 159-165.
28. Wood, B., *Origin and evolution of the genus Homo.* Nature, 1992. **355**(6363): p. 783.
29. de Lumley, M.-A., et al., *Les restes humains du Pliocène final et du début du Pléistocène inférieur de Dmanissi, Géorgie (1991–2000). I–Les crânes, D 2280, D 2282, D 2700.* L'anthropologie, 2006. **110**(1): p. 1-110.
30. Gabounia, L., et al., *Découverte d'un nouvel hominidé à Dmanissi (Transcaucasie, Géorgie).* Comptes Rendus Palevol, 2002. **1**(4): p. 243-253.
31. Martinón-Torres, M., et al., *Dental remains from Dmanisi (Republic of Georgia): morphological analysis and comparative study.* Journal of Human Evolution, 2008. **55**(2): p. 249-273.
32. Tattersall, I., *Species concepts and species identification in human evolution.* Journal of Human Evolution, 1992. **22**(4-5): p. 341-349.
33. Schwartz, J. and I. Tattersall, *The human fossil record. Volume two. Craniodental morphology of genus Homo (Africa, Asia).* 2003, New York: Wiley.
34. Schwartz, J.H. and I. Tattersall, *The Human Fossil Record. Vol. 4: Craniodental Morphology of Early Hominids (Genera, Australopithecus, Paranthropus, Orrorin), and Overview*. 2005: NJ: John Wiley & Sons.
35. Harvati, K., et al., *Apidima Cave fossils provide earliest evidence of Homo sapiens in Eurasia.* Nature, 2019. **571**(7766): p. 500-504.
36. Bookstein, F.L., *Principal warps: Thin-plate splines and the decomposition of deformations.* IEEE Transactions on pattern analysis and machine intelligence, 1989. **11**(6): p. 567-585.
37. Bookstein, F.L., *Morphometric tools for landmark data: geometry and biology.* 1991, Cambridge: Cambridge University Press. 435.
38. Bookstein, F.L., *Morphometric tools for landmark data: geometry and biology*. 1997: Cambridge University Press.
39. Mitteroecker, P. and P. Gunz, *Advances in Geometric Morphometrics.* Evolutionary Biology, 2009. **36**(2): p. 235-247.
40. Rohlf, F.J. and D. Slice, *Extensions of the Procrustes Method for the Optimal Superimposition of Landmarks.* Systematic Biology, 1990. **39**(1): p. 40-59.
41. Adams, D.C. and M.L. Collyer, *A general framework for the analysis of phenotypic trajectories in evolutionary studies.* Evolution, 2009. **63**(5): p. 1143-1154.
42. Athreya, S., *The frontal bone in the genus Homo: a survey of functional and phylogenetic sources of variation.* J. Anthropol. Sci., 2012. **90**: p. 1-22.
43. Baab, K.L., *Defining Homo erectus*, in *Handbook of paleoanthropology*, W. Henke and I. Tattersall, Editors. 2015, Springer: Berlin, Heidelberg. p. 2189-2219.
44. Bastir, M., A. Rosas, and P. O'Higgins, *Craniofacial levels and the morphological maturation of the human skull.* Journal of Anatomy, 2006. **209**(5): p. 637-654.
45. Gunz, P., P. Mitteroecker, and F.L. Bookstein, *Semilandmarks in three dimensions*, in *Modern morphometrics in physical anthropology*, D.E. Slice, Editor. 2005, Springer: Boston, MA. p. 73-98.
46. Gunz, P., et al., *Neandertal introgression sheds light on modern human endocranial globularity.* Current Biology, 2019. **29**(1): p. 120-127. e5.
47. Neubauer, S., P. Gunz, and J.-J. Hublin, *Endocranial shape changes during growth in chimpanzees and humans: A morphometric analysis of unique and shared aspects.* Journal of Human Evolution, 2010. **59**(5): p. 555-566.

48. O'HIGGINS, P., *The study of morphological variation in the hominid fossil record: biology, landmarks and geometry.* The Journal of Anatomy, 2000. **197**(1): p. 103-120.
49. Profico, A., et al., *Filling the gap. Human cranial remains from Gombore II (Melka Kunture, Ethiopia; ca. 850 ka) and the origin of Homo heidelbergensis.* J. Anthropol. Sci., 2016. **94**: p. 1-24.
50. Reyes-Centeno, H., et al., *Genomic and cranial phenotype data support multiple modern human dispersals from Africa and a southern route into Asia.* Proceedings of the National Academy of Sciences of the United States of America, 2014. **111**(20): p. 7248-7253.
51. Smith, H.F., et al., *A 3-D geometric morphometric study of intraspecific variation in the ontogeny of the temporal bone in modern Homo sapiens.* Journal of Human Evolution, 2013. **65**(5): p. 479-489.
52. Bräuer, G., *The origin of modern anatomy: By speciation or intraspecific evolution?* Evolutionary Anthropology: Issues, News, and Reviews, 2008. **17**(1): p. 22-37.
53. Gunz, P., et al., *Principles for the virtual reconstruction of hominin crania.* Journal of Human Evolution, 2009. **57**(1): p. 48-62.
54. Weber, G.W., *Virtual anthropology.* American Journal of Physical Anthropology, 2015. **156**: p. 22-42.
55. Weber, G.W. and F.L. Bookstein, *Virtual anthropology: a guide to a new interdisciplinary field*. 2011, Wien, Austria: SpringerWienNewYork.
56. Aytek, A.İ. and K. Harvati, *The human fossil record from Turkey*, in *Paleoanthropology of the Balkans and Anatolia*, K. Harvati and M. Roksandic, Editors. 2016, Springer: Dordrecht. p. 79-91.
57. Baab, K.L., *A re-evaluation of the taxonomic affinities of the early Homo cranium KNM-ER 42700.* Journal of human evolution, 2008. **55**(4): p. 741-6.
58. Spoor, F., et al., *Implications of new early Homo fossils from Ileret, east of Lake Turkana, Kenya.* Nature, 2007. **448**: p. 688.
59. Spoor, F., et al., *The taxonomic status of KNM-ER 42700: A reply to Baab (2008a).* Journal of human evolution, 2008. **55**(4): p. 747-750.
60. Bauer, C.C. and K. Harvati, *A virtual reconstruction and comparative analysis of the KNM-ER 42700 cranium.* Anthropologischer Anzeiger, 2015. **72**(2): p. 129-140.
61. Baab, K.L., *The role of neurocranial shape in defining the boundaries of an expanded Homo erectus hypodigm.* Journal of Human Evolution, 2016. **92**: p. 1-21.
62. Neubauer, S., et al., *Reconstruction, endocranial form and taxonomic affinity of the early Homo calvaria KNM-ER 42700.* Journal of Human Evolution, 2018.
63. Lieberman, D.E., *The evolution of the human head*. 2011: The belknap press of Harvard university press.
64. Antón, S.C., *Cranial growth in Homo erectus: how credible are the Ngandong juveniles?* American Journal of Physical Anthropology, 1999. **108**(2): p. 223-236.
65. Dean, C. and H.M. Liversidge, *Age estimation in fossil hominins: comparing dental development in early Homo with modern humans.* Annals of Human Biology, 2015. **42**(4): p. 415-429.
66. Robson, S.L. and B. Wood, *Hominin life history: reconstruction and evolution.* Journal of Anatomy, 2008. **212**(4): p. 394-425.
67. Smith, B.H., *Dental development as measure of life history in primates.* Evolution, 1989. **43**(3): p. 683-688.
68. Smith, S.L., *Skeletal age, dental age, and the maturation of KNM-WT 15000.* American Journal of Physical Anthropology, 2004. **125**(2): p. 105-120.
69. Gower, J.C., *Generalized procrustes analysis.* Psychometrika, 1975. **40**(1): p. 33-51.

70. Potts, R., et al., *Small Mid-Pleistocene Hominin Associated with East African Acheulean Technology.* Science, 2004. **305**(5680): p. 75-78.
71. Rightmire, G.P., *Cranial remains of Homo erectus from Beds II and IV, Olduvai Gorge, Tanzania.* American Journal of Physical Anthropology, 1979. **51**(1): p. 99-115.
72. Tamrat, E., et al., *Revised magnetostratigraphy of the Plio-Pleistocene sedimentary sequence of the Olduvai Formation (Tanzania).* Palaeogeography, Palaeoclimatology, Palaeoecology, 1995. **114**(2-4): p. 273-283.
73. Kappelman, J., et al., *First Homo erectus from Turkey and implications for migrations into temperate Eurasia.* American Journal of Physical Anthropology, 2008. **135**(1): p. 110-116.
74. Lebatard, A.-E., et al., *Dating the Homo erectus bearing travertine from Kocabaş (Denizli, Turkey) at at least 1.1 Ma.* Earth and Planetary Science Letters, 2014. **390**: p. 8-18.
75. Vialet, A., G. Guipert, and M. Cihat Alçiçek, *Homo erectus found still further west: Reconstruction of the Kocabaş cranium (Denizli, Turkey).* Comptes Rendus Palevol, 2012. **11**(2): p. 89-95.
76. Guipert, G., A. Vialet, and M.C. Alcicek. *The Homo erectus from Kocabaş in Turkey and the first settlements in Eurasia*. in *American Journal of Physical Anthropology*. 2011. WILEY-BLACKWELL 111 RIVER ST, HOBOKEN 07030-5774, NJ USA.
77. Vialet, A., et al., *La calotte crânienne de l'Homo erectus de Kocabaş (Bassin de Denizli, Turquie).* L'Anthropologie, 2014. **118**(1): p. 74-107.
78. Vialet, A., et al., *The Kocabaş hominin (Denizli Basin, Turkey) at the crossroads of Eurasia: New insights from morphometric and cladistic analyses.* Comptes Rendus Palevol, 2018. **17**(1): p. 17-32.
79. Adams, D.C., E. Otárola-Castillo, and E. Paradis, *geomorph: an r package for the collection and analysis of geometric morphometric shape data.* Methods in Ecology and Evolution, 2013. **4**(4): p. 393-399.
80. Collyer, M.L. and D.C. Adams, *Analysis of two-state multivariate phenotypic change in ecological studies.* Ecology, 2007. **88**(3): p. 683-692.
81. Collyer, M.L. and D.C. Adams, *Phenotypic trajectory analysis: comparison of shape change patterns in evolution and ecology.* Hystrix, the Italian Journal of Mammalogy, 2013. **24**(1): p. 75-83.
82. Antón, S.C., *Developmental age and taxonomic affinity of the Mojokerto child, Java, Indonesia.* American Journal of Physical Anthropology, 1997. **102**(4): p. 497-514.
83. Balzeau, A., D. Grimaud-Hervé, and T. Jacob, *Internal cranial features of the Mojokerto child fossil (East Java, Indonesia).* Journal of Human Evolution, 2005. **48**(6): p. 535-553.
84. Gilbert, W.H. and B. Asfaw, *Homo erectus: Pleistocene Evidence from the Middle Awash, Ethiopia*. Vol. 1. 2008, Berkeley and Los Angeles, California: University of California Press.
85. Bruner, E., et al., *The endocast of the one-million-year-old human cranium from Buia (UA 31), Danakil Eritrea.* American journal of physical anthropology, 2016. **160**(3): p. 458-468.
86. Antón, S.C., *Defining Homo erectus: size considered.* Handbook of paleoanthropology, 2007. **3**: p. Chapter 11.
87. Lordkipanidze, D., et al., *A Complete Skull from Dmanisi, Georgia, and the Evolutionary Biology of Early Homo.* Science, 2013. **342**(6156): p. 326-331.
88. Plavcan, J.M., *Body size, size variation, and sexual size dimorphism in early Homo.* Current Anthropology, 2012. **53**(S6): p. S409-S423.
89. Rightmire, G.P., *Brain size and encephalization in early to mid-Pleistocene Homo.* American Journal of Physical Anthropology: The Official Publication of the American Association of Physical Anthropologists, 2004. **124**(2): p. 109-123.

90. Rightmire, G.P., *Homo erectus and Middle Pleistocene hominins: brain size, skull form, and species recognition.* Journal of human evolution, 2013. **65**(3): p. 223-252.
91. Baab, K.L., et al., *Reconstruction and analysis of the DAN5/P1 and BSN12/P1 Gona Early Pleistocene Homo fossils.* Journal of Human Evolution, 2022. **162**: p. 103102.
92. Howell, F.C., *Paleo-Demes, Species Clades, and Extinctions in the Pleistocene Hominin Record.* Journal of Anthropological Research, 1999. **55**(2): p. 191-243.
93. Delson, E., et al., *The Sambungmacan 3 Homo erectus calvaria: a comparative morphometric and morphological analysis.* The Anatomical Record: An Official Publication of the American Association of Anatomists, 2001. **262**(4): p. 380-397.
94. Openoorth, W., *Homo (Javanthropus) soloensis, een pleistoceene mensch van Java.* Wetesch Mededee. Dienst Mijnbauw Nederl Indie, 1932. **20**: p. 49-74.
95. Schwartz, J.H. and I. Tattersall, *Defining the genus Homo.* Science, 2015. **349**(6251): p. 931-932.
96. Tattersall, I., *Homo ergaster and Its Contemporaries*, in *Handbook of Paleoanthropology*, W. Henke and I. Tattersall, Editors. 2015, Springer Berlin Heidelberg: Berlin, Heidelberg. p. 2167-2187.
97. Weidenreich, F., *Morphology of Solo man.* Anthropological Paper of the American Museum of Natural History, 1951. **43**(3): p. 205-290.
98. Widianto, H. and V. Zeitoun, *Morphological description, biometry and phylogenetic position of the skull of Ngawi 1 (east Java, Indonesia).* International Journal of Osteoarchaeology, 2003. **13**(6): p. 339-351.
99. Wolpoff, M.H., et al., *The case for sinking Homo erectus: 100 years of Pithecanthropus is enough.* Courier Forschungsinstitut Senckenberg, 1994. **171**: p. 341-361.
100. Zeitoun, V., et al., *Solo man in question: Convergent views to split Indonesian Homo erectus in two categories.* Quaternary International, 2010. **223-224**: p. 281-292.
101. Antón, S.C., R. Potts, and L.C. Aiello, *Evolution of early Homo: An integrated biological perspective.* Science, 2014. **345**(6192): p. 1236828.
102. Delson, E. and C. Stringer, *The naming of Homo bodoensis by Roksandic and colleagues does not resolve issues surrounding Middle Pleistocene human evolution.* Evolutionary Anthropology: Issues, News, and Reviews, 2022. **n/a**(n/a).
103. Rightmire, G.P., *Homo in the Middle Pleistocene: Hypodigms, variation, and species recognition.* Evolutionary Anthropology: Issues, News, and Reviews: Issues, News, and Reviews, 2008. **17**(1): p. 8-21.
104. Roksandic, M., P. Radović, and J. Lindal, *Revising the hypodigm of Homo heidelbergensis: A view from the Eastern Mediterranean.* Quaternary International, 2018. **466**: p. 66-81.
105. Roksandic, M., et al., *Resolving the "muddle in the middle": The case for Homo bodoensis sp. nov.* Evolutionary Anthropology: Issues, News, and Reviews, 2022. **31**(1): p. 20-29.
106. Altunel, E., *Pamukkale travertenlerinin morfolojik özellikleri, yaşları ve neotektonik önemleri.* MTA dergisi, 1996. **118**: p. 47-64.
107. Engin, B., O. Güven, and F. Köksal, *Electron spin resonance age determination of a travertine sample from the southwestern part of Turkey.* Applied Radiation and Isotopes, 1999. **51**(6): p. 689-699.
108. Muttoni, G., G. Scardia, and D.V. Kent, *Early hominins in Europe: The Galerian migration hypothesis.* Quaternary Science Reviews, 2018. **180**: p. 1-29.
109. Baab, K.L., et al., *Assessing the status of the KNM-ER 42700 fossil using Homo erectus neurocranial development.* Journal of Human Evolution, 2021. **154**: p. 102980.
110. Granger, D.E., et al., *Cosmogenic nuclide dating of Australopithecus at Sterkfontein, South Africa.* Proceedings of the National Academy of Sciences, 2022. **119**(27): p. e2123516119.

111. Gabunia, L. and A. Vekua, *A plio-pleistocene hominid from Dmanisi, East Georgia, Caucasus.* Nature, 1995. **373**(6514): p. 509.
112. Boulbes, N., et al., *Les grands mammifères du Villafranchien supérieur des travertins du Bassin de Denizli (Sud-Ouest Anatolie, Turquie).* L'Anthropologie, 2014. **118**(1): p. 44-73.
113. Khatib, S., et al., *Études stratigraphique, sédimentologique et paléomagnétique des travertins de Kocabaş, Bassin de Denizli, Anatolie, Turquie, contenant des restes fossiles quaternaires.* L'anthropologie, 2014. **118**(1): p. 16-33.
114. Matsu'ura, S., et al., *Age control of the first appearance datum for Javanese Homo erectus in the Sangiran area.* Science, 2020. **367**(6474): p. 210-214.
115. Rightmire, G.P., *Middle and later Pleistocene hominins in Africa and Southwest Asia.* Proceedings of the National Academy of Sciences, 2009. **106**(38): p. 16046-16050.
116. Stringer, C., *The status of Homo heidelbergensis (Schoetensack 1908).* Evolutionary Anthropology: Issues, News, and Reviews, 2012. **21**(3): p. 101-107.
117. Benazzi, S. and S. Senck, *Comparing 3-dimensional virtual methods for reconstruction in craniomaxillofacial surgery.* Journal of Oral and Maxillofacial Surgery, 2011. **69**(4): p. 1184-1194.
118. Bosman, A., et al., *The Kabua I cranium: Virtual anatomical reconstructions* in *Modern Human Origins and Dispersal*, Y. Sahle, H. Reyes-Centeno, and C. Bentz, Editors. 2019, Kerns Verlag: Tübingen.
119. Noback, M.L. and K. Harvati, *Covariation in the Human Masticatory Apparatus.* The Anatomical Record, 2014. **298**(1): p. 64-84.
120. Noback, M.L. and K. Harvati, *The contribution of subsistence to global human cranial variation.* Journal of Human Evolution, 2015. **80**: p. 34-50.
121. Bosman, A.M., H. Reyes-Centeno, and K. Harvati, *A virtual assessment of the suprainiac depressions on the Eyasi I (Tanzania) and Aduma ADU-VP-1/3 (Ethiopia) Pleistocene hominin crania.* Journal of Human Evolution, 2020. **145**: p. 102815.
122. Mori, T., et al., *Frontal bone virtual reconstruction and geometric morphometric analysis of the mid-Pleistocene hominin KNM-OG 45500 (Olorgesailie, Kenya).* Journal of Anthropological Sciences, 2020. **98**: p. 49-72.
123. Garcia, T., et al., *Earliest human remains in Eurasia: New 40Ar/39Ar dating of the Dmanisi hominid-bearing levels, Georgia.* Quaternary Geochronology, 2010. **5**(4): p. 443-451.
124. Asfaw, B., et al., *Remains of Homo erectus from Bouri, Middle Awash, Ethiopia.* Nature, 2002. **416**(6878): p. 317.
125. Lepre, C.J. and D.V. Kent, *Chronostratigraphy of KNM-ER 3733 and other Area 104 hominins from Koobi Fora.* Journal of human evolution, 2015. **86**: p. 99-111.
126. McDougall, I., et al., *New single crystal 40Ar/39Ar ages improve time scale for deposition of the Omo Group, Omo–Turkana Basin, East Africa.* Journal of the Geological Society, 2012. **169**(2): p. 213-226.
127. Yokoyama, Y., et al., *Gamma-ray spectrometric dating of late Homo erectus skulls from Ngandong and Sambungmacan, Central Java, Indonesia.* Journal of Human Evolution, 2008. **55**(2): p. 274-277.
128. Storm, P., et al., *Late Pleistocene Homo sapiens in a tropical rainforest fauna in East Java.* Journal of Human Evolution, 2005. **49**(4): p. 536-545.
129. Larick, R., et al., *Early Pleistocene 40Ar/39Ar ages for Bapang formation hominins, central Jawa, Indonesia.* Proceedings of the National Academy of Sciences, 2001. **98**(9): p. 4866-4871.
130. Shen, G., et al., *Age of Zhoukoudian Homo erectus determined with 26Al/10Be burial dating.* Nature, 2009. **458**(7235): p. 198-200.

131. Nomade, S., et al., *First 40Ar/39Ar age of the Ceprano man (central Italy).* Quaternary Geochronology, 2011. **6**(5): p. 453-457.
132. Manzi, G., et al., *The new chronology of the Ceprano calvarium (Italy).* Journal of human evolution, 2010. **59**(5): p. 580-585.
133. Falguères, C., et al., *New ESR and U-series dating at Caune de l'Arago, France: A key-site for European Middle Pleistocene.* Quaternary Geochronology, 2015. **30**: p. 547-553.
134. Rightmire, P.G., *The human cranium from Bodo, Ethiopia: evidence for speciation in the Middle Pleistocene?* Journal of Human Evolution, 1996. **31**(1): p. 21-39.
135. Buck, L.T. and C.B. Stringer, *A rich locality in South Kensington: the fossil hominin collection of the Natural History Museum, London.* Geological Journal, 2015. **50**(3): p. 321-337.
136. Grün, R., *A re-analysis of electron spin resonance dating results associated with the Petralona hominid.* Journal of Human Evolution, 1996. **30**(3): p. 227-241.
137. Xiao, J., C. Jin, and Y. Zhu, *Age of the fossil Dali Man in north-central China deduced from chronostratigraphy of the loess–paleosol sequence.* Quaternary Science Reviews, 2002. **21**(20-22): p. 2191-2198.
138. Grün, R. and C.B. Stringer, *Electron spin resonance dating and the evolution of modern humans.* Archaeometry, 1991. **33**(2): p. 153-199.
139. Richter, D., et al., *The age of the hominin fossils from Jebel Irhoud, Morocco, and the origins of the Middle Stone Age.* Nature, 2017. **546**: p. 293.
140. Grün, R., *Direct dating of human fossils.* American Journal of Physical Anthropology, 2006. **131**(S43): p. 2-48.
141. Schlager, S., *Morpho and Rvcg–Shape Analysis in R: R-Packages for geometric morphometrics, shape analysis and surface manipulations*, in *Statistical shape and deformation analysis*, G. Zheng, S. Li, and G. Székely, Editors. 2017, Academic Press: Cambridge. p. 217-256.
142. Mitteroecker, P. and F. Bookstein, *Linear discrimination, ordination, and the visualization of selection gradients in modern morphometrics.* Evolutionary Biology, 2011. **38**(1): p. 100-114.
143. Sokal, R.R., *A statistical method for evaluating systematic relationships.* Univ. Kansas, Sci. Bull., 1958. **38**: p. 1409-1438.
144. Lachenbruch, P.A. and M. Goldstein, *Discriminant analysis.* Biometrics, 1979: p. 69-85.
145. Field, A., *Discovering statistics using IBM SPSS Statistics (4th edition)*. 2013, London: Sage.
146. R Core Team, *R: A language and environment for statistical computing.* 2018.
147. Profico, A., et al., *Arothron: R functions for geometric morphometrics analyses.* R package version, 2015. **314**(1.0).
148. Profico, A., et al., *Reproducing the internal and external anatomy of fossil bones: Two new automatic digital tools.* American journal of physical anthropology, 2018. **166**(4): p. 979-986.
149. Schliep, K.P., *phangorn: phylogenetic analysis in R.* Bioinformatics, 2010. **27**(4): p. 592-593.
150. Manzi, G., *Humans of the Middle Pleistocene: The controversial calvarium from Ceprano (Italy) and its significance for the origin and variability of Homo heidelbergensis.* Quaternary international, 2016. **411**: p. 254-261.
151. Manzi, G., E. Bruner, and P. Passarello, *The one-million-year-old Homo cranium from Bouri (Ethiopia): a reconsideration of its H. erectus affinities.* Journal of Human Evolution, 2003. **44**(6): p. 731-736.
152. Maslin, M.A. and A.J. Ridgwell, *Mid-Pleistocene revolution and the 'eccentricity myth'.* Geological Society, London, Special Publications, 2005. **247**(1): p. 19-34.

153. Mounier, A., F. Marchal, and S. Condemi, *Is Homo heidelbergensis a distinct species? New insight on the Mauer mandible.* Journal of Human Evolution, 2009. **56**(3): p. 219-246.
154. Leakey, M.D., *Olduvai Gorge: Volume 3, excavations in beds I and II, 1960-1963*. Vol. 3. 1971, Cambridge: Cambridge University Press.
155. Erten, H., S. Sen, and M. Özkul, *Pleistocene mammals from travertine deposits of the Denizli basin (SW Turkey).* Annales de Paléontologie, 2005. **91**(3): p. 267-278.
156. Berger, L.R., et al., *Homo naledi, a new species of the genus Homo from the Dinaledi Chamber, South Africa.* Elife, 2015. **4**: p. e09560.
157. Berger, L.R., et al., *Homo naledi and Pleistocene hominin evolution in subequatorial Africa.* Elife, 2017. **6**: p. e24234.
158. Wold, S., K. Esbensen, and P. Geladi, *Principal component analysis.* Chemometrics and intelligent laboratory systems, 1987. **2**(1-3): p. 37-52.
159. Profico, A., et al., *A new tool for digital alignment in virtual anthropology.* The Anatomical Record, 2019. **302**(7): p. 1104-1115.
160. Mori, T. and K. Harvati, *Basicranial ontogeny comparison in Pan troglodytes and Homo sapiens and its use for developmental stage definition of KNM-ER 42700.* American journal of physical anthropology, 2019.
161. Tattersall, I., *Homo ergaster and its contemporaries.* Handbook of paleoanthropology, 2007. **3**: p. 1633-1654.

List of Publications

Original articles:

Alessandro Riga; **Mori, Tommaso**; Fabio, Di Vincenzo; Pasquinelli, Filippo; Carpi, Roberto; Moggi-Cecchi, Jacopo. " 3D Methods for the Anthropological Cultural Heritage". *IOP conference series: Florence Heritech*. (In Press) 2022

Mori, Tommaso; Riga, Alessandro; Dionisio, Giulia; Bigoni, Francesca; Moggi-Cecchi, Jacopo; "Cranial modification and trepanation in pre-Hispanic collections from Peru in the Museum of Anthropology and Ethnology, Florence, Italy", *Medicina Historica* ,6,1,e2022002, 2022,

Riga, Alessandro; Begni, Claudia; Sala, Susanna; Erriu, Stella; Gori, Silvia; Moggi-Cecchi, Jacopo; **Mori, Tommaso**; Dori, Irene. "Is root exposure a good marker of periodontal disease?",*Bulletin of the International Association for Paleodontology*,15,1,21-30,2021,International Association for Paleodontology

Oxilia, Gregorio; Menghi Sartorio, Jessica C; Bortolini, Eugenio; Zampirolo, Giulia; Papini, Andrea; Boggioni, Marco; Martini, Sergio; Marciani, Filippo; Arrighi, Simona; Figus, Carla; **Mori, Tommaso**; … & Benazzi, Stefano. "Exploring directional and fluctuating asymmetry in the human palate during growth", *American journal of physical anthropology*,175,4,847-864,2021,"John Wiley & Sons, Inc. Hoboken, USA"

Dionisio, Giulia; Bigoni, Francesca; **Mori, Tommaso**; Moggi- Cecchi, Jacopo. "La collezione di maschere facciali del Museo di Antropologia e Etnologia di Firenze",*Museologia Scientifica*,14,,12-28,2020,

Mori, Tommaso; Beier, Judith; de Matos, Daniela; Mentzer, Susan M. "Seventh Annual Meeting of the European Society for the Study of Human Evolution",*Evolutionary Anthropology: Issues, News, and Reviews*,27,1,3-4,2018,Wiley Online Library

Mori, Tommaso; Profico, Antonio; Reyes-Centeno, Hugo; Harvati, Katerina. "Frontal bone virtual reconstruction and geometric morphometric analysis of the mid-Pleistocene hominin KNM-OG 45500 (Olorgesailie, Kenya)",*Journal of Anthropological Sciences*,98,,49-72,2020,

Mori, Tommaso; Harvati, Katerina. "Basicranial ontogeny comparison in Pan troglodytes and Homo sapiens and its use for developmental stage definition of KNM-ER 42700", *American Journal of Physical Anthropology*,170,4,579-594,2019,"John Wiley & Sons, Inc. Hoboken, USA"

Riga, Alessandro; **Mori, Tommaso**; Pickering, Travis Rayne; Moggi-Cecchi, Jacopo; Menter, Colin G. "Ages-at-death distribution of the early Pleistocene hominin fossil assemblage from Drimolen (South Africa)",*American Journal of Physical Anthropology*,168,3,632-636,2019,"John Wiley & Sons, Inc. Hoboken, USA"

Dionisio, Giulia; **Mori, Tommaso**; Bigoni, Francesca; Moggi-Cecchi, Jacopo. "Antropologia Integrata: approcci innovativi per lo studio delle collezioni al Museo di Antropologia e Etnologia di Firenze", *Museologia scientifica Memorie*.

Published conference abstracts

Mori, Tommaso; Profico, Antonio; Reyes-Centeno, Hugo; Harvati, Katerina. "Frontal bone virtual reconstruction and geometric morphometric analysis of the mid-Pleistocene hominin KNM-OG 45500 (Olorgesailie, Kenya)", Pecha Kucha presentation. In: *Proceedings of the European Society for the Study of Human Evolution,* 9, 80, Worldwide.

Mori, Tommaso; Harvati, Katerina. “Basicranial ontogeny comparison in Pan troglodytes and Homo sapiens and its use for developmental stage definition of KNM-ER 42700”, Poster presentation. In: *Proceedings of the European Society for the Study of Human Evolution,* 8, 135, Liège.

Mori, Tommaso; Moggi-Cecchi Jacopo; Pickering, Travis Rayne; Menter, Colin G. “Distribution of Ages-at-Death of Fossil Hominins from the Early Pleistocene site of Drimolen, South Africa: Preliminary Results and Behavioral Implications”, Poster presentation. In: *Proceedings of the European Society for the Study of Human Evolution*, 3, 158, Vienna

Acknowledgments

At the end of my Ph.D. I cannot stop thinking of the many fantastic people I met and all the times I chatted, discussed, and laughed with many of you. All of this could not have been possible without the support of many people. In these few lines, I want to sincerely thank all the people who crossed their paths with me during the time of my Ph.D.

I am immensely grateful to my first supervisor, Professor Katerina Harvati, for giving me the chance to be part of her amazing lab. Your thoughts and comments were and will always be priceless for any paleoanthropologist. Thank you for having supported my work and believing in me. I would like to thank also my former supervisor at the time of my Master's degree, Professor Jacopo Moggi-Cecchi; you have always been present during my scientific growth. Thank you for turning on my interest in this field and the fantastic time in South Africa. Visiting the different sites and the extraordinary collections really changed my life. I hope I will be able to keep the same enthusiasm you have about paleoanthropology and any news that come from such a field. I am also grateful to Professor Sireen El Zaatari for being part of the committee; I look forward to fantastic news from Libano! As a final committee member but the first person I met in Tuebingen, I want to thank Professor Cosimo Posth. You have been my guide during my first period in Tuebingen. The time spent together was priceless, and you helped me a lot not feeling the distance from home, may the cantuccini spirit guide you. Thanks also to Hugo Reyes-Centeno; you were always willing to help me since the earliest stage of my path in Tuebingen. Your comments and advice were fundamental for this doctorate. This doctorate would not be accomplished without the help of super secretaries who helped me find the path in the bureaucracy's dedalous. Thank you, Moni and Karin, for the help you gave me during these years. I would like to thank all the people from the INA and the Paleoanthropology group. You all have always been friendly and ready to help me when I needed it; being your colleague has been a pleasure.

Many friends I met in Tuebingen, and there I found a second family that gives me the feeling of a second home. My gratitude goes to everybody I have met, even if not everyone is named here. Thoughts of gratitude for the 509ers: Dome, Hannes, Judith, Viola, Anto. Dome and Hannes, you are like brothers, and I could not ask for better persons next to me during these years. Science, saunas, pools, hiking, skiing, lakes, rivers, pubs, concerts, raves, amazing new years eve, dinners, beers, all these things come to my mind thinking of you. Thank you for making me part of your life, not only your job. And thank you, Hannes for the Zusammenfassung!! Many thanks also to the Greek gang; you have always being amazing. The TSR time was fantastic, and I hope to be able to come again and find new nails (the earliest evidence of iron age culture in the Villafranchian, I must say!!). Georgos and Vangelis, thank you. Also, other greeks cross their life with mine. Alexandros (and Enora) and Melania. Thank you Alexandros; you always be the best prosciutto lover I will ever meet. Not only that, I must say, I am really grateful for the very nice discussion I had with you in the earliest phase of my Ph.D.; you helped me a lot with finding the right ways to achieve the results of this Ph.D. thank you. Also, the Italians were in town, so I want to thank all the Italians I met. Armando and Ele, thank you for your friendship and the pizzas at your place; these were good food for the soul, I will never forget them together with our Italian chat and searching for Italian things here and there in Tubi and beyond (clams, fiori di zucca, orate)! At the beginning of this journey, I need to thank also Alex Bertacchi, you will rock in the USA. A thought to the D&D gang, Shyama, Abel, Sarah, Alex, and Hannes, all of you were

amazing; I will never forget the goblin's slayers 😊 hope you will enjoy many more adventures in your life. Also, cheers to all the "people from the castle", parties there will always be in my memories!

Most importantly, I really owe everything to my family. You always supported me and gave me the chance to pursue my interest. Thank you for your endless approval and motivation. Life is not easy, but you helped me to keep going.

Last but not least, I really want to thank you. My rock, my confidant, my love. Thank you for your patience. Over these many years, we had to live our relationship in half, but it probably is thanks to this that now I feel we are really strong together. And thank you for giving me the most important thing in my life, our son. To you, my son, the last words, thank you for putting my view of the world in a completely different perspective. Stay curious and enjoy your life; I will be there anytime you need it.